Flow patterns and flow pattern maps for adiabatic and diabatic gas liquid two phase flow in microchannels: fundamentals, mechanisms and applications

CHENG, Lixin and XIA, Guodong

Experimental Thermal and Fluid Science 148 (2023) 110988

Contents lists available at ScienceDirect

Experimental Thermal and Fluid Science

journal homepage: www.elsevier.com/locate/etfs

Flow patterns and flow pattern maps for adiabatic and diabatic gas liquid two phase flow in microchannels: fundamentals, mechanisms and applications

Lixin Cheng [a,b,*], Guodong Xia [a,*]

[a] Key Laboratory of Enhanced Heat Transfer and Energy Conservation, Ministry of Education, Beijing University of Technology, Beijing 100124, China
[b] Department of Engineering and Mathematics, Sheffield Hallam University, City Campus, Howard Street, Sheffield, S1 1WB, UK

ARTICLE INFO

Keywords:
Flow patterns
Bubble dynamics
Flow pattern maps
Microchannels
Unstable and transient flow patterns
Mechanism

ABSTRACT

This paper mainly presents comprehensive review on the research regarding adiabatic and diabatic gas–liquid two-phase flow patterns, bubble growth, flow pattern transitions and flow pattern maps in microchannels over the past 15 years. First, criteria for distinction of macro- and micro-channels are discussed. Then, fundamentals of gas liquid two-phase flow patterns, flow pattern maps and techniques for two phase flow visualization and sensing are presented. Next, experimental studied of adiabatic and diabatic two phase flow patterns, bubble behaviour, flow pattern transitions and flow pattern maps in microchannels with plain and enhanced structures are reviewed. Finally, applications of flow patterns and flow pattern maps are discussed. Flow pattern based mechanistic heat transfer prediction methods are focused on and studies on unstable and transient two phase flow patterns and heat transfer in microscale channels are addressed. According to the review and analysis, recommendations on the future research needs have been given. Systematic and accurate experimental data on flow patterns, bubble growth, flow pattern transitions are still needed. In particular, there are lacks general flow pattern transition criteria. Therefore, effort should be made to develop generalized flow pattern transition criteria based on well documented experimental observation and data. Furthermore, studies of mechanistic and theoretical models for flow patterns, flow pattern transitions bubble growth in microchannels should be further conducted. As an important topic, unstable and transient gas liquid two phase flow patterns and heat transfer in microchannels should be systematically investigated as well in order to understand the flow pattern transition mechanisms in microchannels with plain and enhanced structures.

1. Introduction

Due to the rapid development in fabrication techniques, the miniaturization of devices and components is increasing in a wide range of engineering applications. Advanced reliable and effective high heat flux cooling technologies are crucial in a wide spectrum of industrial processes such as high power electronics, microelectronics, microprocessers in the computer and information technology, micro reactors, microfluidics, fuel cells, turbine blades, concentrator photovoltaic systems, battery packs in hybrid vehicles, advanced military avionics, defence radars, directed-energy lasers, electromagnetic weapons, space, thermal energy conversion and utilisation, renewable and sustainable energy technologies and nuclear energy etc. [1–14]. Breakthroughs in many of today's cutting-edge technologies require advanced high heat flux and ultra high heat flux cooling technologies which are becoming increasingly dependent upon the ability to safely dissipate enormous amounts of heat from very small areas. Two ranges of heat flux can be loosely identified relative to the magnitude of the heat dissipation and the type of coolant permissible in a particular application. These are the high fluxes of $10^2 - 10^3$ W/cm^2, and the ultra high fluxes of 10^2-10^5 W/cm^2. The high heat fluxes must be removed while maintaining the material temperatures below prescribed limits, for example, the current high heat flux for power electronics in electric vehicles reaches up to 300 W/cm^2 at the chip level, while in some applications, such as defence power electronics, it can reach up to 1000 W/cm^2 [11]. Two phase flow cooling using flow boiling in microchannel heat exchangers is an enabling method to remove high heat flux. However, microscale and nanoscale two phase fluid flow and heat transfer phenomena are quite different from those in macroscale

* Corresponding authors.
E-mail addresses: lixincheng@hotmail.com, l.cheng@shu.ac.uk (L. Cheng), xgd@bjut.edu.cn (G. Xia).

https://doi.org/10.1016/j.expthermflusci.2023.110988
Received 28 February 2023; Received in revised form 11 May 2023; Accepted 9 June 2023
Available online 11 June 2023

Nomenclature

A	annular flow
a	constant in Eq. (8)
Acs	cross sectional area, m^2
AR	aspect ratio
B	bubbly flow
b	constant in Eq. (8)
Bd	Bond number, defined by Eq. (5)
Bo	Bond number, defined by Eq. (5), Boiling number, defined by Eq. (15)
CB	confined bubble flow
CHF	critical heat flux, W/m^2
Co	confinement number
c_p	specific heat at constant pressure, J/kgK
$Eö$	Eotvös number defined by Eq. (4)
Fr	Froude number
Fr_L	Liquid Froude number defined by Eq. (17)
f_A	frequency, Hz
D	length scale defined by Eq. (6), m, diameter, m, dryout
D_h	internal tube hydraulic diameter, m
d	diameter, m; length, m
e	thickness of base wall, m
G	total gas and liquid two-phase mass velocity, kg/m^2s
g	gravitational acceleration, 9.81 m/s^2
H	height, m
h	heat transfer coefficient, W/m^2K, heigh, m
I	intermittent flow
IB	isolated bubble flow
J	superficial velocity, m/s
j	superficial velocity, m/s
L	Laplace number, defined by Eq. (1); length, m.
M	mass flow rate, kg/s, mist flow
P	plug flow
p	pressure, N/m^2
p_r	redcued pressure $[p/p_{crit}]$
q	heat flux, W/m^2
q''	heat flux, W/m^2
T	temperature, K
Re	Reynolds number
Re_L	Liuqid Reynolds number defined by Eq. (14)
Re_V	Liuqid Reynolds number defined by Eq. (13)
r	distance, m
S	stratified flow, slug flow
$SLUG$	slug flow
SW	stratified wave flow
T_{sat}	saturation temperature, K
t	time, s, fin thickness, m
u	velocity, m/s
W	width, m
We	Weber number
We_L	liquid Weber number defined by Eq. (16)
We_l	liquid Weber number
We_g	gas phase Weber number
x	vapor quality
z	location, m

Greek symbols

μ	Dynamics viscosity, Pa.s
δ	liquid film thickness, m
ε	void fraction
θ	Angle, rad
ρ	density, kg/m^3
σ	surface tension, N/m
ΔL_{Laser}	distance between two laser measurement points, m
ΔT_{sub}	subcooled temperature, C

Subscripts

b	base
c	channel
$crit$	critical
cs	cross section
dry	dry perimeter
e	exit
f	liquid phase
G	gas phase
g	gas phase
in	inlet
L	liquid phase
l	liquid phase
sat	saturation
sub	subcooled
T	total
th	threshold
V	vapor phase
W	wall
w	tube wall

systems. Over the past decades, a large number of studies have been conducted to understand the very complicated two phase flow and heat transfer in microchannels and to propose the relevant new mechanisms, models and theory [3–5,11–13]. There are still many issues to be clarified from both theoretical and applied aspects.

Flow patterns, flow pattern maps and bubble growth are the fundamentals to understanding gas liquid two phase flow dynamics, flow boiling and condensation heat transfer characteristics and mechanisms in macro- and micro-channels. Both adiabatic and diabatic gas–liquid two-phase flows are very complex physical processes and affected by a deformable interface, channel shape, flow direction and the compressibility of one of the phases in some cases [1–6]. Flow patterns, flow pattern transitions and bubble growth in a channel vary with the channel geometry, channel size, the aspect ratio of rectangular channels, wall wettability, gas and liquid input into the microchannels, working fluid physical properties, flow orientation, flow parameters, adiabatic and diabatic gas liquid two phase flow [7–9]. Furthermore, transient gas liquid two-phase flow, heat transfer and flow oscillations may significantly the flow patterns, flow pattern transitions and bubble behaviours [10–13].

Flow patterns and flow pattern maps at adiabatic and diabatic conditions are quite different from each other due to quite different gas liquid interfacial phenomena, bubble growth and coalescence, heat transfer mechanisms in the phase change processes such as flow boiling and condensation, critical heat flux (CHF) and gas liquid two phase flow instability. In most cases, the gas and liquid flow rates are constant for adiabatic flows. Diabatic two-phase flows with heat transfer occur in flow boiling, flow condensation or gas–liquid two-phase flows with heat addition or removal [1–5,9–11]. Different heat transfer mechanisms are dominant in flow boiling and flow condensation for different flow patterns. Therefore, it is essential to relate the local flow patterns to the gas liquid two phase thermal–hydraulic parameters for determining the two phase flow and heat transfer behaviour in order to design various gas liquid two phase flow systems and phase change heat exchangers such as evaporators, condensers and mixers. In essence, gas liquid two-phase pressure drops, heat transfer coefficients of flow boiling and flow

condensation and the physical mechanisms are intrinsically related to the local flow patterns [14–20]. The prediction methods for gas–liquid two phase flow heat transfer and pressure drops should be based on the local flow patterns. Therefore, it is essential to develop complete flow pattern transition criteria and comprehensive flow pattern maps.

In general, two dimensional flow pattern maps are used to predict the local flow patterns in gas liquid two phase flow. So far, numerous studies of flow patterns have been conducted for various tube configurations such as inside vertical, horizontal and inclined channels covering both macro- and micro-channels, and other complex geometries such as inside enhanced tubes, in compact heat exchangers, across tube bundles, under microgravity conditions, and many flow pattern maps have been proposed for adiabatic and diabatic two phase flow [1,2,21–27]. In principle, adiabatic two phase flow pattern maps are not applicable to diabatic conditions although adiabatic flow pattern maps are often used to compare to diabatic flow patterns in flow boiling and condensation. Such extrapolation of adiabatic flow maps to diabatic conditions are in general not reliable and also lack the influence of heat transfer on the local flow patterns and their transitions. A diabatic flow pattern map should include the effect of heat flux, CHF and dryout on the flow pattern transition boundaries [2,4,10]. A properly developed diabatic flow map should be able to revert to an adiabatic flow pattern map when the heat flux tends to zero. However, such a universal flow pattern map for both diabatic and adiabatic two phase flows are not available in the literature. Although characteristics of two-phase flow in microchannels such as flow patterns, pressure drop, void fraction, and heat transfer are now being extensively studied by numerous groups, one of the major drawbacks in this area to date is the lack of a universal flow patten map enabling the prediction of flow regimes in microchannels for both adiabatic and diabatic conditions [1, 2, 4. 7, 10, 19].

Microscale gas liquid two phase flow and heat transfer have found extensive applications in traditional industries and highly specialized micro-fabricated fluidic systems since the late 20th century [3–8,28–36]. Flow boiling and condensation in microchannels are essential processes involved in a wide range of industrial applications such as micro-heat exchangers, micro reactors, microfluidic device, high heat flux cooling, aerospace, automotive, energy and renewable energy, electronic and microelectronic, hydrogen production and utilisation, biological and medical engineering etc. [3,5,6–9,11–13,37–43]. As shown in Fig. 1, flow boiling in microchannels is an enabling high heat flux cooling technology [14,43,44]. However, flow patterns, bubble behaviours and flow pattern transitions in microchannels are quite different from those of macrochannels. The channel confinement has a great effect on flow patterns, bubble growth, flow pattern transitions, heat transfer and pressure drop in flow boiling and flow condensation and the corresponding mechanistic prediction methods based on flow patterns [2–6,43,45–48,81,98–107]. In particular, stability of liquid vapor two-phase flow is the key to the efficiency and safety of heat dissipation of high heat flux devices. Flow instabilities may greatly affect flow patterns, bubble growth, flow pattern transitions and the corresponding two phase pressure drop, heat transfer and CHF in microchannel evaporators [3–5,9,11].

In recent years, extensive studies have been conducted to enhance flow boiling heat transfer performances in microchannels [49–51]. Various heat transfer enhancement approaches including modifying surface properties, intensifying mixing or disturbance and enhancing nucleate boiling have been exploited to significantly increase flow boiling heat transfer performances and CHF in multi-microchannel evaporators [52–75]. Furthermore, microchannels with various surface structures have attracted much attention to mitigate two-phase flow instabilities in flow boiling. For example, artificial micro cavities, porous layers and nano coatings have been proposed to promote bubble nucleation, increase heat transfer areas, and mitigate rapid bubble growth in stabilities [76–86]. Using nanofluids is another emerging approach to enhance flow boiling heat transfer [87–89]. However, feasibility of using nanofluids in microchannels needs to be carefully

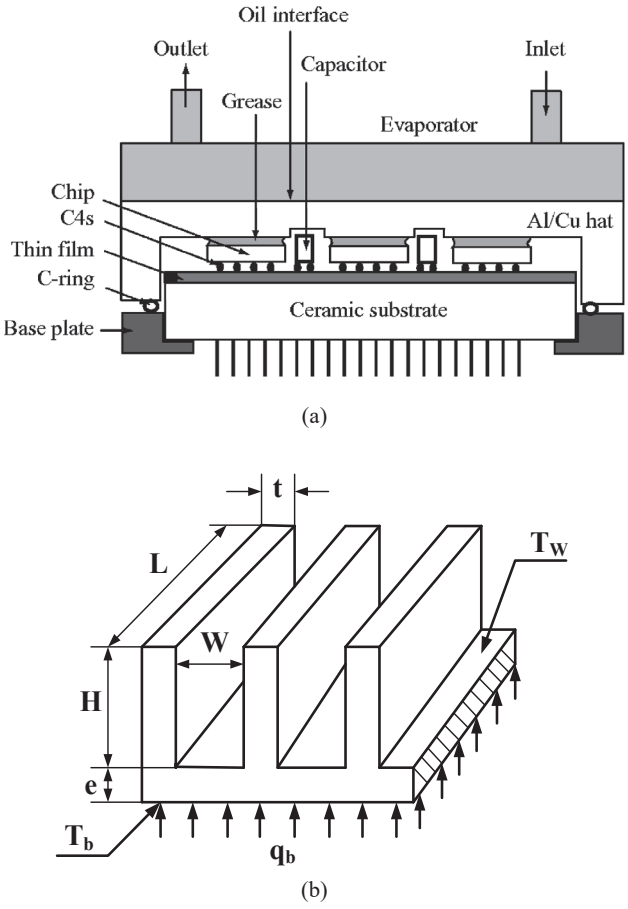

Fig. 1. (a) Cross-section of computer chips with an evaporator by Schmidt and Notohardjono [44]. (b) Schematic diagram of a silicon multi-microchannel evaporator used for chips cooling by Cheng and Thome [14].

evaluated as deposition of nanoparticles on the channel surface may block the microchannels although a number of studies on flow boiling with nanofluids are available in the literature. Flow patterns, bubble growth, flow pattern transitions and the physical mechanisms are yet to be explored for two phase flow phase change heat transfer and two phase flow of nanofluids. Furthermore, there are limited research regarding two phase flow patterns of nanofluids in microchannels. Therefore, the topic of two phase flow patterns, bubble growth, flow pattern transitions with nanofluids are beyond the scope of this review but worth to be mentioned here.

Fundamentals and mechanisms of both adiabatic and diabatic flow patterns and flow pattern maps in microchannels are the key to the development of relevant cutting-edge technologies. Advanced measurement techniques specially for microscale two phase flow patterns, bubble growth, flow pattern transitions, flow instabilities are the key to obtaining accurate experimental results in the research of flow boiling in microchannel evaporators [1–4]. Precisely measuring local flow boiling heat transfer, flow patterns and bubble growth in microchannels is difficult for commonly-used thermal sensors. Verification of heat transfer mechanisms based on direct observation of fundamental heat transfer phenomena at a small and micro spatiotemporal scale is insufficient. Due to the large discrepancies between experiment results from different researchers, systematic knowledge of understanding the fundamentals of diabatic two phase flow patterns, bubble growths, flow pattern transition mechanisms and model development in microchannels is urgently needed. Although there are some studies involving diabatic two-phase flow patterns in flow boiling and condensation, the study of diabatic two phase flow patterns in

microchannels is very complex, and needs to be better understood. Furthermore, the flow distribution and back flow had significant effect on the observed flow patterns, called unstable flow patterns or flow regimes [76–80,82,84–86]. Dryout and flow instability during flow boiling makes it difficult to document an accurate flow pattern map [4,5]. In particular, most of the available studies of flow patterns and flow pattern maps in microchannels are only based on limited fluid types, channel geometry and test parameters such as one or two saturation temperature. Such flow pattern maps can only be applicable to limited fluids and flow conditions. There are disagreements of the observed flow patterns for similar test conditions by different researchers. Therefore, it is necessary to address all these issues in the research of flow patterns, bubble growth, flow pattern transition mechanisms and flow pattern maps in microchannels.

Over the past decades, great efforts have been made to understand the fundamentals of gas liquid two phase flow patterns and development of flow pattern maps. In the early research of gas liquid two phase flow patterns, adiabatic two phase flow patterns in microchannels were mainly studied [1]. With the development of enabling measurement techniques, diabatic flow patterns are being extensively studied. Furthermore, extensive studies of two phase flow and heat transfer in microchannels with enhanced structures have been performed. Although there are several reviews on the relevant topics, none of them cover the recent studies. Two phase flow patterns and flow pattern maps yet need to be investigated and understood. In particular, relating to flow patterns to two phase flow heat transfer prediction methods is important. Flow pattern based heat transfer methods have some mechanistic basis but are less concerned in the available reviews. Therefore, the objectives of the present paper are to review many of these related topics over the past 15 years, to provide a comprehensive knowledge of what has been learned from the available research regarding fundamentals and mechanisms of flow patterns, flow pattern maps and bubble behaviours in microchannels, and to further discus the applications of flow pattern and flow pattern maps in predicting two phase flow and heat transfer behaviours.

2. Criteria for distinction between macro- and micro-channels

Due to the significant differences of flow patterns, flow pattern transitions and bubble behaviours in micro-channels as compared to those in macro-channels, it is essential to address the distinction between macro- and micro-channels at first before addressing various aspects of the available research in the literature. Fig. 2 illustrates the size characteristics of different microfluidic systems [15]. For gas liquid two phase flow in microchannels, a number of macro-to-micro-channel transition criteria based on physical channel size classifications to criteria based on bubble confinement using dimensionless numbers have been proposed by various researchers. The physical channel size classifications are of engineering practice but lack the physical mechanisms of two phase flow phenomena. The bubble confinement criteria are based on the confined growth of a bubble in microchannels. For such criteria, the role of the surface tension force becomes important as the maximum bubble radius decreases at the expense of a gradual suppression of the gravity force as the channel size decreases. However, all such criteria have been proposed according to limited fluids and test conditions by different research groups. There is still a significant difference of opinion regarding the macro-to-micro-channel transitions. Several typical classification criteria are presented here to address the issue.

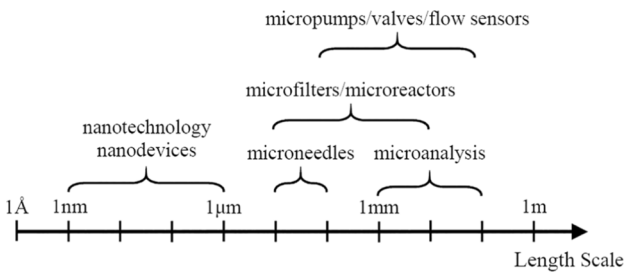

Fig. 2. The size characteristics of different microfluidic systems [15].

2.1. Criteria for classification of macro- and micro-channels according to physical channel sizes

Due to the significantly different transport phenomena in micro channels as compared to conventional channels, one very important issue should be clarified about the distinction between macro-channels and micro-channels at first. However, a universal agreement is not clearly established in the literature. Instead, there are various definitions on this issue.

Based on engineering practice and application areas such as refrigeration industry in the small tonnage units, compact evaporators employed in automotive, aerospace, air separation and cryogenic industries, cooling elements in the field of microelectronics and micro-electro-mechanical-systems (MEMS), several criteria for distinction macro- and micro-channels have been proposed. Shah [90] defined a compact heat exchanger as an exchanger with a surface area density ratio $> 700\ m^2/m^3$. This limit translates into a hydraulic diameter of < 6 mm. Mehendale et al. [91] defined various small and mini heat exchangers in terms of hydraulic diameter D_h, as:

- Micro heat exchanger: $D_h = 1 – 100$ μm.
- *Meso* heat exchanger: $D_h = 100$ μm – 1 mm.
- Compact heat exchanger: $D_h = 1 – 6$ mm.
- Conventional heat exchanger: $D_h > 6$ mm.

Based on engineering practice and application areas such as refrigeration industry in the small tonnage units, compact evaporators employed in automotive, aerospace, air separation and cryogenic industries, the application in the field of microelectronics and micro-electro-mechanical-systems (MEMS), Kandlikar [6] defined different channels according to the following ranges of hydraulic diameters D_h, as.

- Conventional channels: $D_h > 3$ mm.
- Minichannels: $D_h = 200$ μm – 3 mm.
- Microchannels: $D_h = 10$ μm – 200 μm.

2.2. Criteria for classification of macro- and micro-channels according to dimensionless numbers

Several dimensionless numbers are used to represent the feature of gas liquid two phase flow in micro-channels by various researchers. According to these dimensionless numbers, the distinction between macro- and micro-channels may be classified.

Triplett et al. [92] defined flow channels with hydraulic diameters D_h of the order, or smaller than, the Laplace constant L as micro-channels:

$$L = \frac{\sigma}{g(\rho_l - \rho_g)} \tag{1}$$

where σ is surface tension, g is gravitational acceleration, and ρ_l and ρ_g are respectively liquid and gas/vapor densities. Flow channels less than L are applied in compact heat exchangers, microelectronic cooling systems, research nuclear reactors, chemical processing, and small-sized refrigeration systems.

Examination of studies of capillary flow and flooding in vertical upflow and of heat transfer in confined spaces under a variety of conditions suggests that the effects of confinement will be significant for channels having hydraulic diameters such that the confinement number, Kew and Cornwell [93] proposed the Confinement number *Co* for the distinction

of macro- and micro-channels, which is actually based on the Laplace number Eq. (1) as follows:

$$Co = \frac{1}{D_h}\sqrt{\frac{\sigma}{g(\rho_l - \rho_g)}} \tag{2}$$

When the confinement number Co is<0.5, the channel is considered as microscale channel.

Li and Wang [94] defined a threshold diameter as $D_{th} = 1.75L_{cap}$ and their critical diameter as $D_{crit} = 0.224L_{cap}$ according to experimental study of the channel size effects on two-phase flow regimes for in-tube condensation in microchannels. The capillary length L_{ca} is the same as the Laplace constant L in Eq. (1). Their observations based on the flow patterns with respect to the internal tube diameter D resulted in the following classification criteria:

- $D < D_{crit}$: Gravity forces are insignificant compared to surface tension forces. The flow regimes are symmetrical (equivalent to $Co > 4.46$).
- $D_{crit} < D < D_{th}$: Gravity and surface tension forces are equally dominant. A slight stratification of the flow distribution is observed (equivalent to $0.57 < Co < 4.46$).
- $D_{th} < D$: Gravity forces are dominant and the flow regimes are similar to macroscale flows (equivalent to $Co < 0.57$).

Considering for the dominance of surface tension in microchannels, Brauner and Moalem-Maron [95] derived the Eotvös number *Eö* criterion for micro-channels as

$$E\ddot{o} = \frac{(2\pi)^2\sigma}{(\rho_l - \rho_g)D_h^2 g} > 1 \tag{3}$$

Cheng and Mewes [33] compared some of the available classification criteria for micro-channels to identify their difference. Fig. 3 shows the comparable results using channel diameter versus reduced pressure for water and CO_2. It shows clearly the big difference among these classification criteria for microchannels. The fluid types have also a significant effect on the classification criteria for microchannels. No general agreed microchannel classification criteria are available so far.

According to the experimental observation and heat transfer behaviour, Harirchian and Garimella [96] have proposed the following macro to micro-scale criterion using dimensionless numbers based on their experimental flow patterns:

$$Bd^{0.5} \times Re = \frac{1}{\mu_l}\left(\frac{g(\rho_l - \rho_g)}{\sigma}\right)^{0.5} GD^2 = 160 \tag{4}$$

$$Bd = \left(\frac{g(\rho_l - \rho_g)}{\sigma}\right)^{0.5} \tag{5}$$

$$Re = \frac{GD}{\mu} \tag{6}$$

$$D = \sqrt{A_{cs}} \tag{7}$$

where *Bd* is the Bond number, *Re* is the Reynolds number, *G* is mass velocity and *D* is length scale, A_{cs} is cross-sectional area of microscale channels. This distinction criterion is based on the convective confinement number which is the product of the Bond number and the Reynolds number with the assumption that the total gas liquid two-phase mixture flows as liquid. Fig. 4 shows the macro- and micro-channel transition from confined flow to unconfined flow. However, their criterion is only based on their own experimental data obtained at limited test conditions, channel size and shape. Evaluation with extensive experimental flow pattern data is needed. In fact, their experiments were conducted in multi micro-channels. As such, all flows should be actually confined in the microchannels. Therefore, it essential to clarify what unconfined flow means in their study. However, such definition is not presented and explained in their study.

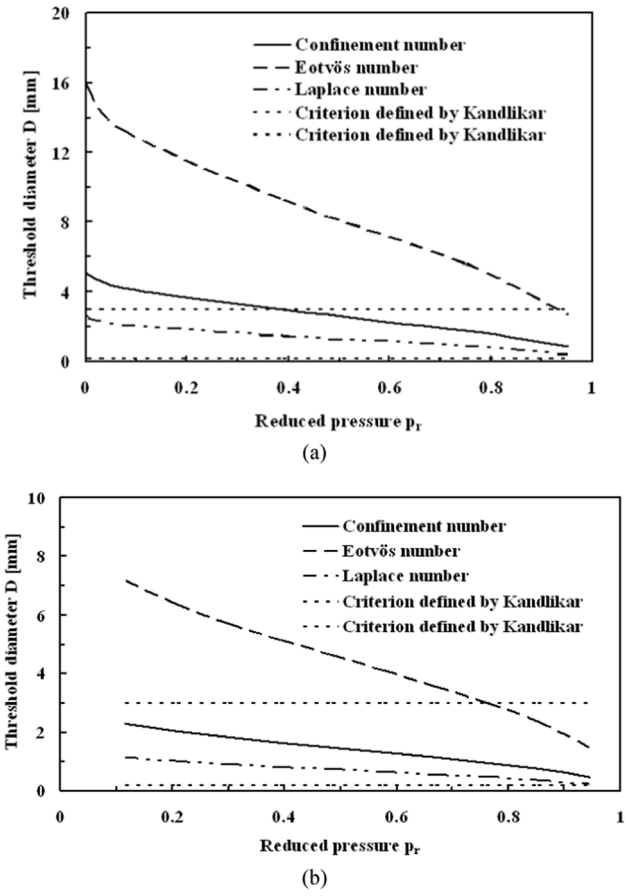

Fig. 3. Comparison of various definitions of threshold diameters for microscale channels: (a) Water, (b) CO_2, by Cheng and Mewes [33].

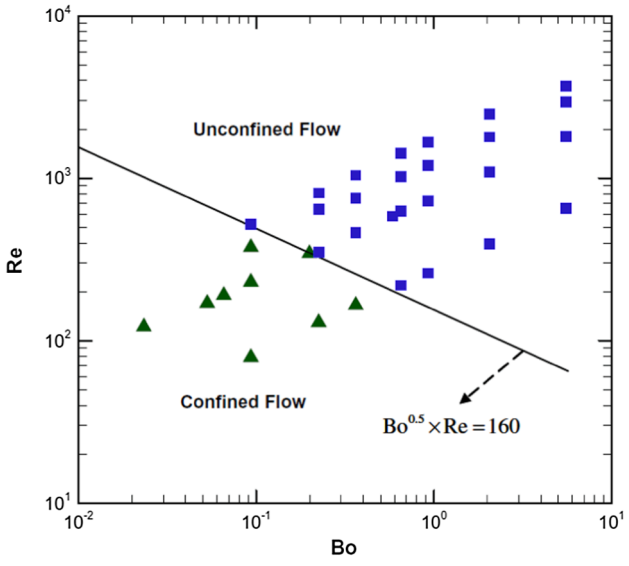

Fig. 4. Transition from confined flow to unconfined flow using flow behaviours defined by Harirchian and Garimella [96].

Ong and Thome [97] have proposed a new macro-to-micro-channel criterion using the confinement number *Co* defined by Eq. (2) according to their observed flow patterns and measured liquid films for different flow patterns. For the confinement numbers>1, they observed symmetric liquid film distribution along the channel wall. For the

confinement numbers lower than about 0.3, they observed non-symmetric liquid film distribution along the channel wall. They observed isolated bubbles and bubble coalescence and the flow boiling is microscale behaviour for the confinement number>1. For the confinement number is<0.3, they observed the plug-slug flow pattern and flow boiling exhibits macroscale channel behaviours. For confinement numbers between 1.0 and values within the range of 0.3 to 0.4, they observed the mesoscale channel behaviour according to their test conditions and test channels.

Although several such criteria based on the confinement number have been proposed by various researchers, the confinement numbers have quite different values according to their individual experimental flow patterns and flow boiling behaviour. It should be pointed out that each individual research was conducted for specific test fluids, different microchannels and experimental parameter ranges. No generalised classification criteria are available so far. Agreed classification criteria should be further investigated according to well established experimental database including a wide range of fluids, channel sizes, channel shapes and working conditions.

It should be pointed out that the transition from macro-to-micro- gas liquid two phase flow is a continuous and progress process which corresponds to the bubble growth, flow pattern evolution, heat transfer behaviours and mechanisms [1,2]. Therefore, for diabatic two phase flow such as flow boiling and flow condensation, the most important point is to relate flow patterns to flow boiling heat transfer behaviours such as heat transfer, CHF and fluid behaviour such as pressure drops [3–11]. In particular, relating flow patterns to the corresponding gas liquid two phase heat transfer and two phase flow behaviours is a practical and effective method to develop mechanistic prediction methods for both macro- and microchannels due to the continuously progressive flow pattern transitions alongside with the corresponding two phase flow and heat transfer behaviours and mechanisms from macro-channels to micro-channels [1,2]. One good example is the flow pattern based CO_2 flow boiling heat transfer and two phase pressure drop models developed by Cheng et al. [98–100] for both macro- and micro-channels. The generalized flow pattern based heat transfer model favourably predicts a large amount of independent experimental data in macro- and micro-channels. In particular, their CO_2 flow pattern map based on the heat transfer behaviours and mechanisms favourably captures the independent flow pattern observations in microscale channels. It means that the macro- and micro-channels could be classified according to the flow boiling heat transfer behaviour due to the intrinsic links between the heat transfer mechanisms and the corresponding flow patterns in macro- and micro-channels. In fact, mechanistic classification criteria may be more of practice and effectiveness in developing two phase heat transfer prediction models based on flow patterns. Such classification criteria should be systematically investigated in future.

Due to the lack of agreed classification criteria for distinction of macro- and micro-channels. In this review, the threshold diameter of 3 mm is adopted for classifying the macro- and micro-channels. This is in line with the criteria recommended by Kandliar [6] and also meets the engineering applications.

3. Techniques for flow visualization and sensing, flow patterns and flow pattern maps in microchannels

Numerous studies on flow patterns and flow pattern maps have been extensively investigated for macro-channels since 1950 s [1]. The available studies cover observed flow regimes in horizontal and vertical pipes, different types of flow pattern maps, experimental techniques for direct and indirect determination of flow patterns and flow pattern transition criteria based on correlations and theoretical derivations, and also the effects of wall roughness, heat flux and flow accelerations on flow regime transitions [5,9,11]. Generally, they have provided an introduction to the fundamental knowledge for conventional size channels with various orientations, such as horizontal, vertical and inclined channels. Flow patterns and flow patterns maps in macro-channels are the basis for further investigating flow patterns and flow pattern maps in microchannels. However, advanced measurement techniques are specially needed for identifications of two phase flow patterns, flow pattern transitions and bubble growth in microchannels.

3.1. Fundamentals of gas liquid two phase flow patterns and flow pattern maps

Flow patterns macro-channels are usually divided into groups consisting of bubbly, stratified, stratified-wavy, annular, and mist flow [1]. Flow patterns and their transitions are strongly affected by the physical properties of test fluids and conditions such as mass flux, operation pressure, channel geometry and size, the aspect ratio of rectangular channels, wall wettability, gas and liquid input into the microchannels etc. There is a complicated two-way coupling between the flow in each of the phases or components and the geometry of the flow (as well as the rates of change of that geometry). For diabatic condition such as flow boiling and condensation, understanding the bubble dynamics such as bubble generation, growth and coalesces is extremely important.

In general, a phenomenological description of flow patterns is presented in common gas–liquid two phase flows, flow boiling and flow condensation with various flow visualization techniques. The observed results are often presented in the form of a flow pattern map which can be used to identify the flow patterns occurring at various two phase flow and heat transfer conditions. Usually, gas liquid two flow parameters are used to define a coordinate system on which the boundaries between the different flow patterns are charted, such as the superficial gas and liquid velocities or mass velocity and vapor quality. Transition boundaries are then proposed to distinguish the location of the various flow regimes as in a flow pattern map. Although efforts have been made to develop generalized flow pattern maps, all the available flow pattern maps are only valid for a specific set of conditions and/or fluids. The accuracy in determining transition lines on a flow pattern map depends on the number of experiments carried out and coordinate systems adopted. There are many coordinate systems for flow pattern maps, which are divided into three groups [1,2]:

(1) Phase velocities or fluxes: gas and liquid superficial velocities J_g and J_l in (m/s), or gas and liquid superficial mass fluxes G_g and G_l in (kg/m^{2}s) and gas and liquid mass flow rates M_g and M_l in (kg/s) Use of these parameters, while undoubtedly being the most convenient, does not assure creation of a universal flow pattern map for different two-phase mixtures.
(2) Quantities referring to the two-phase flow homogeneous model are the transformations of the parameters from group (1) such as total velocity u_T, total mass flux G_T, Froude number based on total velocity Fr_T, void fraction ε, and quality $\times$, and they are only useful for the description of some flow pattern maps.
(3) Parameters including the physical properties of phases such as liquid and gas Reynolds numbers Re_l and Re_g, and others; this formulation gives the best possibility for attaining a universal flow pattern map.

The boundary between any two flow patterns in a flow pattern map occurs because a flow pattern becomes unstable. The boundary is approached and growth of this instability causes transition from one flow pattern to another. However, these gas–liquid two phase transitions can be rather unpredictable since they may depend on otherwise minor features of the flow, such as the roughness of the walls or the entrance conditions. Hence, the flow pattern boundaries are not distinctive lines but more poorly defined transition zones.

Many of the available flow pattern maps are for adiabatic flow conditions and do not include dryout regime which occurs in flow boiling. In the case of diabatic two-phase flows such as flow boiling,

important factors influencing these flows and their transitions are nucleate boiling, evaporation on what could otherwise be dry parts of the perimeter, and acceleration of the flows. For example, nucleate boiling in an annular film tends to increase the film thickness and change the void profile near the wall or vigorous nucleate boiling in an otherwise stratified flow can completely wet the upper perimeter, thus increasing liquid entrainment in the vapor core. It is desirable that diabatic flow pattern maps include the influences of heat flux, vapor quality and dryout, etc. on the flow pattern transition boundaries [98–107]. Just to give one example here, Cheng et al. [98] developed a flow pattern map for CO_2 evaporation inside horizontal tubes on the basis of the Wojtan et al. [104,105] flow pattern map. Cheng et al. [99,100] further modified the CO_2 flow pattern map for a wide range of parameters and developed an updated flow boiling heat transfer model based on their flow map. There is an essential arbitrariness in the interpretation of flow patterns and thus it is unlikely that perfect prediction methods will ever emerge.

There are other serious difficulties with most of the existing literature on flow pattern maps. One of the basic fluid mechanical problems is that these maps are often dimensional and therefore apply only to specific channel sizes and fluids employed in the relevant studies [1,2]. Effort has been made to find generalized coordinates that would allow the map to cover different fluids and different channel sizes. However, such generalizations can only have limited value because several transitions are represented in most flow pattern maps and the corresponding instabilities are governed by different sets of fluid properties. For example, one transition might occur at a critical Weber number, whereas another boundary may be characterized by a particular Reynolds number. Hence, there exist no universal, dimensionless flow pattern maps that incorporate the full, parametric dependence of the boundaries on the gas liquid two phase flow characteristics.

3.2. Techniques for flow visualization and sensing in micro-channels

Various flow pattern identification methods have been used in the experimental studies for macro-scale two phase flow, including direct visual observation and observation through high speed photography or camera, X-ray absorption, multi-beam gamma densitometry, signal processing of pressure fluctuations, void fraction fluctuations and light intensities, spectral distribution of wall pressure fluctuations, pressure gradient variations, neutron radiography, electrical conductance probes, etc. [1,2,108–110]. Most of these methods developed for gas liquid two phase flow in macro-channels are not applicable to gas liquid two phase flow in microchannels. The difficulty of identifying gas liquid two phase flow patterns and their transitions in microchannels comes from the difficulties in obtaining good quality high speed images, adopting proper measurement techniques, interpreting the flow patterns (subjectivity and pattern definition by various researchers) and also in conducting experiments of different fluids in various channel sizes and shapes, the aspect ratio of rectangular channels, wall wettability, gas and liquid input into the microchannels under different test parameters. In particular, advanced techniques for flow visualisation and specially purpose designed measurement methods should be adopted for micro-scale gas liquid two phase flow.

Over the past decades, many advanced measurement techniques have been developed and applied to micro-scale multiphase flow and gas liquid two phase flow in microchannels [111–130]. Table 1 summarizes different experimental techniques for characterizing microscale multiphase flow as well as the spatial and temporal measurement resolutions [111]. The dynamic nature of multiphase microfluidic systems imposes unique requirements on the time resolution of the flow characterization techniques. Intrusive measurement probes are generally not an option for micro- and nanofluidic systems. Microscopy is the most often used imaging technique for gas liquid two phase flow pattern identifications in microchannels. Digital cameras which acquire several thousand frames per second are often used to record fast transient gas liquid two phase flow patterns in microchannels. For camera shutter times below 10 μs, image quality can generally be improved if the continuous light source of a microscope (typical power: 100 W) is replaced by a stroboscopic source. However, microscopy often implies an expensive means to observe gas liquid two phase flow patterns in microchannels. There is an interest in the availability of scalable and non-intrusive sensors integrated in gas liquid two phase flow systems to observe flow patterns in microchannels. Combined IR-absorption with a capacitance sensor is often used to analyse multiphase flows in microchannels and total internal reflection (TIR) of laser light at a fluid interface is used to characterize flow patterns in microchannels. The latter measurement system may be then integrated in a multilayer, multichannel device to demonstrate its scalability and application in situations where direct optical access to the flow channel is not available.

Tomographic techniques are powerful but expensive tools to obtain gas liquid two phase flow patterns in microchannels, particularly where direct optical access is not available, in multilayer stacked microreactors or inside micro-structured reaction channels [115,116]. Nuclear Magnetic Resonance Imaging (MIR) is used for characterizing single and multiphase flows inside parallel flow channels of monolith reactors [113,114]. The single excitation multiple image rapid acquisition with relaxation enhancement (SEMI-RARE) technique provides a temporal resolution. Very high spatial resolution phase distribution measurements in single microchannels can be achieved with X-ray tomographic microscopy (XTM) using synchrotron radiation. Synchrotron XTM is has been applied to multiphase flow patterns in porous materials.

Optical measurement technique is an effective and unexpensive method to characterize gas liquid two phase flow in microchannels [120,121,124–126]. The most important parameters controlling two-phase flow in microchannels are bubble frequencies, lengths and velocities, coalescence of bubbles and flow pattern transitions. These can be measured and/or detected by an optical measurement technique developed specifically for this purpose. Revellin et al. [120] used an optical method to count bubbles and determine the two-phase flow characteristics. Fig. 5 shows their experimental setup consisting of two laser beams with a power<1 mW. The beams are directed through a

Table 1
Experimental techniques available to study multiphase flow in microsystems with their spatial and temporal resolution [111].

Technique	Spatial dimension	Spatial resolution	Temporal resolution/ms
Brightfield microscopy [112]	2D	~1 μm	0.2–33 ms, 18 ns (stroboscopic white light source)
Fluorescence microscopy	2D	~1 μm	33 ms, 7 ns (pulsed Nd:YAG/YLF laser)
Confocal microscopy	2D/3D (SC)[a]	~1 μm	~500 ms (2D), ~1 min (3D) ~70 ms (2D), 0.1–1 min (3D)
	2D/3D (SD)[a]	~1 μm	
Transient magnetic resonance imaging (MRI) [113]	2D/3D	800 μm	150 ms
X-ray tomography microscopy (XTM) [114–115]	2D/3D	1.1–4 μm	30–90 min (3D)
	2D/3D	<100 nm	
Total internal reflectance sensor [117–118]	1D	~200 μm	0.1–1 ms
Infrared and conductivity sensor [119]	1D	Distance between probes 10 mm	0.1 ms

a SC = scanning confocal microscope, SD = spinning disk confocal microscope.

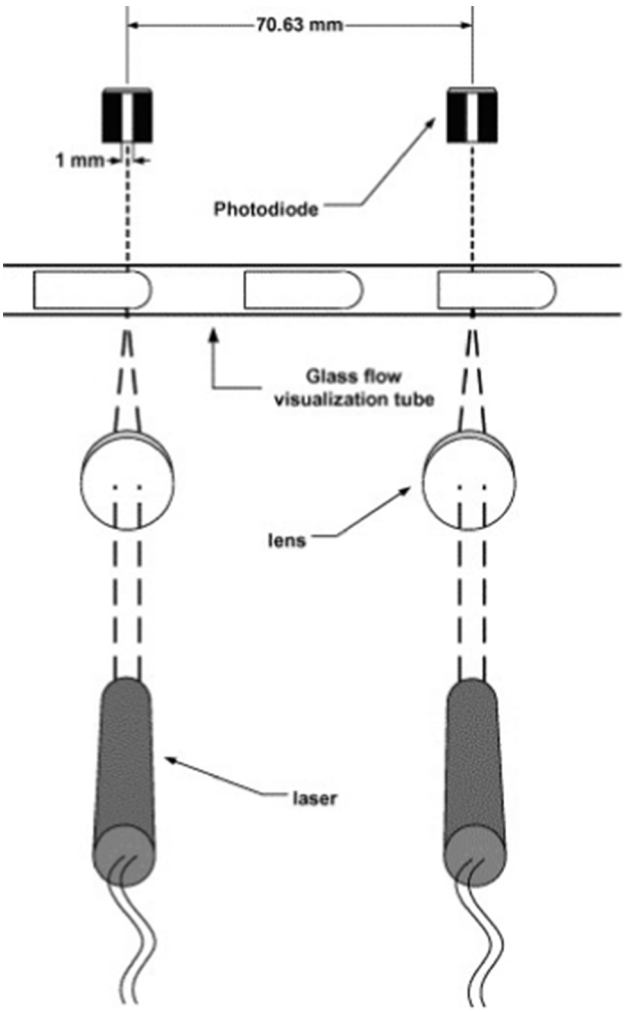

Fig. 5. Schematic diagram of the laser instrumentation [120].

glass visualization tube and the fluid inside at two different locations are separated by a distance of $\Delta L_{Laser} = 70.63$ mm. Two lenses focus the laser beams to the middle of the microtube. Two photodiodes are placed on the opposite side of the microtube and their faces are painted over but leaving only a vertical 1 mm wide opening in the middle to isolate the signal. The resulting voltage signals from the two diodes are measured. The laser beams interact locally with the structure of the flow and by signal processing and thus determine the velocity, length and frequency of vapor bubbles. Fig. 6 shows the observed flow patterns taken with a high definition video camera and Fig. 7 shows the corresponding signals. The signals from the diodes obtained by this technique for the different flow patterns are similar to those obtained by Lowe and Rezkallah [122] using a void fraction probe for a microgravity air/water two-phase flow patterns in a macro-channel. Seven flow patterns including bubbly flow, bubbly/slug flow, slug flow, slug/semi-annular flow, semi-annular flow, wavy annular flow and smooth annular flow are identified in the micro-channels. Kuznetsov et al. [126] used a high-speed video and a dual-laser flow scanning to identify the flow patterns of nitrogen–water two phase flow in vertical and horizontal microchannels with cross section of 1500 μm × 720 μm. Their observed flow patterns in the microchannel are elongated bubble flow, churn flow, and annular flow. Fig. 8 shows their measured optical signal for the elongated bubbles which combines the bubbly-slug flow and slug flow. The slug flow is defined as elongated bubbles flow when the length of the gas slug exceeds the liquid plug length. This flow is characterized by periodicity and by the lack of small bubbles in the flow.

One of the main methods for visualizing flow irregularities in

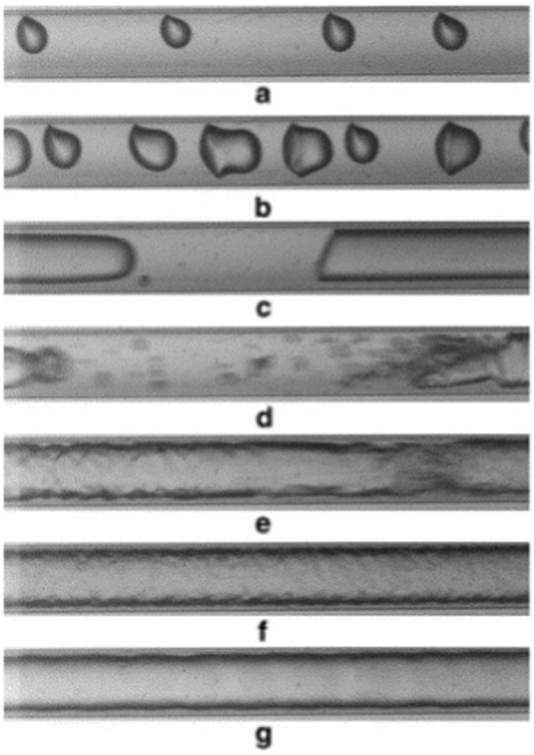

Fig. 6. Flow patterns and transitions for D = 0.5 mm, L = 70.7 mm, G = 500 kg/(m^{2}s), T_{sat} = 30 °C and ΔT_{sub} = 3 °C at entrance to heater: (a) bubbly flow at × = 2 % and f_A = 131 Hz; (b) bubbly/slug flow at × = 4 % and f_A = 520 Hz; (c) slug flow at × = 11 % and f_A = 136 Hz; (d) slug/semi-annular flow at × = 19 % and f_A = 33 Hz; (e) semi-annular flow at × = 40 % and f_A = 0 Hz; (f) wavy annular flow at × = 82 % and f_A = 0 Hz; (g) smooth annular flow at × = 82 % and f_A = 0 Hz [120].

microchannels is the schlieren method. A combination of the schlieren-system and interferometry principles is generally used. Ronshin and Chinnov [124] have developed a new technique to measure the local void fraction, size of characteristic regions of the liquid films on the upper and lower walls of a microchannel, frequency of bubble formation, and other quantitative characteristics. The two-phase flow patterns in a microchannel of 50 μm height and 10 mm width were identified. Interaction between the gas and liquid flows was recorded with digital video- and photo-cameras. The schlieren method was used to register and visualize deformations on the surface of a thin liquid film. Based on the experimental observations, criteria identifying the two phase flow pattern transitions and a flow pattern map have been proposed. As shown in Fig. 9, the void fractions and characteristic regions of the films are calculated as: Image (1) obtained by modification of the schlieren method are cleared of glares and other noise by using special filters and by subtracting background (2) from the original image. The background is either recorded by the camera during the experiment or calculated by finding the average frame. The result is a cleaned image (3). Further, by choosing a colour shade, the studied quantity (4): void fraction or characteristic region of the film on the upper wall of the channel, is determined. Then, the image gradients (5) are analyzed, and the characteristic value of investigated time is calculated, as well as the average value. As shown in Fig. 10, the frequency of bubble formation is calculated in a similar way as: Image (1) obtained by modification of the schlieren method are cleared of glares and other noise by using special filters and by subtracting background (2) from the original image. The result is a cleaned image (3). Next, a colour shade corresponding to the bubbles (4) is chosen. Then, the image gradients are analyzed and using a special algorithm, the image is divided into areas, where each area corresponds to a bubble. In the example, four areas are marked out: a, b,

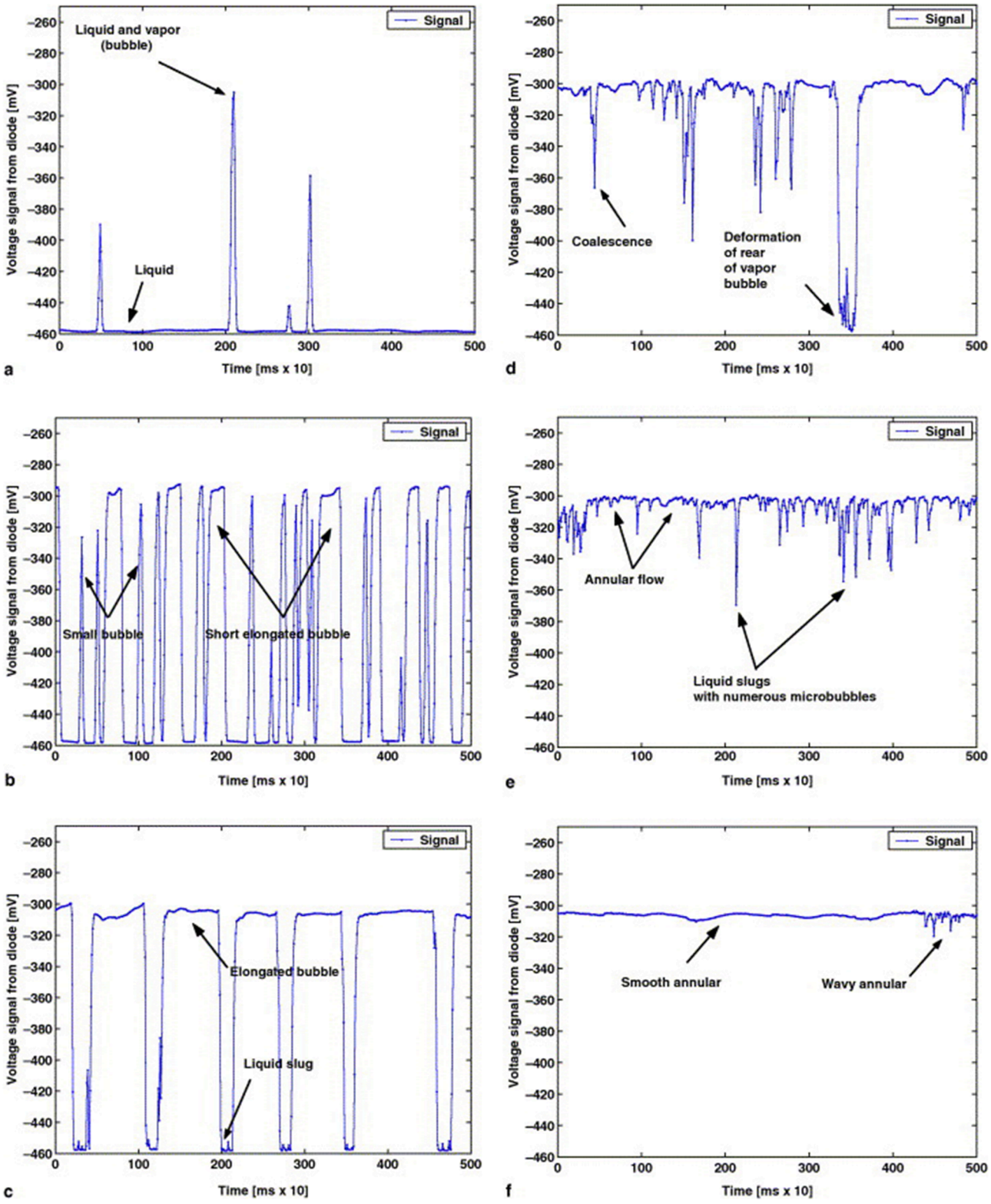

Fig. 7. Flow pattern laser signals for D = 0.5 mm, L = 70.7 mm, G = 500 kg/(m^2s), T_{sat} = 30 °C and ΔT_{sub} = 3 °C: (a) bubbly flow signal at × = 2 % and f_A = 131 Hz; (b) bubbly/slug flow signal for at × = 4 % and f_A = 520 Hz; (c) slug flow signal at × = 11 % and f_A = 136 Hz; (d) slug/semi-annular flow signal at × = 19 % and f_A = 33 Hz; (e) semi-annular flow signal at × = 40 % and f_A = 0 Hz; (f) annular flow signal at × = 82 % and f_A = 0 Hz. [120].

c, and d. The number of such areas corresponds to the number of bubbles. To measure the size of a bubble, an algorithm similar to the algorithm for measuring void fraction is used, only in this case, the size of the region corresponding to the gas bubble in the binary image is measured. Chinnov et al. [125] experimentally investigated gas liquid two-phase flow in short horizontal rectangular microchannels with a height of 100–500 μm and a width of 9–40 mm. They used the schlieren method and fluorescent methods to reveal the flow of liquid in the channel and to determine its characteristics quantitatively and study the features of the churn, jet and drop flow patterns. The two-phase flow patterns and

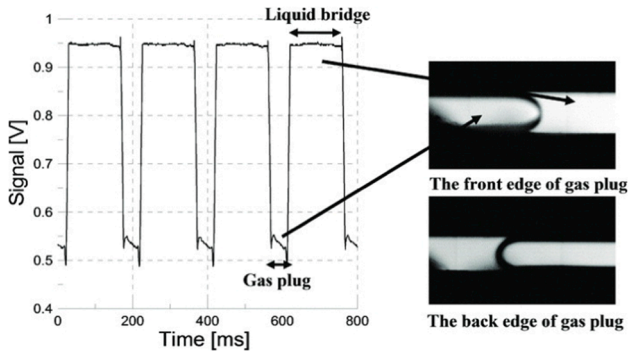

Fig. 8. Optical signal from the photodiode and flow visualization of slug flow at $j_{liq} = 0.17$ m/s, $j_{gas} = 0$ 0.16 m/s [126].

flow pattern transitions are determined. The schlieren method is used to register deformation and visualize the liquid film surface, the video camera is used to record the intensity of light reflected from the surface separating gas and liquid depending on the angle of this surface inclination from the axis of reference radiation. The laser induced fluorescence method, which is based on the detection of light reradiated by phosphor with a spectrum different from that of the exciting laser radiation, is used to analyze the interaction of gas and liquid phases in the microchannels. Their observed flow patterns are churn flow, stratified flow, annular flow, bubbly flow, pulsating jet flow and stationary jet flow. In particular, the jet flow patterns occur at low superficial gas and liquid velocities when the gas flow occupies no more than a half of the micro-channel cross-section. The upper wall of the channel is not wetted for the jet flow patterns. With increasing superficial liquid velocity, liquid moving along the channel sides, occupies a larger volume, and the dry area decreases. At sufficiently high superficial velocities of liquid ($j_l > 0.05$ m/s), the liquid film is formed on the upper channel wall due to liquid floats from its sides as shown in Fig. 11, the pulsating jet flow pattern occurs. Liquid moving along the side walls of the channel occupies the main part of the channel and gas occupies the channel center for the jet flow pattern. At a certain moment, liquid is discharged from the sides and forms a film on the upper wall of the channel. Then, the film moves along the channel, entrained by gas. In a certain time, this process is repeated and a pulsating jet flow pattern occurs.

One of the most interesting modern methods of flow analysis in micro-dimensional systems is the modification of the Particle Image

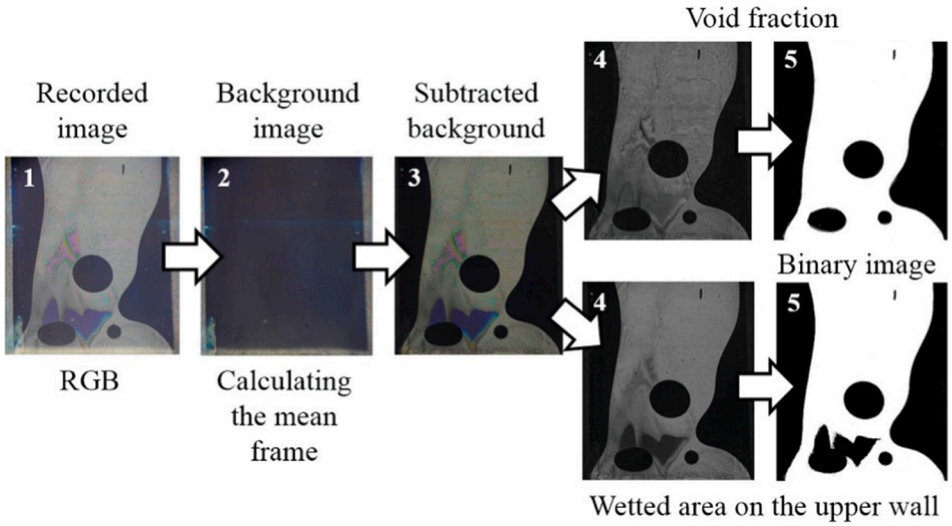

Fig. 9. Calculation of the local void fraction and characteristic region of the liquid film on the upper wall of microchannel [124].

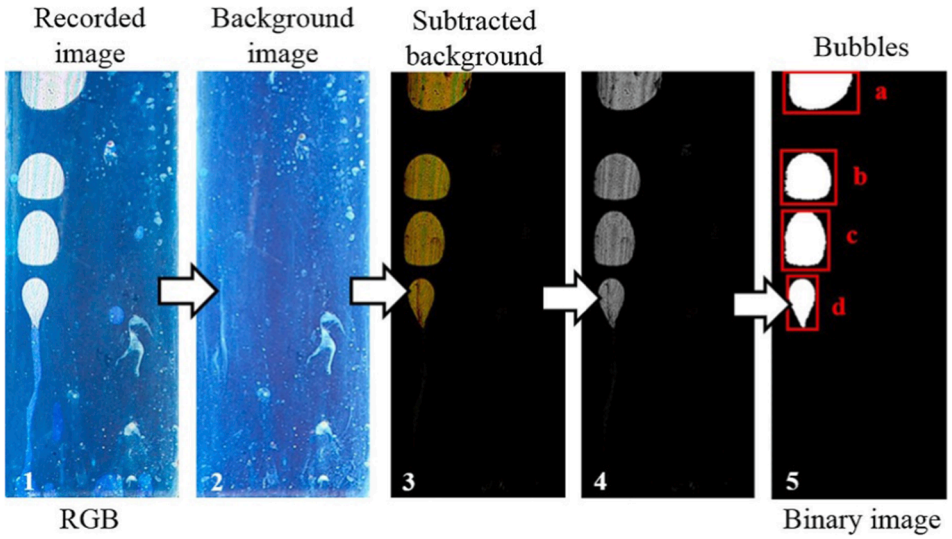

Fig. 10. Calculation of the number of bubbles in the microchannel [124].

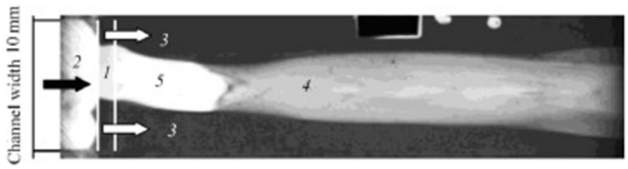

Fig. 11. The schlieren photograph of the jet flow in the channel of 0.3 × 10 mm^2 at $j_g = 3.3$ m/s, $j_l = 0.092$ m/s, top view: (1) slot in the lower channel wall for liquid inflow to the channel; (2) gas inlet to the channel; (3) liquid; (4) liquid film on the upper channel wall; (5) unwetted zone on the upper channel wall. Black arrow – direction of gas motion, white arrows – direction of liquid motion [125].

Velocimetry (PIV) method: micro-PIV [131–135]. The main feature of micro-PTV is that the algorithm can track the individual particles for velocity calculations in contrast to the frequently used PIV, based on correlations between intensity values of interrogation regions. Therefore, micro-PTV can better distinguish the higher flow gradients than PIV. Despite the enormous prospects of micro-PIV methods, it is quite difficult to apply micro-PIV methods to study gas–liquid two phase flow in a microchannel because the thickness of the liquid layer can be below 1 μm while micro-PIV has been extensively used for single-phase flow visualization in microchannels. Xia et al. [131] investigated the laminar flow behavior of water in circular micro pin–fin (C-MPF), square micro pin–fin (S-MPF) and diamond micro pin–fin (D-MPF) heat sinks using micro-PIV flow visualization technology. They compared the numerical simulation results of the fluid flow characteristics in these heat sinks with CFD to the experimental results of fluid flow behaviors measured with the micro-PIV flow visualization. It shows that the experimental results favorably agree with the numerical results.

4. Experimental studies of two phase flow patterns and flow pattern maps in microchannels

Over the past decades, both adiabatic and diabatic flow patterns and flow pattern maps in mini-channels and microchannels have been extensively studied by numerous research groups [136–198]. Both single microchannels and multi-microchannels with various channel shapes and sizes have been used in the available studies of gas liquid two phase flow patterns and flow pattern maps. In this section, experimental studies of adiabatic and diabatic gas liquid two phase flow patterns and flow pattern maps are reviewed respectively.

4.1. Adiabatic two phase flow patterns and flow pattern maps in microchannels

Triplett et al. [92] investigated the flow patterns of air–water in circular microchannels with inner diameters of 1.1 and 1.45 mm and semi-triangular channels with hydraulic diameters of 1.09 and 1.49 mm. The observed flow patterns are bubbly, churn, slug, slug-annular and annular flows. The flow patterns are compared the criteria of Suo and Griffith [140]. The criteria of Suo and Griffith significantly disagreed with their data. Chung and Kawaji [138] studied the effect of channel diameter on two-phase flow in circular channels of with diameters of 530, 250, 100, and 50 μm. In the 530 and 250 μm channels, the two-phase flow characteristics are similar to those typically observed in minichannels of up to 1 mm diameter. In the 100 and 50 μm channels, the two-phase flow behaviour departs from that observevtions in mini-channels - the occurrence of slug flow dominated. Fig. 12 shows the observed two-phase flow patterns in a 250 μm microchannel for flow condition (j_l = 4.25 m/s and j_g = 5.71 m/s). Kawaji and Chung [139] have illustrated the representatives of flow patterns in minichannels and microchannels according to the definitions of Kandlikar [6] as shown in Fig. 13.

Chen et al. [148] experimentally investigated the effect of tube

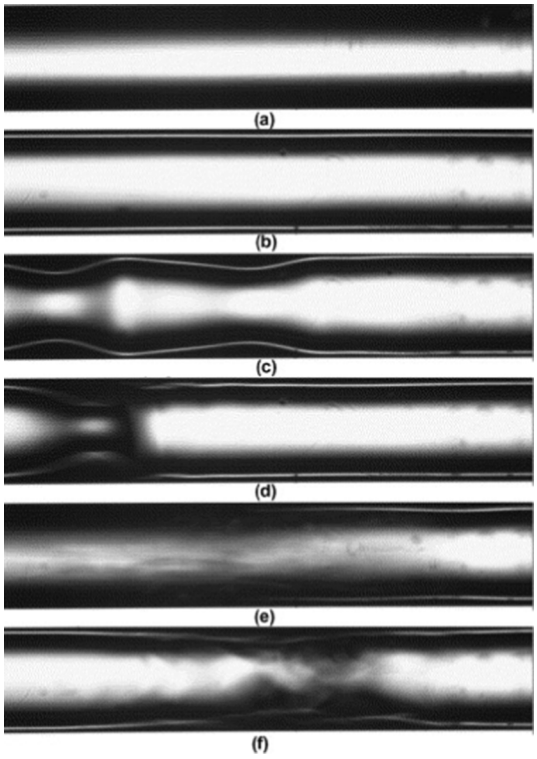

Fig. 12. Two-phase flow patterns in a 250 μm microchannel for the same flow condition (j_L = 4.25 m/s and j_G = 5.71 m/s): (a) single-phase liquid; (b) gas core with a thin-smooth liquid film; (c) gas core with a wavy liquid film; (d) gas core with a wavy liquid film; (e) streaked pattern; (f) serpentine-like gas core [138].

diameters on flow patterns observed in a glass tube (at adiabatic condition) connected to flow boiling with R134a in vertical circular tubes with four different diameters of 1.10, 2.01, 2.88 and 4.26 mm. Their observed flow patterns include dispersed bubble, bubbly, confined bubble, slug, churn, annular and mist flow. The flow patterns in the 2.88 and 4.26 mm tubes are similar to those typically described in macro-channels while the smaller tubes with diameters 1.10 and 2.01 mm illustrate strong effects of the channel confinements on the flow patterns and the transitions from slug flow to churn flow and from churn flow to annular flow move to higher vapor velocities. The transition from the dispersed bubble to bubbly flow moves to higher liquid velocities when the tube diameter decreases from 4.26 to 1.1 mm. Zhao and Bi [142] investigated upward air–water two-phase flow patterns in vertical equilateral triangular channels with hydraulic diameters of 2.886, 1.443 and 0.866 mm. Their observed flow patterns include dispersed bubbly flow, slug flow, churn flow and annular flow in the channels with larger hydraulic diameters 2 and 1.443 mm. They are similar to flow patterns in vertical macro-channels. For the channel with a hydraulic diameter 0.866 mm, dispersed bubbly flow pattern which is characterized by randomly dispersed bubbles in continuous liquid phase was not found in their study. In particular, they observed a so-called capillary bubbly flow pattern which is characterized by a single train of bubbles, essentially ellipsoidal in shape and spanning almost the entire cross-section of the channel, existed at low gas flow rates. In the slug flow pattern, slug-bubbles are substantially elongated. Liu and Wang [146] investigated flow patterns of upward air–water flow in circular channels with diameters of 1.47, 2.37, and 3.04 mm. Their observed flow patterns include bubbly, slug, Taylor, bubble-train slug, churn, and annular flows. They found that the effects of capillary diameter on the flow patterns were not remarkable. Their flow patterns agreed with the flow patterns of Triplett et al. [92] while they did not agree well with the observed flow patterns of Zhao and Bi [142] in triangular channels.

Sur and Liu [147] investigated the effects of channel size on the flow

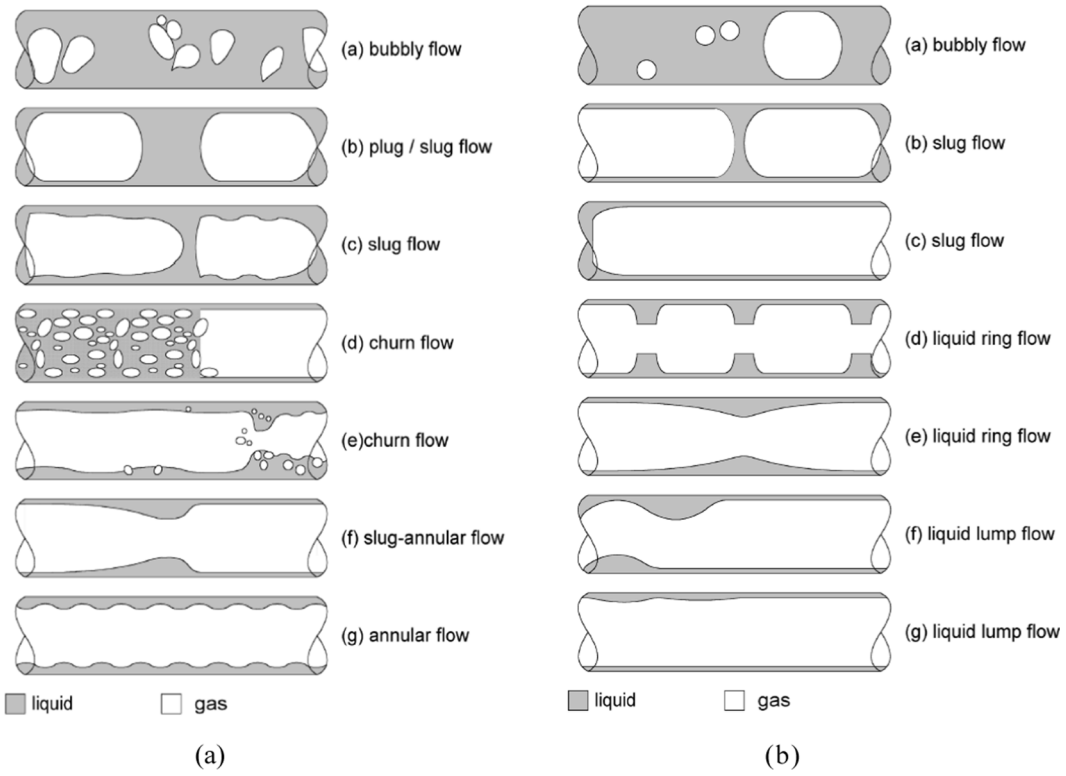

Fig. 13. (a) Two-phase flow patterns in a horizontal minichannel; (b) Two-phase flow patterns in a horizontal microchannel [139].

patterns of air–water flow in circular microchannels with diameters of 100, 180 and 324 μm. Fig. 14 shows their observed flow patterns: bubbly flow, slug flow, ring flow and annular flow. With decreasing the channel size, the flow pattern transitions in the flow pattern map in Fig. 15 shift mainly as the result of the force competition between the inertia and surface tension. Furthermore, they have proposed a new flow pattern map which use the modified liquid and gas phase Weber numbers as the coordinates to unify the transitions for the flow patterns in micro-channels with different channel diameters. Fig. 16 shows their flow map based on their experimental data and Weber numbers. The channel diameters in their study are much smaller than the studies by Chen et al. [148], Liu and Wang [146] and Zhao and Bi [142]. As the channel dimension decreases, the flow pattern transition boundary lines shift mainly as the result of the force competition between the inertia and surface tension.

Quite different flow patterns have been observed in microchannels in the available studies. For instance, Serizawa et al. [150] investigated flow patterns of air–water flow in circular tubes with inner diameters of 20, 25 and 100 μm and for steam-water flow in a 50 μm inner diameter circular tube. As show in Fig. 17, their observed dispersed bubbly flow, gas slug flow, liquid ring flow, liquid lump flow, annular flow, frothy or wispy annular flow, rivulet flow and liquid droplets flow. The two-phase flow patterns are sensitive to the surface conditions of the inner wall of the test tubes. A stable annular flow and gas slug formation with partially stable thin liquid film formed between the tube wall and gas slugs appeared at high velocities under carefully treated clean surface conditions. At lower velocities, dry and wet areas exist between gas slug and the tube wall. Compared to the flow patterns of Sur and Liu shown in

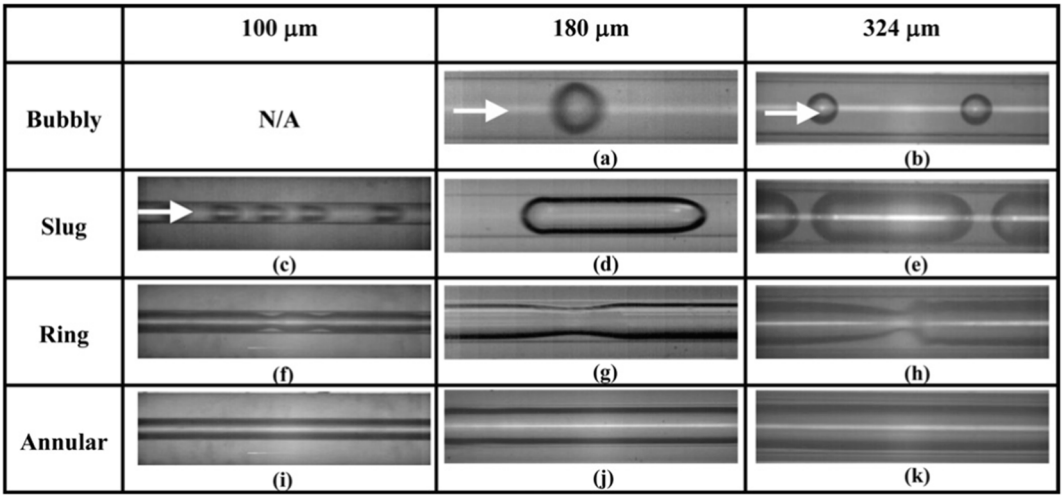

Fig. 14. Photographs of two-phase flow patterns of air–water flow in horizontal circular microchannels of Sur and Liu [147].

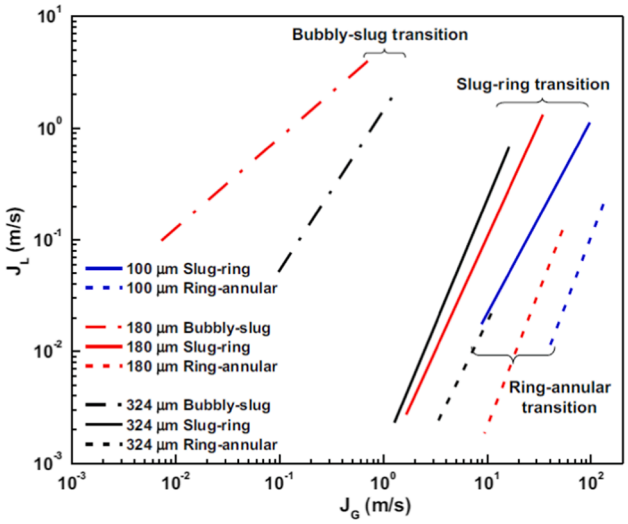

Fig. 15. Effects of channel size on the flow regime transition lines by Sur and Liu [147].

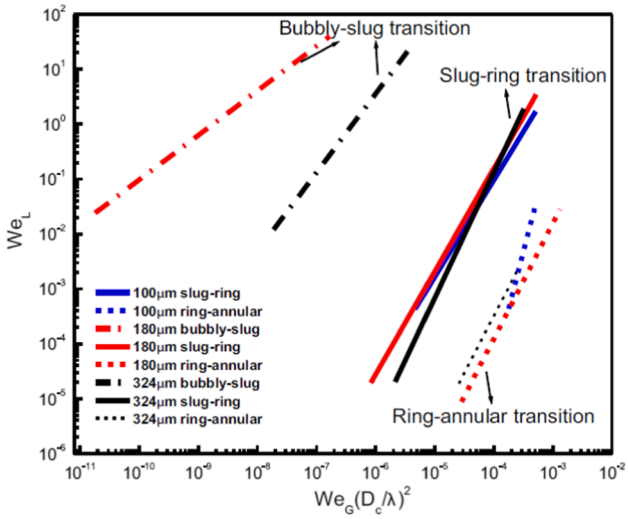

Fig. 16. Two-phase flow map reconstructed with the proposed dimensionless parameters as the coordinates by Sur and Liu [147].

Fig. 14, some different flow patterns were observed.

Cubaud and Ho [153] studied air–water flows in 200 and 525 μm square microchannels made of glass and silicon and observed bubbly flow, wedge flow, slug flow, annular flow and dry flow as shown in Fig. 18. The newly defined wedge flow is proposed. Wedge flow exhibits some differences from the Taylor bubbly flow. For a partially wetting system, as a function of the bubble velocity, the perimeter of the bubbles can dry out at the center face of the channel creating triple lines (liquid–gas-solid) while liquid still flows in the corners.

An aspect ratio is an important parameter for two-phase flow in a rectangular microchannel. Choi et al. [154] studied the aspect ratio effect on the flow pattern, pressure drop and void fraction of adiabatic liquid water and nitrogen gas two-phase flow in rectangular microchannels. The aspect ratios of the rectangular microchannels are 0.92, 0.67, 0.47 and 0.16; and the hydraulic diameters of the rectangular microchannels are 490, 490, 322 and 143 μm, respectively. Fig. 19 (a) shows their observed flow patterns: (a) Bubbly flow; (b) Slug bubble flow; (c) Elongated bubble flow; (d) Liquid ring flow; (e) Multiple flow. Bubbles in a rectangular microchannel have non-uniform thickness of the liquid film due to the corner effect. Fig. 19 (b) shows the effect of

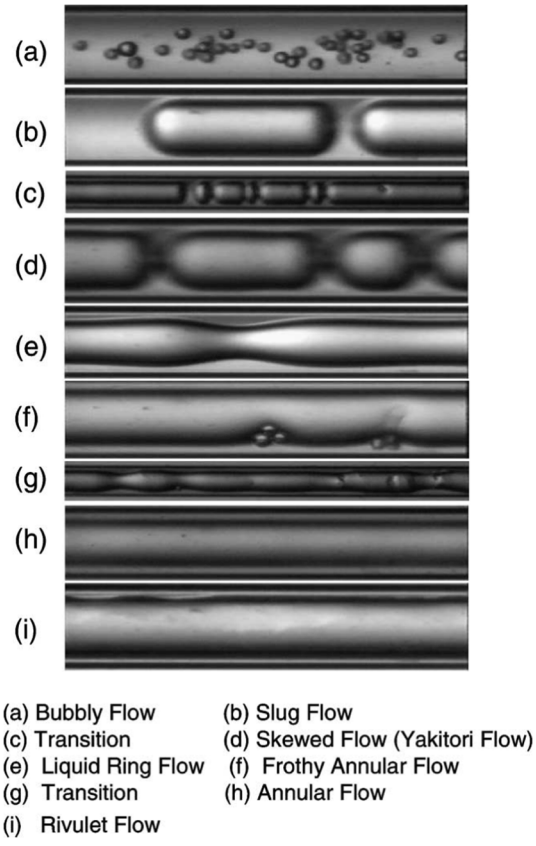

Fig. 17. Air-water two-phase flow patterns in a 100 μm I.D. tube by Serizawa et al. [150].

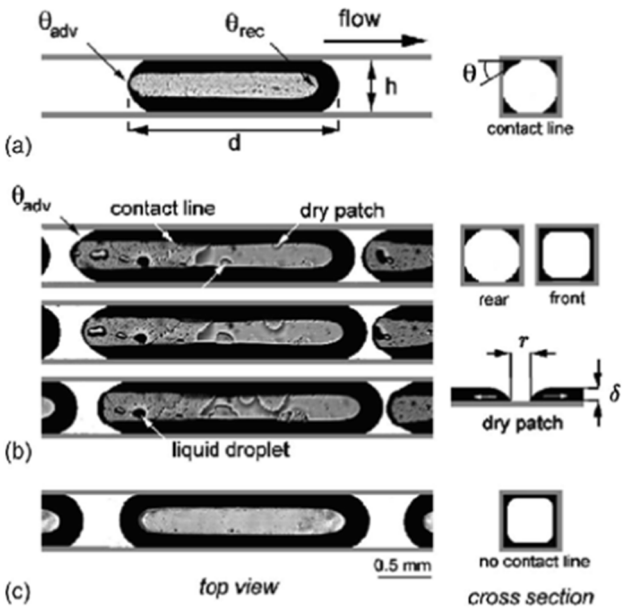

Fig. 18. Wedge flow regime: (a) drying bubble, (b) consecutive images of a hybrid bubble, and (c) lubricated bubble, observed by Cubaud and Ho [153].

aspect ratio on the flow patterns at three different aspect ratios (AR). A darker region is a thick liquid film. With decreasing the AR, the liquid film thickness decreases due to the confinement effect. Fig. 20 shows the flow patten map for $AR = 0.91$ and $D_h = 490$ μm and comparison of the observed flow patterns to the flow pattern maps of Chung and Kawaji [138] and Triplet et al. [92]. With increasing the superficial gas velocity

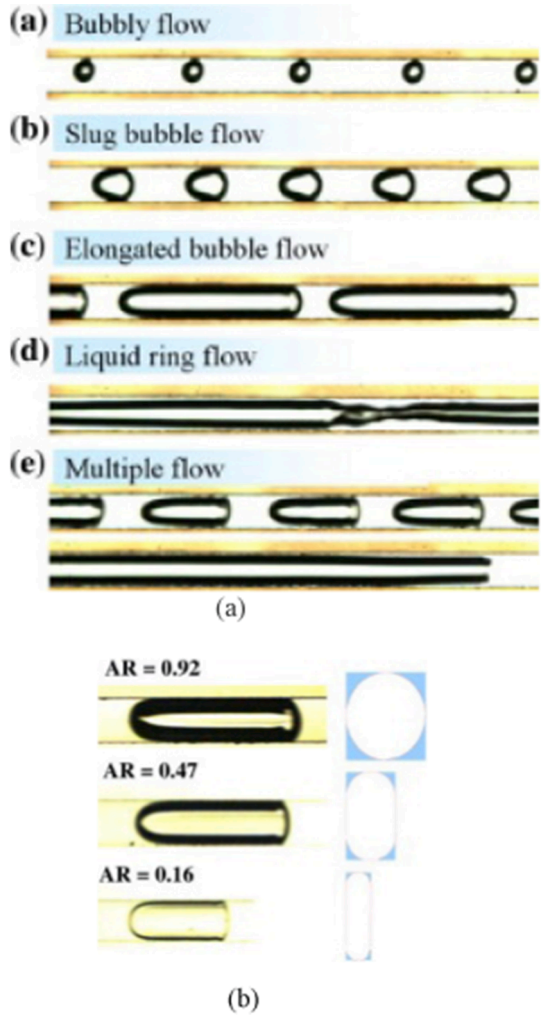

Fig. 19. (a) Classification of flow patterns in rectangular microchannel for AR = 0.92. (b) Aspect ratio effect on bubble flow regime at j_L = 0.2 m/s and j_G = 0.6 m/s by Choi et al. [154].

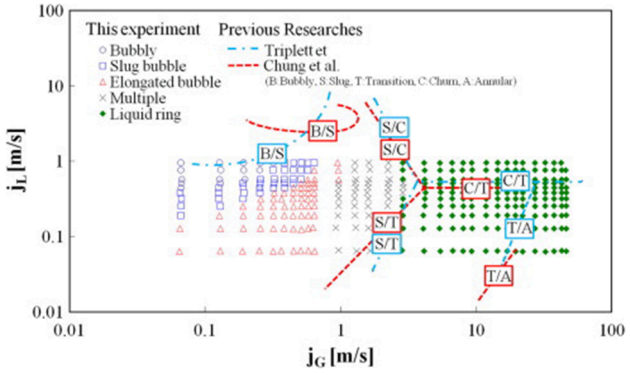

Fig. 20. Flow pattern map for AR = 0.92, D_h = 490 μm and comparison with different flow regime map: Chung and Kawaji [138] and Triplet et al. [92] by Choi et al. [154]. (The two phase flow is liquid water and nitrogen gas two-phase flowThe flow pattern map is applicable to liquid superficial velocities of 0.06–1.0 m/s and gas superficial velocities of 0.06–71 m/s.).

j_G, the bubble flow changes from the slug bubbly flow first and the to the elongated bubble flow. The liquid ring flow is observed after the multiple flow (transition regime). At higher superficial liquid velocities j_l and lower superficial gas velocities j_g, the bubbly flow is observed. With increasing the AR, the transition between the elongated bubble flow and the multiple flow is shifted to the right and the transition between the multiple flow and the liquid ring flow is shifted to higher superficial gas velocities j_g. However, the transition of the bubbly and slug bubble flows is slightly shifted to the left. With decreasing the channel diameter, the elongated bubble pattern become dominate as the effect of the channel confinement. The transitions of slug, elongated and multiple regimes are proposed as following equation:

$$\frac{j_L}{j_G} = a j_G^b \tag{8}$$

For transition of slug between elongated bubble patterns: a = 0.817, b = -0.374. For transition of elongated bubble between multiple patterns: $a = 0.0103e^{0.00784D_h}$, b = 4.576.

Haverkamp et al. [164] experimentally investigated the effect of mixer geometry on the flow patterns. They observed gas–liquid mixture flows in single or multiple rectangular micro-channels with different widths and heights of 100 × 50, 300 × 100, and 1100 × 170 mm^2. Water and isopropanol were used as the liquid phase, and nitrogen was used as the gas phase. Two different mixer geometries, *T*-type and smooth. The mixer configuration affected both the average bubble length and bubble size distribution. Shin and Kim [162] experimentally studied the effect of the gas–liquid mixer configuration on the air water two phase flow patterns in a rectangular channel with a hydraulic diameter of 1.33 mm. Their observed flow patterns are classified into seven categories: slug, aerated-slug, transition, multiple, wavy-annular, smooth-annular, and dispersed-annular flows as shown in Fig. 21. Furthermore, they performed the quantitative characterization of flow patterns and transitions in the micro-channel using the standard deviation of differential pressure fluctuations and have developed a generalized approach for predicting adiabatic two-phase flow patterns in mini/micro-channel flows according to a database of 7391 flow pattern data in mini/micro-channels collected from 25 studied in the literature [163]. The database consists of their own observed flow patterns and experimental flow patterns of 16 different working fluids for both single-component and two/multi-component mixtures with hydraulic diameters of 0.2–4.0 mm, superficial liquid Reynolds numbers of 4.6–918938, superficial gas Reynolds numbers of 0.4–261017, mass velocities of 2.4–6028 $kg/m^2{\cdot}s$, flow qualities of 0–0.99, and the reduced pressures of 0.036–0.78. Fig. 22(a) shows their proposed generalised flow pattern map based on the database and Fig. 22(b) illustrates the schematic of representative flow patterns in the mini and micro-channels. The correlations of the flow pattern transitions can be found in their paper [163]. It is suggested that the generalised flow pattern map be evaluated with extensive new experimental flow pattern data when new flow patterns are available.

The configuration of the mixer, in which the gas and liquid are mixed together before entering the test channel, can affect the two-phase flow patterns in mini/micro-channels. However, However, previous works about the influence of the conditions of gas and liquid input into the channel are not analysed [164,165]. Most microchannels in practical applications have rectangular shape. The influence of the aspect ratio of the rectangular channel on two-phase flow is extremely significant. It is not enough to use only the hydraulic diameter to analyse the two-phase flow in rectangular channels [165]. The two-phase flow patterns are highly affected by the surface wettability [166–169]. In the hydrophilic microchannel, the major flow patterns were bubbly, elongated bubble and liquid ring flow. In the hydrophobic microchannel, the major flow pattern was stratified flow which was governed by capillary force and hydrophobicity. In the channel sizes from 0.01 to 3 mm, adiabatic two phase flow patterns can be quite different as the effect of channel confinement. The effect of channel orientation (vertical or horizontal) tends to disappear with decreasing channel size. Slug flows have much longer bubbles, reaching length to channel diameter ratios of 10 to 100. New flow patterns, such as wedge flow and liquid lump flow appear. A number of flow pattern maps are available. In particular, a generalized

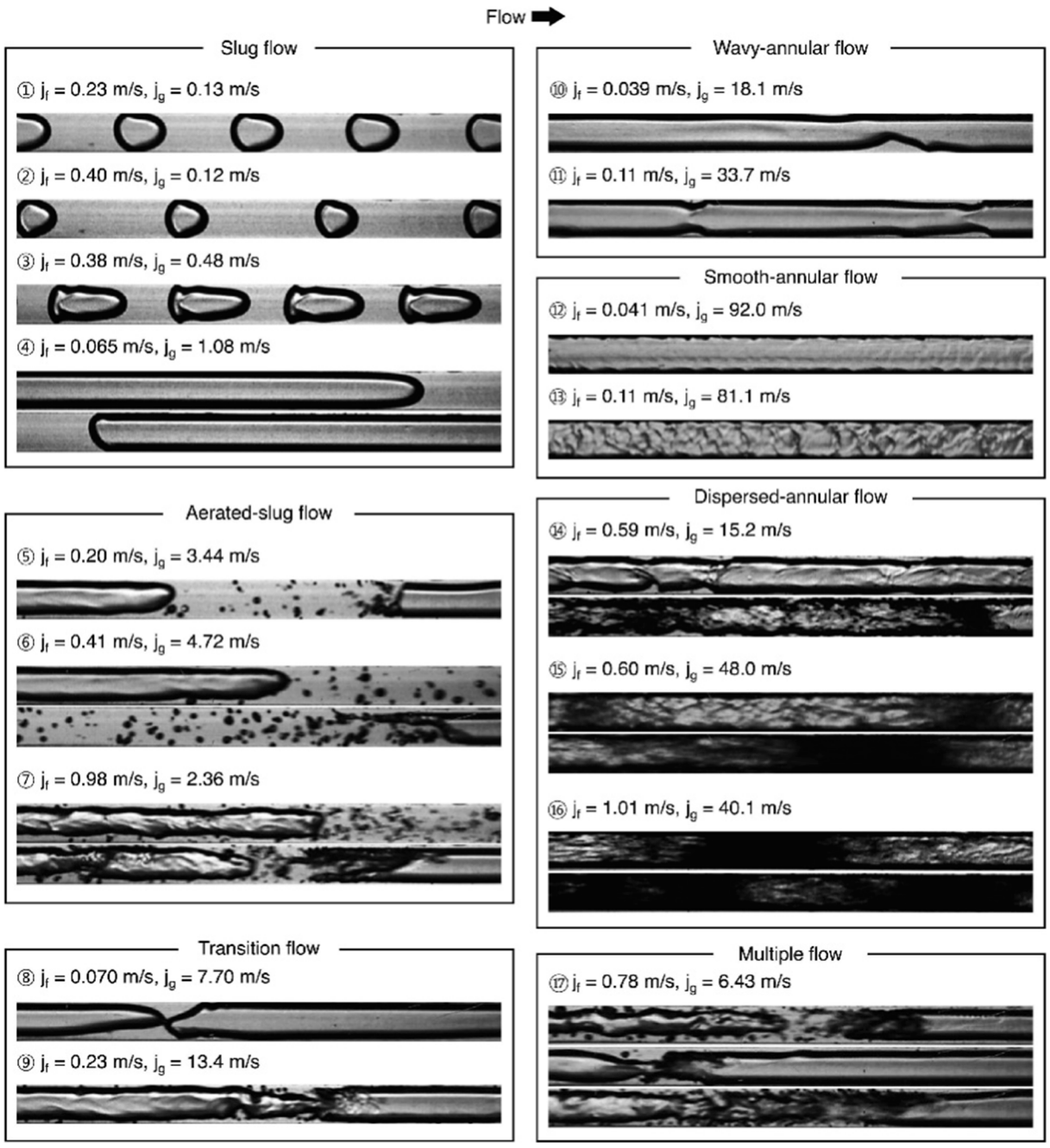

Fig. 21. Representative photographs of air–water flow patterns in $D_h = 1.33$ mm rectangular channel using mixer B: ①-④ for slug flow, ⑤-⑦ for aerated-slug flow, ⑧ and ⑨ for transition flow, ⑩ and ⑪ for wavy-annular flow, ⑫ and ⑬ for smooth-annular flow, ⑭-⑯ for dispersed-annular flow and ⑰ for multiple flow [162].

flow pattern map has been recently developed but needs to be further validated with new experimental flow pattern data in future.

4.2. Diabatic flow patterns and flow pattern maps in microchannels

Similar to the flow patterns in macro-channels, flow patterns at diabatic conditions such as flow boiling and flow condensation are different from those at adiabatic conditions in microchannels. Identification flow patterns at diabatic two phase flow in microchannels is more complicated and challenge due to the channel size effect and quite different bubble growth in the channels. In recent years, much attention has been paid to the research of diabatic gas liquid two phase flow patterns and flow pattern maps. Several flow pattern transition criteria have been proposed for flow boiling in microchannels. However, validation of these transition criteria is still needed by independent data. Further improvement of these flow pattern maps is needed by incorporating a wide range test conditions, fluids and channel sizes.

Revellin and Thome [120,121] experimentally investigated flow patterns in a 0.509 mm micro-channel for flow boiling of R134a and R245fa. As shown in Fig. 6, several flow pattern transitions for R245a such as bubbly/slug flow, slug/semi-annular flow and semi-annular flow have been defined according to their observations, the latter which probably coincides with churn flow in macro-scale channels. Fig. 23 shows their diabatic flow pattern maps observations and boundaries for R134a [120,121]. However, their flow pattern transition boundaries were only drawn according to the experimental observations. No correlations for these boundaries were proposed. Four principal flow patterns (bubbly flow, slug flow, semi-annular flow and annular flow) with

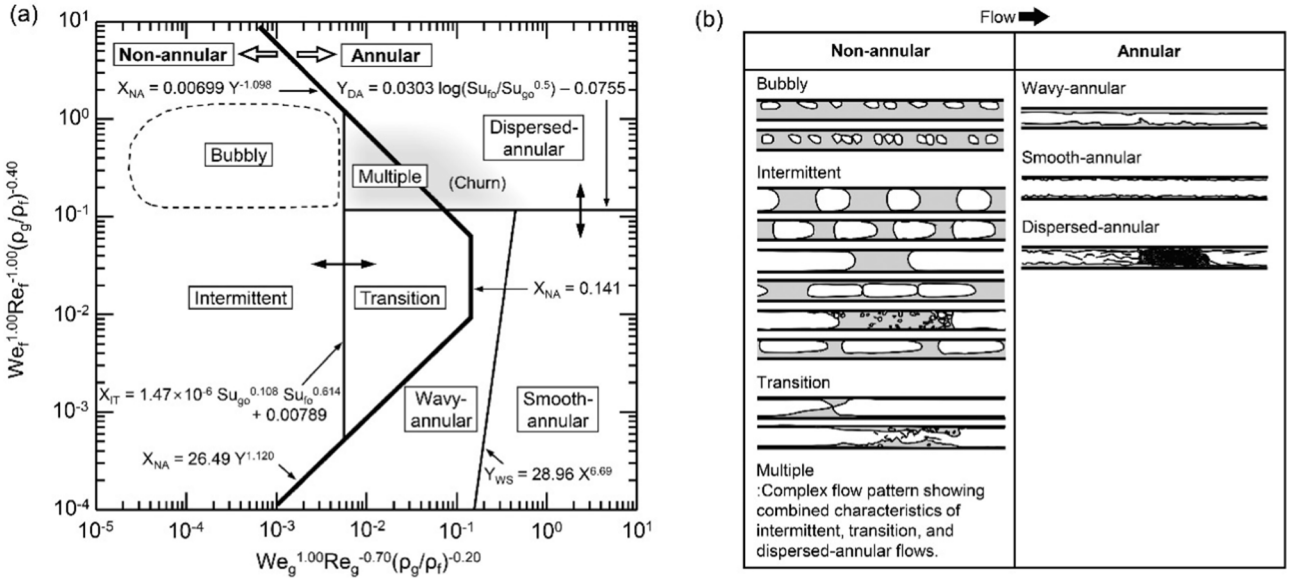

Fig. 22. (a) Proposed generalized flow regime map with flow regime boundary correlations for two-phase mini/micro-channel flows. Churn flow indicated by shaded region reported by five sources of consolidated database shows complicated flow patterns that cannot be classified into one of seven subcategories in their study; (b) Schematic of representative flow regimes for two-phase mini/micro-channel flows [163].

their transitions (bubbly/slug flow and slug/semi-annular flow) were observed in experiments with R-134a and R-245fa in 0.50 mm and 0.80 mm circular channels. Flow pattern changes were detected by signal frequency analysis combined with a small bubble coalescence study. The higher the mass flux is, the earlier the transitions are encountered in terms of vapor quality. Bubbly flow tends to disappear at high mass flux because small bubbles quickly coalesce to form elongated ones.

Celata et al. [178] investigated flow boiling patterns of FC-72 in a horizontal circular microchannel of 0.48 mm at mass fluxes from 50 to 3000 kg/m^2 s. Fig. 24 shows their observed bubbly flow, deformed bubbly flow, bubbly/slug flow, slug flow, slug/annular flow, and annular flow in the microchannels. They developed a flow pattern map which shows the presence of intermittent flow (slug flow) in the subcooled flow boiling region and the presence of instabilities associated mainly to intermediate flow patterns (bubbly/slug flow and slug/annular flow). Churn flow is not observed in the microchannel. The channel size has a significant effect on the transition from bubbly flow to slug flow due to the channel confinement effect. In particular, the presence of intermittent flow spreads toward the subcooled region.

Tibiriçá and Ribatski [171] experimentally studied flow patterns and bubble growth in flow boiling of R134a and R245fa in a horizontal circular microchannel with an inner diameter of 0.4 mm. Fig. 25 illustrate the onset of the nucleate boiling (ONB) observed in the 0.40 mm visualization section. In this sequence of images, the first nucleus appears at 0 ms; around 1.2 ms the nucleation sites move upstream the flow direction to a point at which they become stable and the structure of the flow patterns no longer change along time. As shown in Fig. 26, their observed flow patterns are bubble, slug and annular flow which are similar to those observed by Celata et al. [178]. They also observed static vapor slugs in horizontal tubes with three different inner diameters of 0.4, 1 and 2 mm. With increasing the tube diameter, the interface starts to deform due to the gravity force. However, even with a diameter of 2.00 mm, the surface tension at the interface can hold the liquid pressure and avoid the formation of a stratified flow. They have presented flow pattern maps for R134a and R245fa, respectively. Fig. 27 display the flow pattern transition lines IB-CB (isolated bubbles to coalescing bubbles) and CB-A (coalescing bubbles to annular) from the Ong and Thome [97] flow pattern transition criteria given by Eqs. (9) to (17). Most of the vapor quality range is dominated by annular flow in their study.

Flow patterns and bubble growth of diabatic gas liquid two phase flow in multi-microchannels are very important in understanding the heat transfer behaviours and mechanisms but much more complicated. In general, diabatic gas liquid two phase flow patterns in multi-microchannels are similar to those in single microchannels. However, flow instability and distribution become important in such channels. As such, reversible flow occurs in multi-microchannels. Hetsroni et al. [170] investigated flow boiling of water in the silicon triangular microchannels having hydraulic diameter 103 μm and 129 μm. They observed periodic annular flow and the periodic dry steam flow (periodic wetting and rewetting phenomena). This explosive boiling was triggered by venting of elongated bubble due to very rapid expansion. They also observed dryout in the microchannels. Wang et al. [173] studied the effects of inlet/outlet configurations on flow boiling instabilities in multi parallel microchannels with 8 channels, a length of 30 mm and a hydraulic diameter of 186 μm. Fig. 28 illustrated the arrangement of the multi microchannels. Fig. 29 shows their observed flow patterns in the parallel channels at steady flow condition. Elongated bubbles occur in the microchannels due to the confinement of the microchannels. Other flow patterns include isolated bubble flow, coalescence bubble flow and annular flow. In the unstable flow boiling mode, As shown in Fig. 30, Wang et al. [173,174] observed elongated bubbly/slug flow pattern. The flow pattern also behaved like an annular or semi-annular flow, in which the thin liquid film evaporated between the vapor core and the heating wall. Later, it was observed that upstream vapor plug broke through the liquid front, reaching the long bubble downstream. Local dryout occurred due to the depletion of liquid film between vapor core and heating wall. Subsequent to this, annular/mist flow (alternating dryout and rewetting phenomena) with imminent burnout was observed. Average wall temperature in bubbly/elongated bubbly/slug flow was lower than that in the semi-annular flow and annular/mist flow.

Harirchian and Garimella [172] investigated the effects of channel size and mass flux on the flow boiling patterns of FC-77 in multiple microchannels. The test sections are seven different silicon test pieces with parallel microchannels of width ranging from 100 to 5850 μm, all with a depth of 400 μm. Fig. 31 shows their observed flow patterns include bubbly, slug, churn, wispy-annular, and annular flow. Flow patterns in the 100 μm and 250 μm-wide microchannels are found to be similar and differ from those in microchannels of width 400 μm and larger; the latter group show similar flow patterns. With increasing the

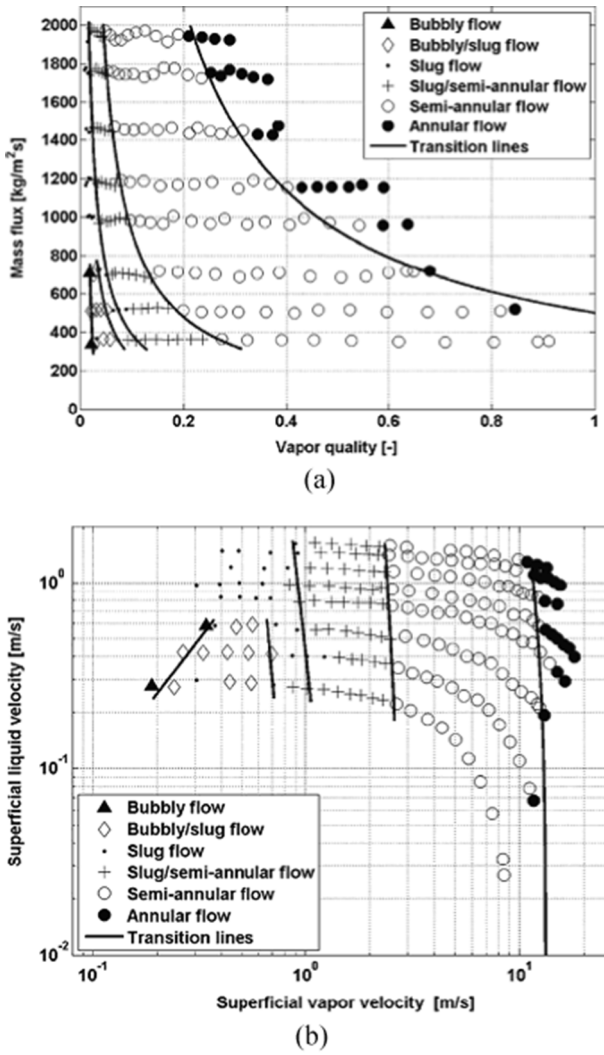

Fig. 23. Flow pattern observations with experimental transition lines for R134a, $D = 0.509$ *mm*, $L = 70.7$ *mm*, $T_{sat} = 35$ °*C*, $\Delta T_{sub} = 5$ °*C* using laser plotted in two different formats: (a) Flow pattern observations with transition lines, (b) Flow pattern map, by Revellin and Thome [120,121]. (The experimental conditions: mass flux G = 350 – 2000 kg/m^{2}s, vapor quality × = 0.4 – 0.852, heat flux: 3.7 – 129.7).

channel width, bubbly flow replaces slug flow and intermittent churn/wispy annular flow replaces intermittent churn/annular flow. Fig. 32 shows the summary of boiling flow patterns in the microchannel test pieces. For each microchannel size, as mass flux increases, the bubbles become smaller and more elongated in the bubbly region, and the liquid layer thickness in the wispy-annular and annular regimes decreases. Since the transition between specific flow patterns occurs at higher heat fluxes as the mass flux increases, different flow patterns were observed at a given heat flux for different mass fluxes. Fig. 33 shows the comprehensive flow pattern map based on the experimental results and flow visualizations performed with FC-77. Plotting all the 390 experimental data points obtained for 12 different microchannel test pieces, four mass fluxes, and heat fluxes in the range of 25–380 kW/m^2 leads to a comprehensive flow regime map with four distinct regions of confined slug flow, churn/confined annular flow, bubbly flow, and churn/annular/wispy-annular flow.

Surface tension plays a more significant role in diabatic gas liquid two phase flows in microchannels than those in macrochannels. The flow patterns which are mainly surface-tension dominated are characterized by large and elongated bubbles of gas, such as the bubbly, plug,

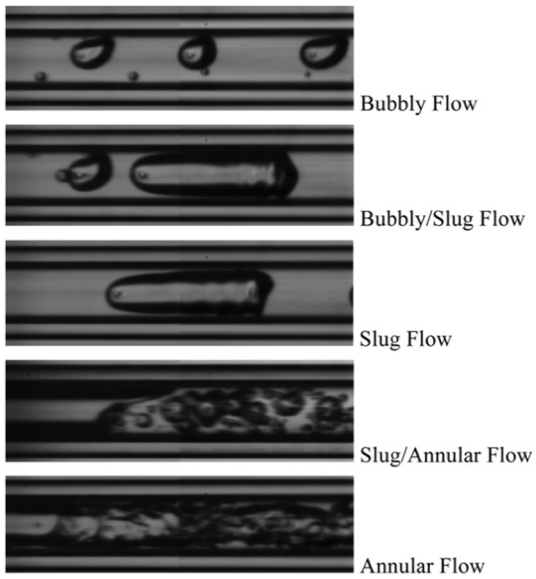

Fig. 24. Flow patterns in a 0.48 mm micro-channel for FC-72 flow boiling, observed by Celata [178] in a heated microchannel.

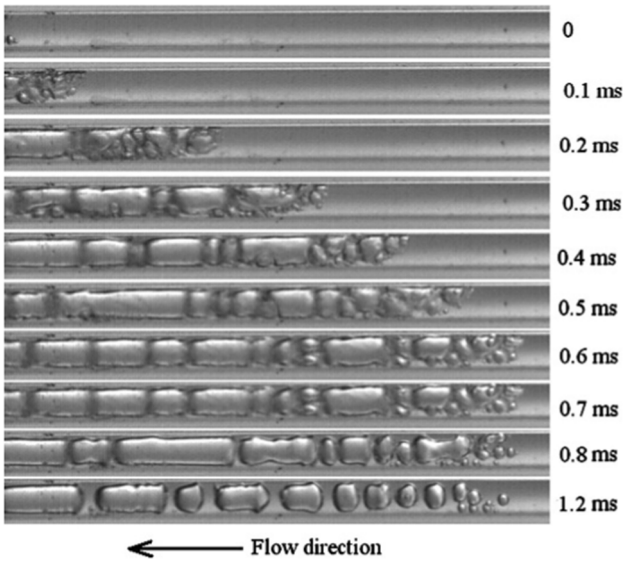

Fig. 25. Onset of nucleated boiling during flow boiling. D = 0.40 mm, R134a at G = 200 kg/m^{2}s, T_{sat} = 31 °C, q = 86 kW/m^2 by Tibiriçá and Ribatski [171].

and slug flows. Also, the flow patterns which are inertia-dominated include annular flows and dispersed flows. When the bubble size approaches the channel size, the result is the annular flow. The most difficult flow patterns are transition flows. On the one hand, there is the scarcity of data related to these transition flow patterns. On the other hand, the definitions of flow patterns are different from one research to another research in the available studies.

Revellin and Thome [121,177] utilized their measured flow patterns and bubble frequency data, and the CHF correlation of Wojtan et al. [184] to produce a new type of flow pattern map for diabatic (evaporating) flows. Their map classifies these evaporating flow regimes: (a) Isolated bubble flow; (b) Slug flow and mixed bubble flows displaying both long and short bubbles. In this regime the bubble frequency increases with heat flux and, thus, vapor quality at a fixed mass velocity; (c) Coalescing bubble regime: this refers to slug flows and churn flows (the latter are long bubbles followed by aerated liquid plugs) but where some short bubbles may still exist and where the frequency of the

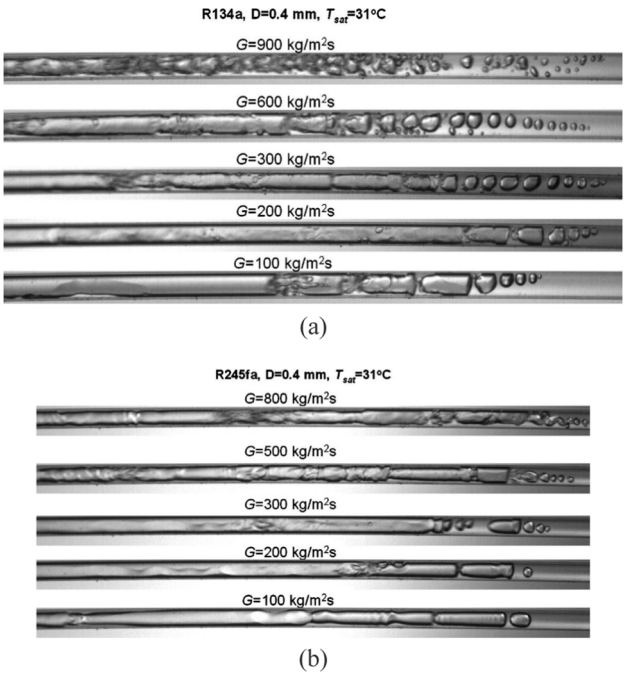

Fig. 26. Flow patterns during a flow boiling development process in a 0.40 mm tube (a) R134a at 31 °C, and (b) R245fa at 31 °C by Tibiriçá and Ribatski [171].

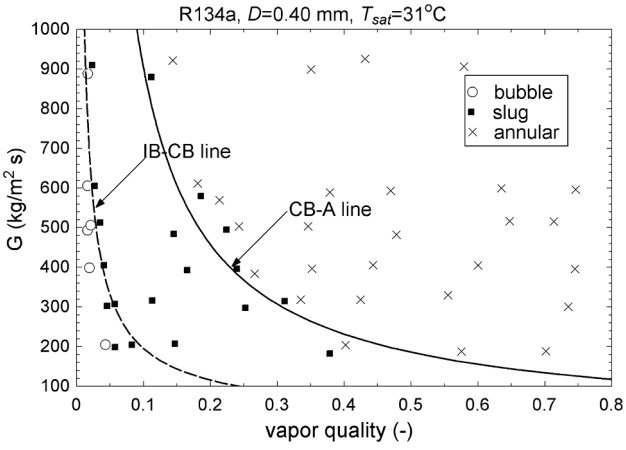

Fig. 27. Flow pattern map for D = 0.40 mm, R134a at 31 °C by by Tibiriçá and Ribatski [171].

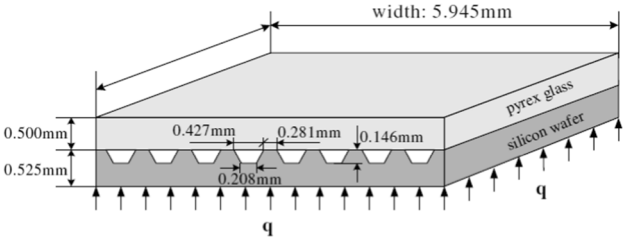

Fig. 28. Arrangement of 8 parallel microchannels having the same length and identical trapezoidal cross-sectional area and etched in a silicon substrate by Wang et al. [171].

bubbles decreases with increasing heat flux and thus vapor quality at a fixed mass velocity; (d) Annular flow regime: this refers to both smooth annular flows with nearly no interfacial waves and wavy annular flow where interfacial waves are very evident and (e) Dryout regime: this refers to the dryout condition encountered after passing through CHF at the critical vapor quality. Fig. 34 shows the diabatic flow pattern map of Revellin and Thome [177] simulated for R-134a at 30 °C for three channel sizes at the indicated conditions. It is important to observe that there are two distinct paths for the transition from annular flow to the dryout regime: (a) increasing the heat flux until it exceeds CHF and (b) increasing the vapor velocity until the shear force is sufficient to cause complete entrainment of the annular liquid film by the vapor core. The CHF transition mechanism tends to dominate in channels operating at high heat fluxes while the shear force mechanism tends to be encountered in channels operating at relatively low heat fluxes or for adiabatic flows. In the flow pattern map of Revellin and Thome, only the CHF mechanism has been addressed.

Ong and Thome [97] proposed updated flow pattern map based on the Revellin and Thome flow map and their experimental two-phase flow pattern transition data together with a top/bottom liquid film thickness comparison for refrigerants R134a, R236fa and R245fa during flow boiling in small channels of 1.03, 2.20 and 3.04 mm diameter. Fig. 35 shows their updated diabatic flow pattern map. The propose flow pattern transition models are as follows:

Isolated bubble/coalescing bubble (IB/CB):

$$X_{IB/CB} = 0.36Co^{0.2}\left(\frac{\mu_V}{\mu_L}\right)^{0.65}\left(\frac{\rho_V}{\rho_L}\right)^{0.9} Re_V^{0.75} Bo^{0.25} We_L^{-0.91} \tag{9}$$

Coalescing bubble/annular (CB/A):

$$X_{CB/A} = 0.47Co^{0.05}\left(\frac{\mu_V}{\mu_L}\right)^{0.7}\left(\frac{\rho_V}{\rho_L}\right)^{0.6} Re_V^{0.8} We_L^{-0.9} \tag{10}$$

Plug–slug/coalescing bubble (*S*—*P*/CB) if ($X_{S-P/CB} < X_{CB/A}$):

$$X_{S-P/CB} = 9Co^{0.2}\left(\frac{\rho_V}{\rho_L}\right)^{0.9} Fr_L^{-1.2} We_L^{0.1} \tag{11}$$

Plug–slug/annular (S—P/A) if ($X_{S-P/CB} > X_{CB/A}$):

$$X_{S-P/CB} = X_{CB/A} \tag{12}$$

where Re_V, Re_L, BO, We_L and Fr_L are respectively defined as:

$$Re_V = \frac{GD}{\mu_V} \tag{13}$$

$$Re_L = \frac{GD}{\mu_L} \tag{14}$$

$$Bo = \frac{q}{GH_{LV}} \tag{15}$$

$$We_L = \frac{G^2 D}{\sigma\rho_L} \tag{16}$$

$$Fr_L = \frac{G^2}{\rho_{LgD}^2} \tag{17}$$

It is important to note that *Bo* above refers to the Boiling number and thus, makes the first transition line $X_{IB/CB}$ diabatic. The transition lines Eqs. (11) and (12) are only used when $Co < 0.34$. This transition criterion was based on their experimental conditions when transition from IB to *S*—*P* flow occurred at $T_{sat} = 31$ °C in the 3.04 mm channel. The flow pattern mas is applicable to the conditions: $Co = 0.27–1.67$, $Re_v = 85.9–452600$, $We_L = 0.58–247$, $Fr_L = 0.24–797$ and $Re_L = 1567–31387$.

In recent years, a number of studies of flow boiling in microchannels with enhanced structures to augment the thermal performance of microchannels. For example, the open microchannel with manifold (OMM) configuration provides stable high heat transfer performance with very low pressure drop. Kalani and Kandlikar [189] obtained high speed images to gain an insight into the nucleating bubble behaviour and flow patterns at high heat fluxes including CHF. The flow patterns

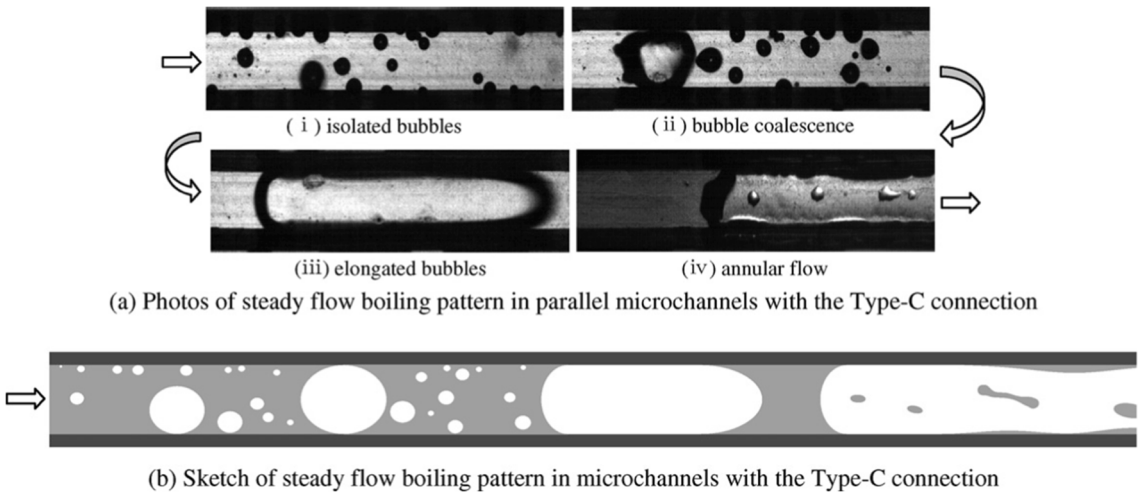

Fig. 29. Photographs and sketch of flow patterns in steady bubbly/slug flow boiling regime in parallel microchannels (D_h = 186 μm) with the Type-C connection at q = 364.68 kW/m^2, G = 124.03 kg/m^2 s and T_{in} = 35 °C (i.e., x_e = 0.359) by Wang et al. [173].

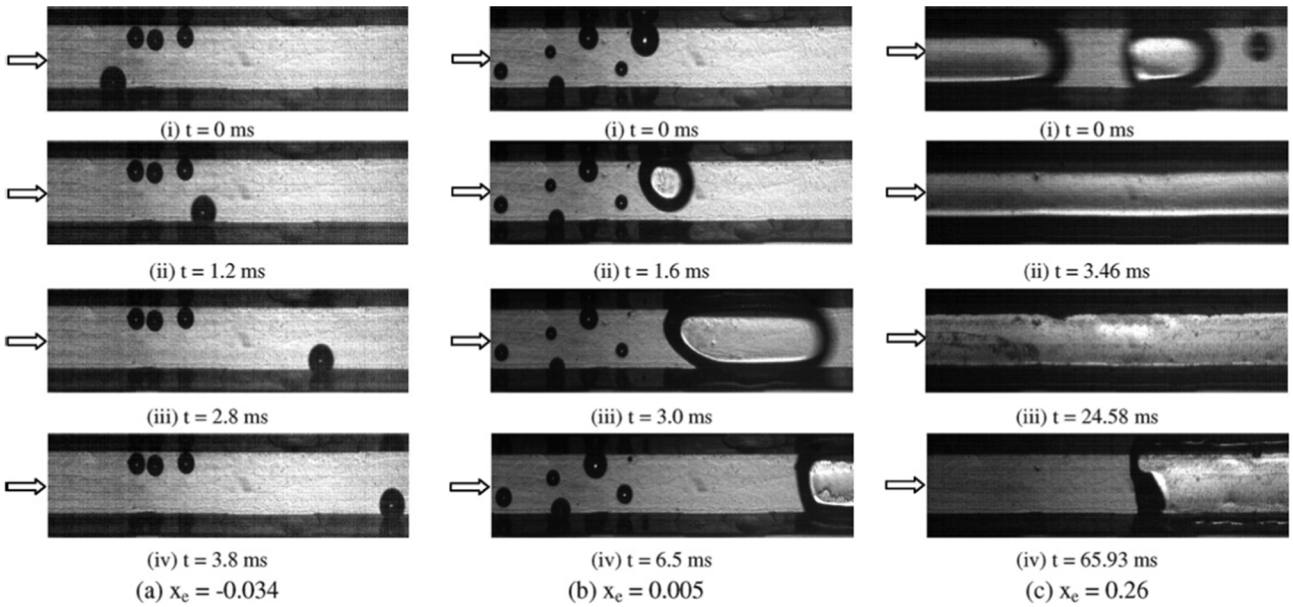

Fig. 30. Photos of steady flow boiling patterns near outlet section of parallel microchannels (D_h = 186 μm) with the Type-C connection at q = 364.68 kW/m^2 and T_{in} = 35 °C: (a) G = 682.11 kg/m^2 s (i.e., x_e = -0.034), (b) G = 471.32 kg/m^2 s (i.e., x_e = 0.005), (c) G = 156.04 kg/m^2 s (i.e., x_e = 0.26), by Wang et al. [174].

are plotted as a function of superficial gas and liquid velocity as shown in Fig. 36. The resulting flow pattern map indicates significant departure from the earlier work on macroscale tubes and confined microchannels. A mechanistic description of the heat transfer mechanism is also presented and the underlying differences between flow boiling in closed microchannels and open microchannels with tapered manifold configuration are highlighted. Furthermore, bubble ebullition cycle in pool boiling is compared with the tapered geometry utilizing plain and microchannel surfaces.

To understand the effect of surface properties on bubble dynamics, flow pattern transition and flow regime development in flow boiling microchannels, Alam et al. [188] conducted high-speed visualization of flow boiling of HFE-7100 in plain wall and SiNW microchannels and observed the flow patterns from the top of both microchannels. Fig. 37 (a) shows the time sequence of flow pattern development in flow boiling on the plain wall microchannels at mass flux, 400 kg/m^{2}s and heat flux, 30 W/cm^2. Nucleate boiling, slug flow, churn flow and annular flow occur throughout its boiling cycle. The cycle starts with rewetting and formation of bubble at the wall. The bubbles do not detach from the wall and form a vapor blanket and later grow and merge with other bubbles to form slugs as time progresses. Afterwards, the slugs merge and grow to form churn flow and evaporation at liquid–vapor interface transforming the churn flow to annular flow. Shortly after the formation of annular flow, rewetting takes place to renew the boiling cycle. It takes approximately 124 ms to complete the cycle in the plain wall channels. As shown in Fig. 37(b), quite different flow patterns and transitions occur in flow boiling in SiNW microchannels at the same working conditions. Numerous micro bubbles form on the heated wall just after rewetting in the SiNW microchannels. There are more nucleating bubbles with significantly reduced sizes in the SiNW microchannel as compared to the plain wall microchannels. Bubbles in the SiNW microchannel depart very quickly from the heated wall, then merge in the middle of the channel to form long vapor slug. No vapor blanket on the wall of SiNW microchannel is formed and a continuous liquid replenishment on heated wall occurs. The boiling cycle takes approximately 38 ms, which is about one third of the time for the flow pattern

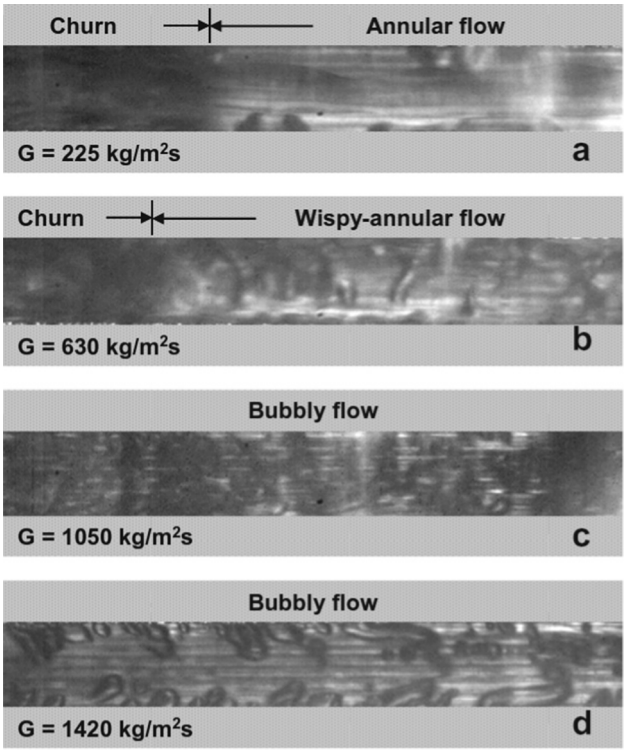

Fig. 31. Effect of mass flux on boiling flow patterns in the 400 μm × 400 μm microchannels at heat flux of 145 kW/m^2 by Harirchia and Garimella [172].

changes in the plain wall microchannel. Fig. 38 illustrates the sketch of typical flow patterns and transitions in flow boiling the plain wall microchannels and the SiNW microchannels. It can be clearly seen that no vapor blockage is observed due to the absence of intermittent flow patterns (slug/churn flow) and smooth flow pattern transition (from explosive nucleate boiling to annular flow) in SiNW microchannel.

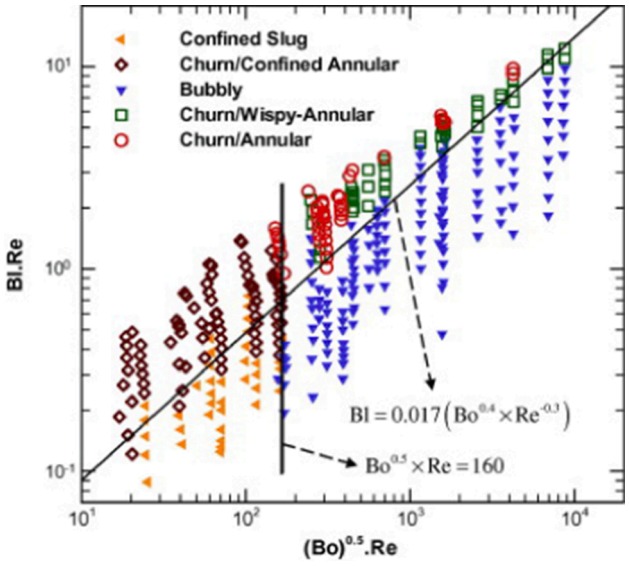

Fig. 33. Comprehensive flow regime map for FC-77 by Harirchia and Garimella [172].

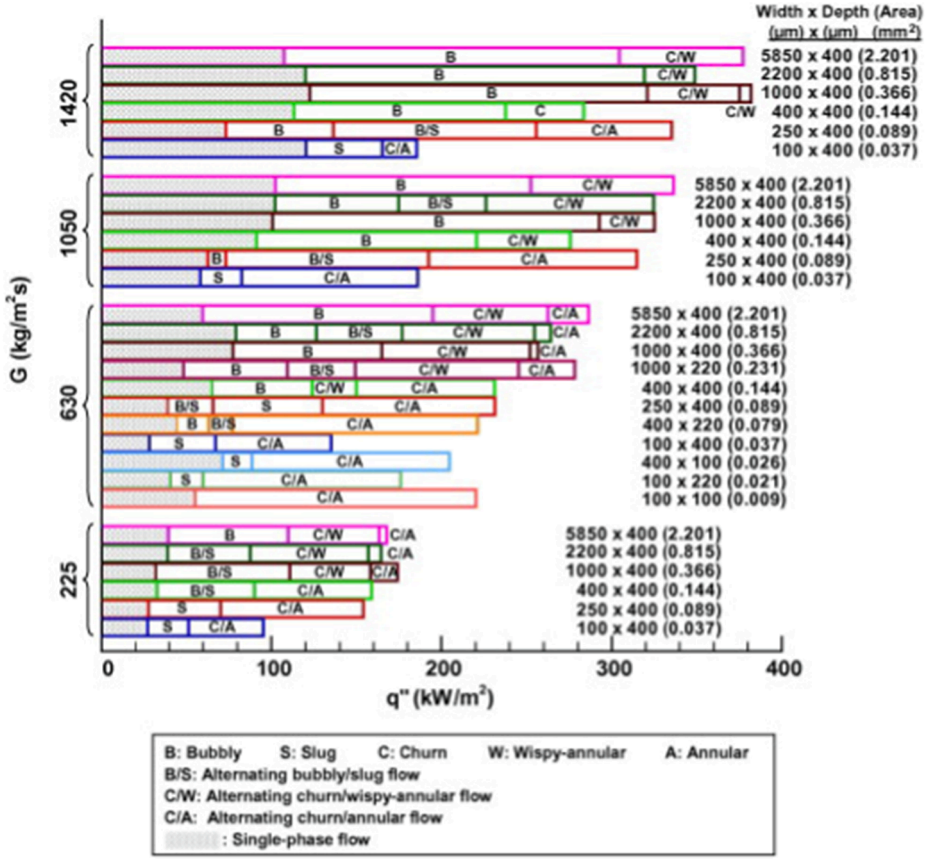

Fig. 32. Summary of boiling flow patterns in the microchannel test pieces; the microchannel dimensions are presented as width (μm) × depth (μm) with a single-channel cross-sectional area (mm^2) in parentheses by by Harirchia and Garimella [172].

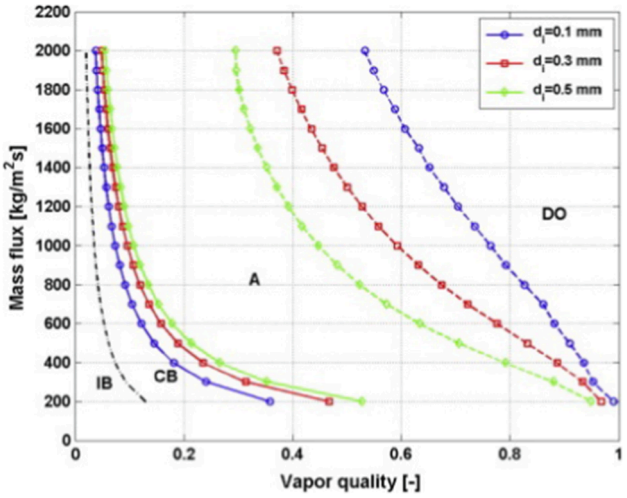

Fig. 34. Diabatic flow pattern map of Revellin and Thome [177] simulated for R-134a at 30 °C for three channel sizes in a horizontal uniformly heated channel (q = 60 kW/m^2 without inlet subcooling and simulated for a channel length of 20 mm) showing the theoretical CHF model transitions from annular flow to dryout (IB: isolated bubble regime; CB: coalescing bubble regime; A: annular flow regime; DO: dry out regime).

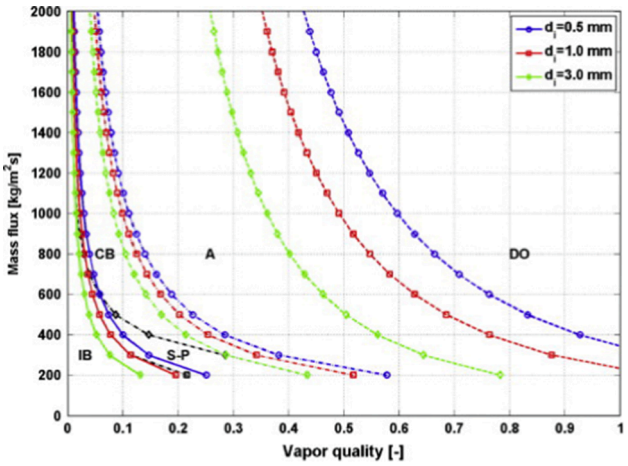

Fig. 35. Updated diabatic flow pattern map of Ong and Thome [97] for R-134a at 30 °C for three channel sizes in a horizontal uniformly heated channel (q = 60 kW/m^2 without inlet subcooling and simulated for a channel length of 20 mm) showing the CHF [49] transitions from annular flow to dryout (IB: isolated bubble regime; CB: coalescing bubble regime; S—P: Slug-Plug regime; A: annular flow regime; DO: dry out regime).

Flow patterns of flow condensation in single and multi-microchannels have been studied to understand the flow structures and mechanisms [191-204]. Ma et al. [194] investigated flow patterns of flow condensation of steam in trapezoidal silicon multi-microchannels with a hydraulic diameter of 0.134, 0.138 and 0.165 mm. They observed four flow patterns: annular, droplet, injection and bubble flow. No slug flow was observed. The annular flow was described as a vapour core surrounded by a liquid film. The condensate film thickness on the side walls in annular flow varies with time for the same location and operating conditions. These variations in liquid film thickness are attributed to two reasons: (1) the interfacial instability arising from the velocity difference between liquid and vapour and (2) the merging of the condensate into the liquid film during the condensation process. The droplet flow was characterized by small droplets growing in size on the bottom wall of the channel while the condensate liquid film covered the side walls. The growth of the droplets was due to condensation and

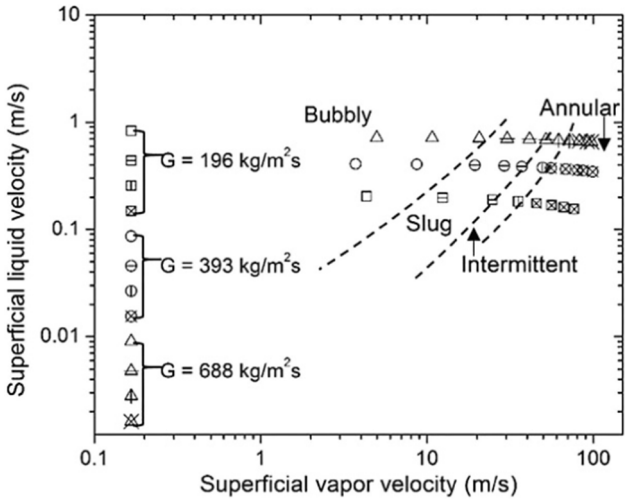

Fig. 36. Flow pattern map on superficial vapor and liquid velocity (j_g and j_l) coordinates with three mass fluxes of 196, 393 and 688 kg/m^{2}s over a heat flux range from 50 − 500 W/cm^2 by Kalani and Kandlikar [189].

merging with other small droplets. The injection flow was found as a transition regime between annular flow and bubble flow. In this flow pattern, the condensate film thickness on the side walls increases along the axial direction. When the condensate thickness becomes large enough, the liquid slug forms and vapour bubbles are released leading to the formation of bubbly flow. Kim et al. [196] experimentally studied flow patterns in flow condensation of FC-72 in a copper multi-microchannels condenser of square cross sectional area and 1 mm hydraulic diameter and length of 299 mm. Their observed flow patterns are smooth-annular, wavy-annular, transition, slug and bubbly flow. The identified flow pattern transition is bridging of liquid ligaments through the vapour core. With increasing the mass flux the smooth-annular flow extends towards the low quality region while the slug flow becomes narrow. Jiang et al. [198] conducted flow visualization of ethanol–water in trapezoidal silicon multi-microchannels with a hydraulic diameter of 0.165 mm and channel length of 50 mm. Their observed flow patterns are annular, annular-streak, annular-streak-droplet, churn, injection, droplet-injection and bubble flow. The annular-streak flow is characterized by a thick streak which is generated from the liquid film on the bottom of the microchannel. Liquid droplets are found in the annular-streak-droplet flow pattern. The injection flow pattern always occurs in the condensation process. According to the available studies in the literature, the transitions in flow patterns in flow condensation differ from one study to another. In fact, the fluid types, test conditions, the channel size and geometry have a significant on the behaviours of flow patterns and transitions.

Al-Zaidi et al. [191] conducted experimental study of HFE-710 condensing a micro- rectangular channel with a hydraulic diameter of 0.57 mm. They observed flow patterns at the channel inlet, middle and outlet to obtain the flow patterns during the condensation. Fig. 39 shows a schematic of their observed flow patterns. When the fluid enters the channels at high vapour quality, the flow pattern is annular flow, which is characterized by a vapour core surrounded by a thin liquid film. The annular flow is distorted at the neck region due to the confinement of the condensation process in the microchannel. When the liquid edges in the neck region join up, a vapour slug separates from the vapour core. With further condensation occurring along the channel, the length of the vapour slug decreases until bubbly flow occurs. Fig. 40(a), (b) and (c) show the typical photographs of the annular flow, slug flow and bubbly flow in the microchannels, respectively.

Wang et al. [202] investigated wo-phase flow pattern transition during the condensation of R134a and R1234ze(E) in a microchannel array consisting of 50 channels with the aspect ratio of 2.46, the

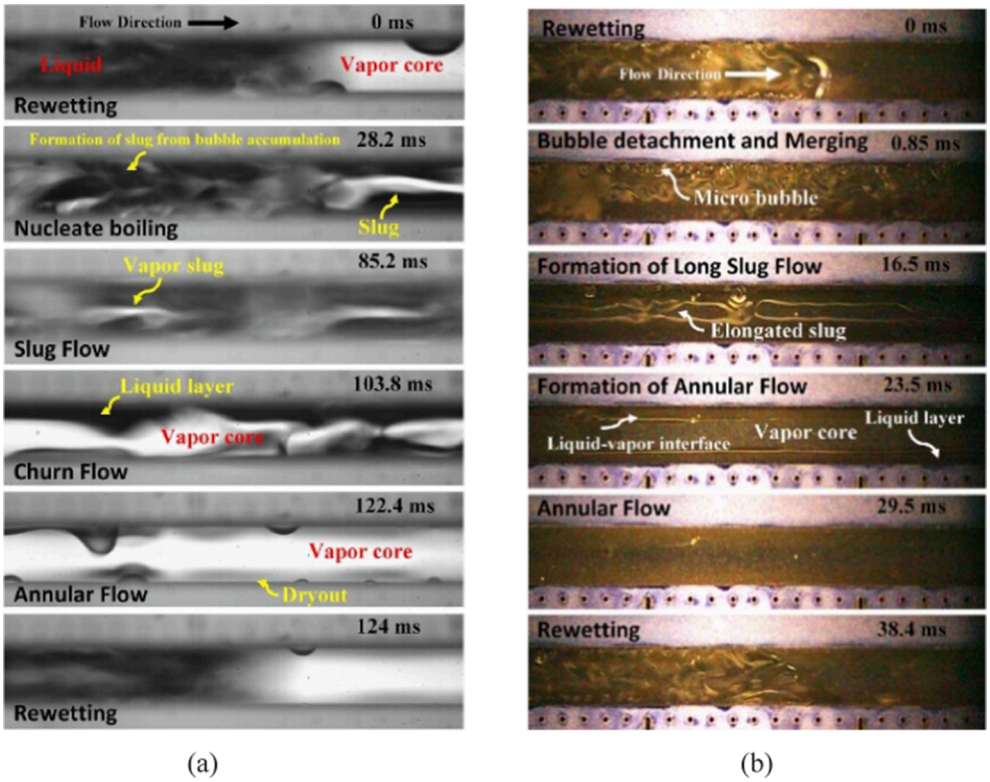

Fig. 37. Flow patterns in flow boiling t mass flux, 400 kg/m^{2}s and heat flux, 30 W/cm^2: (a) Plain wall microchannels; (b) SiNW microchannels by Alam et al. [188].

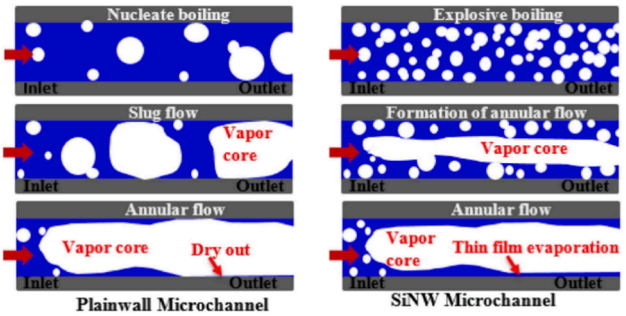

Fig. 38. Typical flow pattern transitions of flow boiling in plain wall microchannels and SiNW microchannels by Alam et al. [188].

hydraulic diameter of 301.6 μm and the length of 50 mm. Their observed patterns are annular flow, steady injection flow, quasi-symmetric wave flow and slug/bubbly flow. Fig. 41 shows the observed quasi-symmetrical wave/annular flow pattern. In addition, three flow pattern transition modes including steady injection, wave-coalescence injection, and liquid bridging are observed and mapped in terms of liquid Webb number versus condensation number. With the increase of refrigerant mass flux, quasi-symmetrical wave/annular flow appears at the upstream region of the channels as shown in Fig. 42 shows the observed steady inject flow which is characterized by three stages: bubble detachment (3 ms), bubble and slug formation (3–5 ms) and bubble growth (5–289 ms). Fig. 43 shows their proposed flow pattern map of R134a and R1234ze(E) in terms of liquid Webb number versus condensation number.

From the afore-going review of the diabatic flow patterns, bubble growth, liquid films and droplets, it is obvious that diabatic flow patterns and bubble and droplet behaviours in microchannels have not yet well understood for both flow boiling and condensation in microchannels. Well documented theoretically based flow pattern transition criteria and generalised flow pattern maps for microchannels have not yet been established although several criteria have been proposed in the literature. However, the transition criteria are only based on limited fluids, test channels and test conditions. Validation of these flow pattern maps are needed to compare with independent flow patterns. Further efforts should be made to develop a generalized flow pattern map for microchannels for a wide range of conditions, channels sizes and shapes and fluids.

Flow patterns and flow pattern maps play a critical role in understanding the complexity of the two-phase flow, flow boiling and condensation heat transfer and physical mechanisms. However, flow patterns, bubble growth and droplet behaviours are still open research topics for flow boiling, condensation and two phase flow in microchannels although numerous research of two-phase flow patterns, bubble growth, droplets and flow pattern maps in microchannels has been performed. Systematic knowledge has not yet fully established due to the very complicated phenomena and flow pattern transition

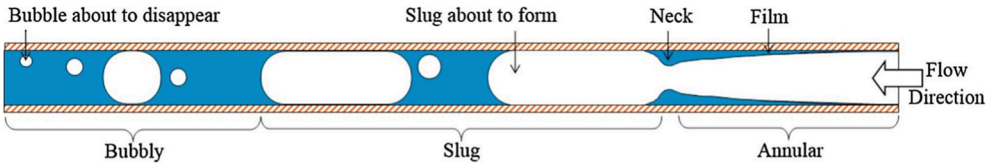

Fig. 39. Condensation flow structure by Al-Zaidi et al. [191].

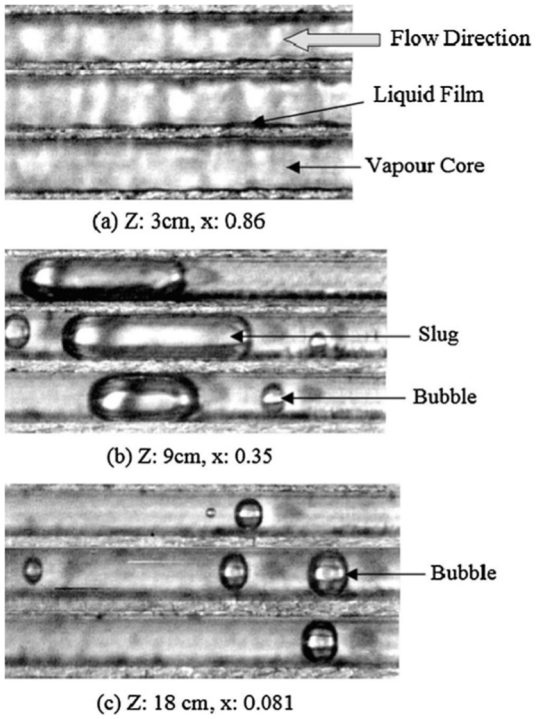

Fig. 40. Flow patterns along the condenser at mass flux of 108 kg/m^2 s, coolant flow rate of 0.8 l/min and inlet coolant temperature of 25 °C with corresponding local quality: (a) Annular, (b) Slug and (c) Bubbly by Al-Zaidi et al. [191].

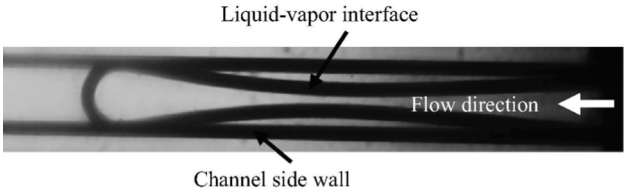

Fig. 41. Quasi-symmetrical wave/annular flow by Wang et al. [202].

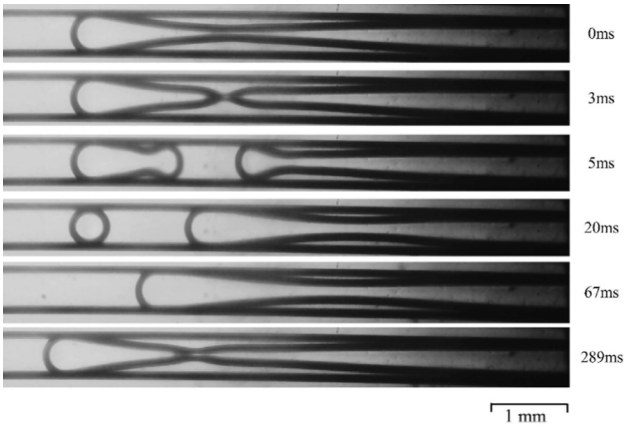

Fig. 42. Steady injection flow Wang et al. [202].

mechanisms in microchannels and quite different results by different research groups. Furthermore, most of the published microchannel flow patterns, bubble growth, droplet behaviour and flow pattern maps are only based on limited fluids and/or test parameters such as one or two saturation temperatures and presented in dimensional parameters

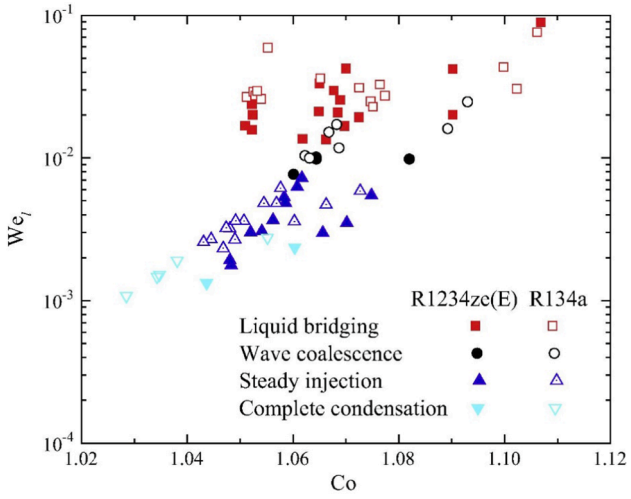

Fig. 43. Proposed condensation flow pattern transition map of R134a and R1234ze(E) Wang et al. [202].

which lack generalization. For flow boiling and condensation in microchannels, the surface tension dominates flow patterns as the channel diameter decreases, and thus the stratified flow basically does not exist in microchannels. Furthermore, confined bubbles and droplets in microchannels have an effect on flow pattern evolution and transitions. In general, the criteria for flow pattern transitions with variation of vapor quality depend on mass flux during the saturation flow boiling and condensation in microchannels, i.e. the pattern transition toward an annular flow occurs in the region of lower vapor quality as the mass flux becomes higher in microchannels compared to these in conventional channels. Quite different flow patterns for similar channels and test conditions have been observed by various researchers. For example, some researcher observed bubbly flow while other did not. Furthermore, bubble dynamics, droplet and liquid film behaviours are very important in understanding the diabatic two phase flow patterns and heat transfer mechanisms during flow boiling and condensation in microchannels, therefore, comprehensive and extensive studies on these topics are yet needed. In particular, the emerging research of diabatic two phase flow patterns, bubble growth, droplet and liquid film behaviours and flow pattern transition mechanisms in microchannels with enhanced structures and coatings are not well understood due to the very complicated phenomena involved in the enhanced microchannels and also the quite different structures of enhanced microchannels.

It should be mentioned that simulations of gas liquid two phase flow patterns and transitions using CFD are emerging but there are limitations and challenges for the research of flow patterns in both macro-microchannels [237–240]. However, this topic is beyond the focus of this review because this paper focuses on the review of experimental studies and correlations for flow pattern transitions and flow pattern maps and their applications as addressed in the next section.

5. Applications of flow patterns and flow pattern maps

Flow patterns, bubble dynamics, droplet and liquid film behvaiours and flow pattern transitions are intrinsically related to diabatic two phase flow and heat transfer behaviours and physical mechanisms. However, many available two phase flow and heat transfer prediction methods do not contain any flow pattern information [205–210]. Kattan et al. [211] developed flow pattern based flow boiling heat transfer model and their model related the flow structures and give good prediction results. For two phase flow and heat transfer in microchannels, most of the available prediction methods for two phase flow and heat transfer do not contain flow pattern information either [212–216]. As shown in Fig. 44, flow boiling and condensation heat transfer

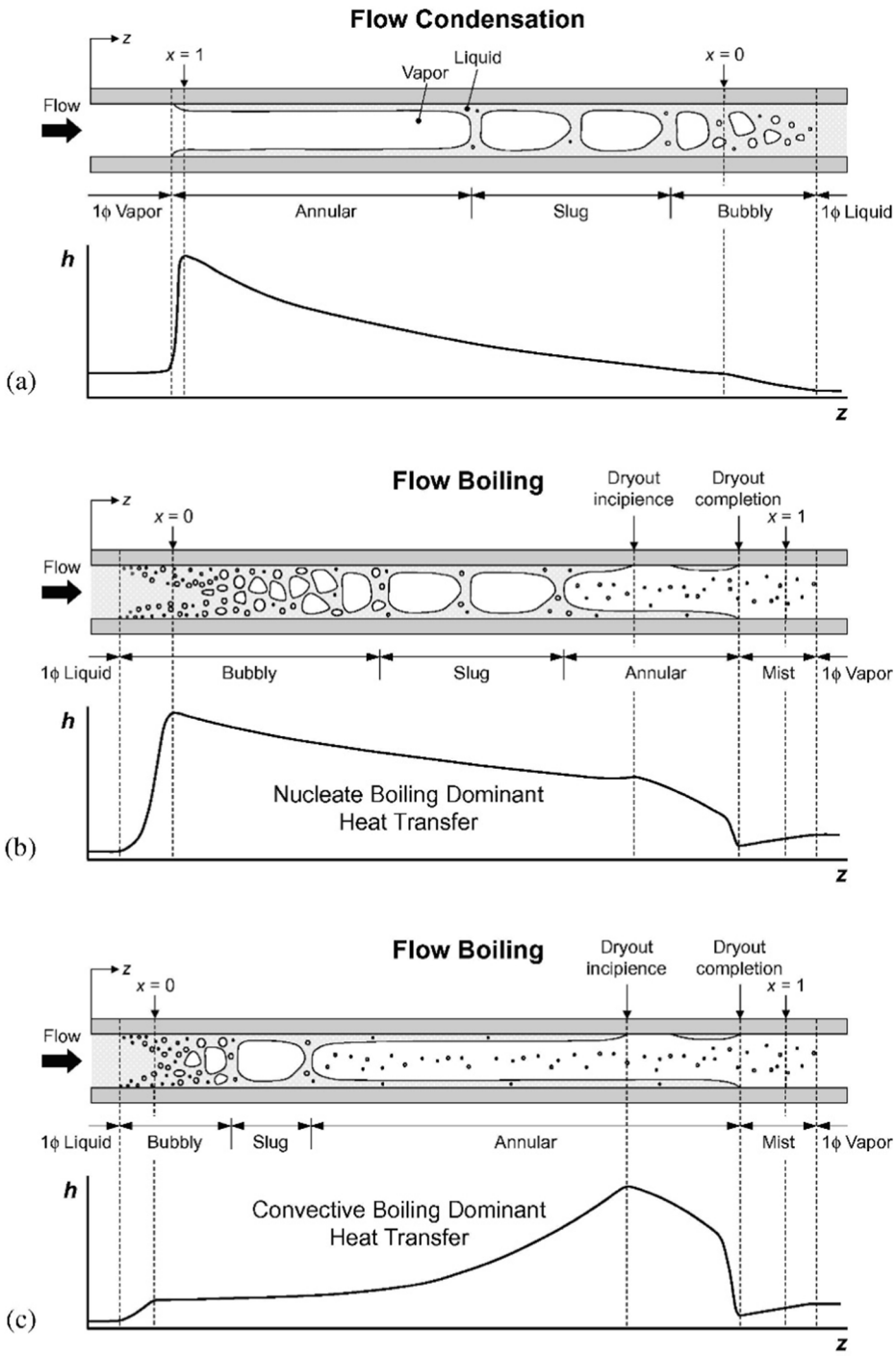

Fig. 44. Schematics of flow regimes, and variation of heat transfer coefficient in mini/microchannels with uniform circumferential heat flux for (a) condensation heat transfer, (b) nucleate boiling dominant heat transfer, and (c) convective boiling dominant heat transfer by Kim and Mudawar [39].

behaviours and mechanisms are strongly dependent on flow patterns and their transitions. Flow boiling is strongly dependent on the heat flux in nucleation dominant boiling while the heat transfer is less dependent on the heat flux and strongly dependent on the mass flux and vapour quality in convection dominant boiling [217–219,223]. The nucleate and convective boiling contributions to the heat transfer can be superimposed by very complex mechanisms which are not yet fully understood in microchannels so far.

From the available studies on flow boiling in microchannels, the heat transfer mechanisms are strongly dependent on the flow patterns and classified into four different categories [5]: (i) Nucleate boiling dominant because the heat transfer data are heat flux dependent; (ii) Convective boiling dominant when the heat transfer coefficient depends on mass flux and vapour quality but not heat flux; (iii) Both nucleate and convective boiling dominant, and (iv) Thin film evaporation of the liquid film around elongated bubble flows as the dominant heat transfer mechanism, which is heat flux dependent via bubble frequency and conduction across the film. (v) Annular flow model for flow boiling in microchannel. Therefore, understanding the fundamentals and mechanisms of diabatic two phase flow heat transfer in microchannels should be relevant to the corresponding flow patterns and bubble dynamics. Flow patterns, bubble behaviours and heat transfer should be observed

and measured simultaneously in experiments for a better understanding the microchannel flow boiling phenomena and mechanisms together with the corresponding flow patterns and bubble behaviour.

5.1. Flow pattern based heat transfer prediction methods in microscale channels

Mechanistic two phase pressure drop and heat transfer prediction methods based on flow patterns behaviours are important and still needed although several such methods have been developed. Several flow pattern-based mechanistic models for two phase flow and heat transfer in microchannels have been developed over the past decades [221,220–222,224–232]. Various new mechanistic models for flow boiling in microchannels such as three zone heat transfer model for elongated bubbles in microchannels by Thome et al. [221], recently updated version of three zone model by Costa-Patry and Thome [230] and annular flow heat transfer models covering both macro- and microchannel by Cioncolini and Thome [231] and Thome and Cioncolini [232]. The three-zone heat transfer models and a flow pattern based heat transfer model the three zone model and the annular flow model were evaluated with the database. Fig. 45 shows the diagram illustrating the three zones: a liquid slug, an elongated bubble and a vapour slug. They proposed this flow boiling heat transfer model, which predicts the local dynamic and the local time-averaged heat transfer coefficient at fixed locations along the channel based on the evaporation of elongated bubbles.

Cioncolini and Thome [231] proposed a heat transfer model for convective evaporation in annular flow in the absence of wall nucleation and proposed a new algebraic turbulence model for the transport of linear momentum and heat through the annular liquid film. Fig. 46 shows their physical model of annular flow. Thome and Cioncolini [232] have recently developed new mechanistic heat transfer model for annular flow covering both macro- and micro-channels and a flow pattern based flow boiling model for microchannel combining with the three zone model and the annular flow model. This model covers more flow patterns of elongated bubbles and annular flows which are dominant flow regimes in microchannel. Both models have been evaluated with the database in the review by Cheng and Xia [5]. It shows very promising predicted results with the flow pattern based heat transfer model as compared to extensive independent experimental data. It shows that adopting flow pattern based heat transfer model combining the three zone model and the annular flow model together with the corresponding flow patterns gives much better results than the three zone model alone. Table 2 summarizes that prediction results of the flow pattern based heat transfer models by Xia and Cheng [5]. The Thome and Cioncolini model predicts the data much better than the three zone heat transfer model for elongated bubbles in microchannels by Thome et al. [221]. Figs. 47 (a) and (b) show the comparative results for R123 and R134a at the indicated conditions respectively. The model favorably predicts the experimental data and capture the heat transfer trends [5]..

The flow pattern based heat transfer models by Cheng et al. [98–100] for CO_2 flow boiling in macro- and micro-channels predicts the flow boiling heat transfer of CO_2 in microchannels reasonably well and it relates the heat transfer mechanisms and behaviours to the corresponding flow patterns. Fig. 48 shows simulation of their flow pattern map and flow boiling model for CO_2 at the indicated conditions, superimposed on the same graphs by Cheng et al. [229]. The process path for the vapor quality variation from 0.01 to 0.99 is shown as the horizontal broken line (dash-dot line) while the variation in the heat transfer coefficient as it changes vapor quality and flow pattern is depicted by the dashed line. The flow pattern boundaries are in solid lines. The line (dash line with arrows) indicates the calculated heat transfer coefficient at the indicated mass velocity and vapor quality. Notice the various changes in trends in the heat transfer coefficient as this occurs. For example, when the flow regime passes from annular flow into the dryout regime, there is a sharp inflection in the heat transfer coefficient as the top perimeter of the tube becomes dry. It has been proved that relating heat transfer behaviours to the corresponding flow regimes may be a better way to understand the flow boiling mechanisms and to develop new prediction models for heat transfer.

Annular flow is a common flow pattern observed in microchannel flow boiling and flow condensation. Analytical model for annular flow may be developed from the mass, momentum and energy conservation with the aid of some assumptions and empirical correlations for wall and interfacial shear stress and droplets entrainment and deposition rates [225–227]. These models have some theoretical basis. However, in order to validate these models, a well-documented universal flow pattern map is needed to segment the heat transfer data but a generalized flow pattern map is not yet available and need to be developed.

Relating heat transfer behaviours to the corresponding flow regimes is a better way to understand the flow boiling mechanisms and to develop mechanistic models based on flow regimes for flow boiling and flow condensation heat transfer and two phase flow pressure drops. The mechanistic heat transfer models for both elongated bubbles and annular flow patterns for microchannels favourably predict the database collecting from the literature [5]. This is very encouraging and promising.

According to the forging analysis and discussion, further development of generalized heat transfer models based on flow patterns is recommended to improve the prediction accuracy in microchannels.

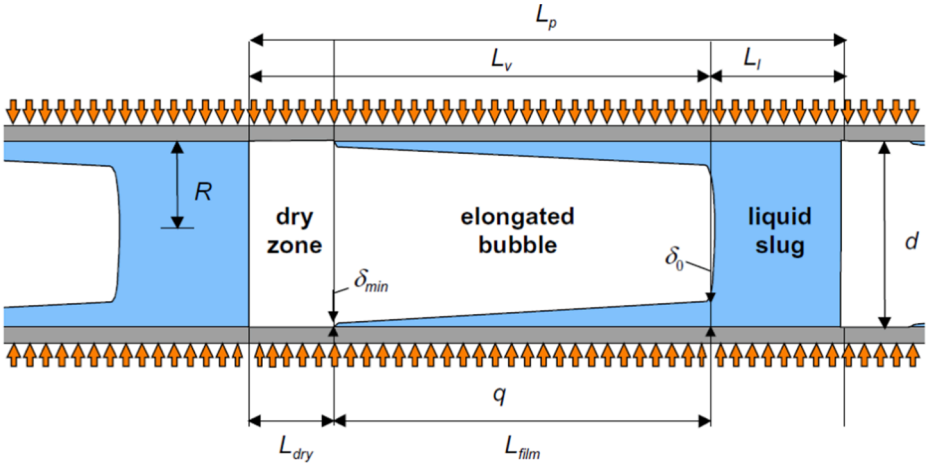

Fig. 45. The Three-zone heat transfer model for elongated bubble flow regime in microscale channels: diagram illustrating a triplet comprised of a liquid slug, an elongated bubble and a vapour slug [221].

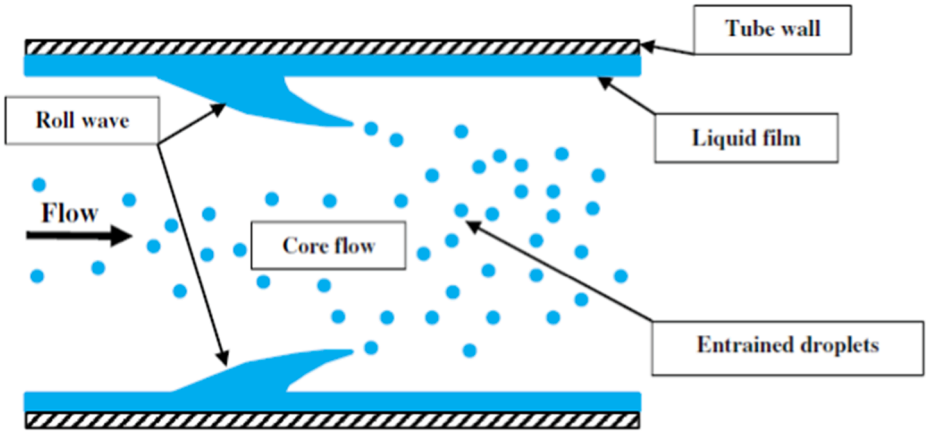

Fig. 46. Annular flow model in tubes [224].

Table 2
Statistical analysis of the two mechanistic heat transfer models for each individual fluid (relative error within ± 30 %) by Cheng and Xia [5].

Model\Fluid	R134a	R245fa	R22	R123	R141b
Three zone heat transfer model [215]	48.3 %	35.5 %	48.7 %	0 %	43.6 %
Flow pattern based heat transfer model combining the three zone model and the annular flow model [226]	69.1 %	68.4 %	76.3 %	64.3 %	66.7 %

Analytical models for flow boiling and flow condensation in microchannels are very complex, and the required assumptions to solve these models restrict the ability to capture the real physics of boiling and flow condensation mechanisms. Also, most empirical correlations are not able to predict other experimental data, even under a similar range of operating conditions where the correlations were obtained. The complex nature of flow boiling and flow condensation in micro channels such as liquid–vapour interactions, bubble growth in the flow as well as in the thin liquid film make analytical or empirical models of the two-phase flow a very difficult task. A serious need was felt to conduct a comprehensive study of phase change phenomena in microchannels to understand the fundamental mechanisms involved in the flow boiling and flow condensation before attempting any modeling. More accurate models for the heat transfer coefficient will be obtained if the modeling efforts are concentrated on each particular flow pattern. Therefore, flow pattern maps with well-developed flow patterns and transition lines may facilitate the modeling efforts but universal diabatic flow pattern maps should be developed at first, at least for a few working fluids at wide range of parameters and channel sizes and shapes.

5.2. Unstable and transient two phase flow patterns and heat transfer in microchannels

It is essential to understand the mechanisms of the unstable and transient two phase flow patterns and heat transfer in microchannels. Flow boiling and two phase instability in macrochannels are divided into dynamic and static instabilities. For dynamic instability, it is related to pressure, mass flux and temperature. It is commonly recognized that three types of oscillations exist in two phase flow and flow boiling in a macroscale channels: pressure drop oscillation, density wave oscillation and thermal oscillation [233–236]. These unstable behaviours may even cause deterioration of heat transfer and thus cause dryout and boiling crisis which may occur in subcooled conditions.

In recent years, a great deal of attention has been paid to the investigation of dynamic flow patterns and flow boiling instability in

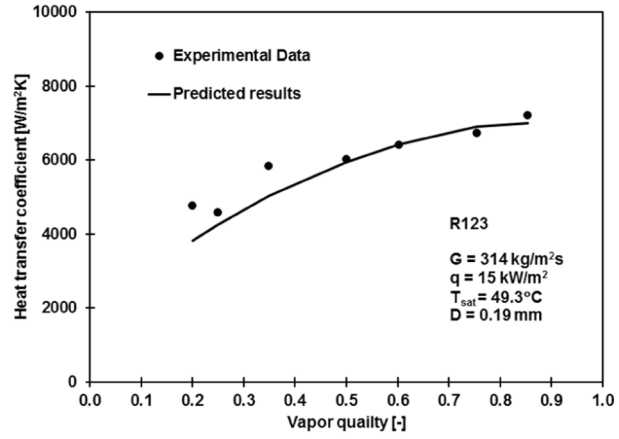

Fig. 47. (a) Comparison of the R123 heat transfer coefficient data to the flow pattern based heat transfer model combining the three zone heat transfer model [221] and the unified annular flow heat transfer model [218,226] at the conditions: mass flux G = 314 kg/m^{2}s, heat flux q = 15 kW/m^2, saturation temperature T_{sat} = 49.3 °C and tube diameter D = 0.19 mm by Cheng and Xia [5]; (b) Comparison of the R134 heat transfer coefficient data to the flow pattern based heat transfer model combining the three zone heat transfer model [221] and the unified annular flow heat transfer model [224,232] at the conditions: mass flux G = 676 kg/m^{2}s, heat flux q = 35.1 kW/m^2, saturation temperature T_{sat} = 24.6 °C and tube diameter D = 1.3 mm by Cheng and Xia [5].

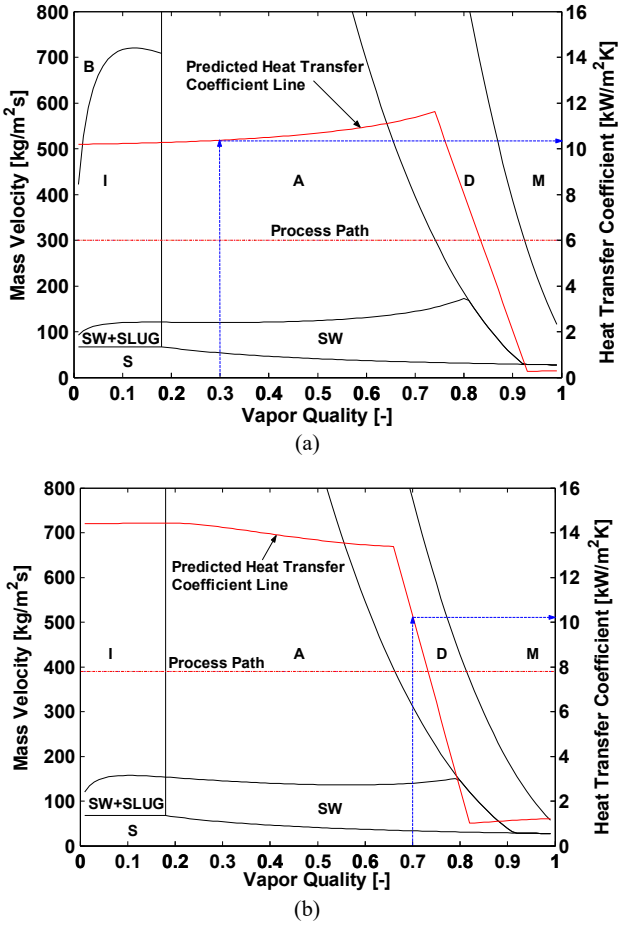

Fig. 48. Simulation of flow boiling model and flow pattern map by Cheng et al. [229]: (a) For 1.15 mm channel at the conditions: $q = 11$ kW/m^2, $T_{sat} = 10$ °C and $G = 300$ kg/m^{2}s with indicated value at × = 0.30; (b) For 3 mm channel at the conditions: $q = 20$ kW/m^2, $T_{sat} = 10$ °C and $G = 390$ kg/m^{2}s with indicated value at × = 0.70. (A- annular flow, B – bubbly flow, D – dryout, I – intermittent flow, M – mist flow, S – stratified flow, SLUG – slug flow and SW – stratified wavy flow).

microchannel. These include both single and parallel microchannels. Hetsroni et al. [233,234] found that small pressure fluctuations in their experiments of water boiling in 21 silicon triangular microchannels of a hydraulic diameter of 0.129 mm and observed periodic annular flow and periodic dry steam flow in the microchannel. In fact, these unstable flow boiling phenomena are caused due to the confined flow regimes changes, back flow and non-uniform flow and so on. Wang et al. [173,174] carried out simultaneous visualisation and measurement study on the effects of inlet/outlet configuration on flow boiling instabilities in parallel microchannel of a length of 30 mm and a hydraulic diameter of 0.186 mm. They found fluctuation of temperature and oscillations in the microchannels which correspond to the unstable flow regime and flow regime transition. Huang et al. [236] experimentally investigated the thermal response of multi-microchannels during flow boiling of R236fa and R245fa under transient heat loads with flow visualization. They investigated the base temperature response of multi-microchannel evaporators under transient heat loads, including cold startups and periodic step variations in heat flux using two different test sections for a wide variety of flow conditions. The effects on the base temperature behaviour of the test section, heat flux magnitude, mass flux, inlet subcooling, outlet saturation temperature, and fluid were investigated. The transient base temperature response, monitored by an infrared (IR) camera, was recorded simultaneously with the flow regime acquired by a high-speed video camera. For cold startups, it was found that reducing the inlet orifice width, heat flux magnitude, inlet subcooling, and outlet saturation temperature but increasing the mass flux decreased the maximum base temperature. Meanwhile, the time required to initiate boiling increased with the inlet orifice width, mass flux, inlet subcooling, and outlet saturation temperature but decreased with the heat flux magnitude. For periodic variations in heat flux, the resulting base temperature was found to oscillate and then damp out along the flow direction. Furthermore, the effects of mass flux and heat flux pulsation period were insignificant.

Lee et al. [76] investigated the interfacial behaviour and heat transfer mechanisms associated with flow boiling of R-134a in a microchannel evaporator. The test evaporator consists of 100 of 1 × 1 mm^2 square micro-channels. Large length of the micro-channels used (609.6 mm) is especially important to capturing broad axial variations of both flow and heat transfer behaviour. The fluid was supplied to the test evaporator in subcooled state to enable assessment of both the subcooled boiling and saturated boiling regions. They employed a combination of temperature measurements along the microchannels and high-speed video to explore crucial details of the flow, including dominant flow regimes, flow instabilities, and downstream dryout effects. As shown in Fig. 49, a series of schematics of transient flow patterns observed in their experimental study based on extensive analysis of video records. From a temporal standpoint, a single oscillation period consists of six sub-periods. Notice that the micro-channel is divided spatially into four distinct sections; flow within each varies during the successive sub-periods [76]. Flow patterns in the micro-channels are featured with transient fluctuations which are induced by flow instabilities. The dominant flow behaviour and related dryout effects are characterized with the aid of a new transient flow pattern map and a dryout map, respectively. Two sub-regions of the subcooled boiling region, partially developed boiling and fully developed boiling, are examined relative to dominant interfacial and heat transfer mechanisms in their study. The saturated boiling region is shown to consist of three separate sub-regions: nucleate boiling dominated for the vapor qualities below 0.3, combined nucleate and convective boiling for the vapor qualities between 0.3 and 0.5, and convective boiling dominated for the vapor qualities above 0.5. For the vapor qualities>0.5, dryout begins to take effect, causing a gradual decrease in the heat transfer coefficient followed downstream by a more severe decrease.

Understanding unstable and transient two phase flow patterns, bubble behaviour and flow pattern transitions is a very important aspect of two phase flow and heat transfer in microchannels and enhanced microchannels. However, this topic is much less concerned in the available research. Unstable and transient two phase flow patterns are very complicated in microchannels and enhanced microchannels but they play a crucial role in understanding the fundamentals of two phase flow and heat transfer in microchannels. Therefore, the relevant research needs to be extensively investigated to achieve systematic fundamental knowledge, mechanisms, theory and applications in developing accurate prediction methods for two phase flow and heat transfer in future.

6. Concluding remarks

Flow patterns, bubble growth and flow pattern transitions in microchannels have not yet completely understood although numerous research has been conducted over the past decades. Different flow patterns and mechanisms have been observed and proposed by different researchers. In particular, many researchers constructed their flow pattern maps according to only their own experimental data and hence these maps are only applicable to those specific conditions and fluids. Some researchers simply compared their flow pattern data to the existing flow pattern maps for macro-channels and microchannels without further modifying these flow pattern maps.

Well documented theoretically based flow pattern transition criteria and flow pattern maps for microchannels are still needed to be

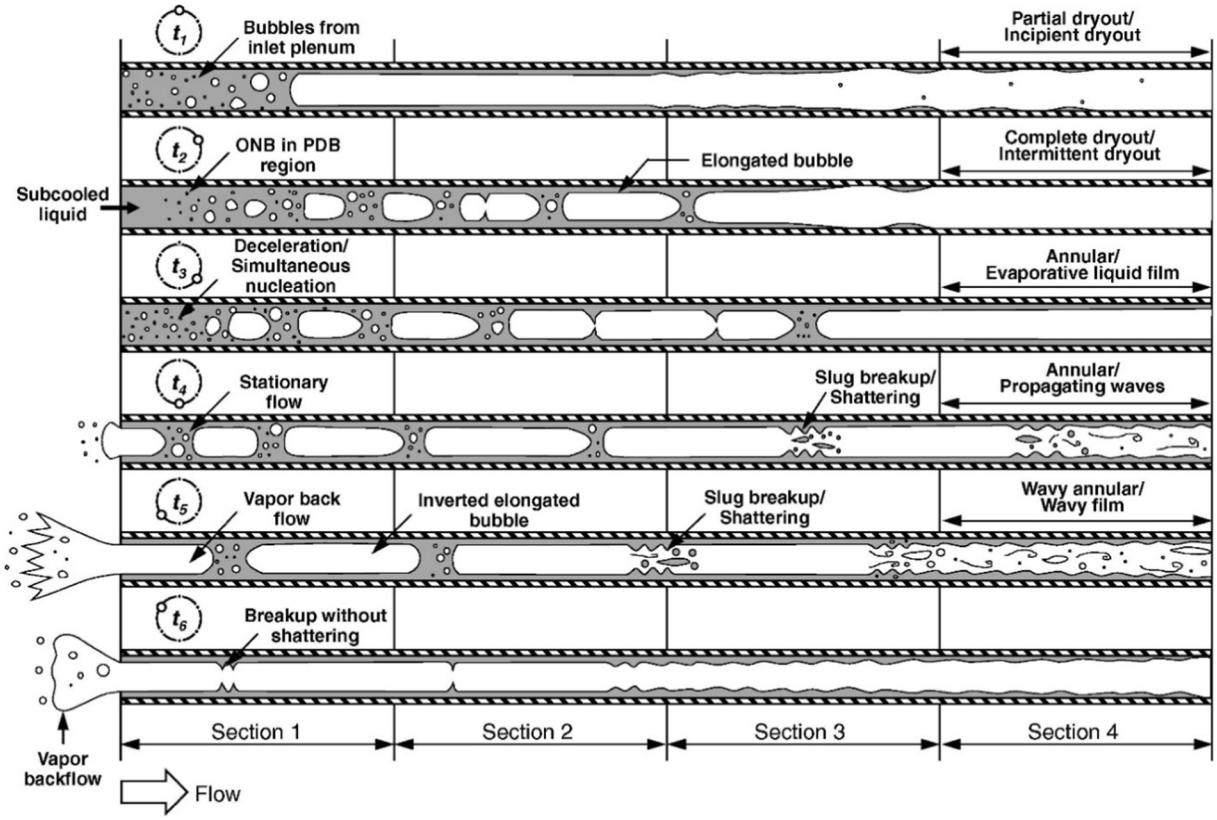

Fig. 49. Schematic of transient flow patterns observed at six different times within a single periodic cycle: t_1: beginning of the cycle, t_2: forward liquid advance, t_3: rapid bubble growth, t_4: commencement of transition pattern, t_5: commencement of wavy annular pattern, and t_6: end of liquid deficient period. The indicated sections are as follows: 1: subcooled boiling dominant, 2: combined saturated nucleate and convective boiling, 3: saturated convective boiling by annular film evaporation, and 4: intermittent dryout dominant region by Lee et al. [76].

established based on well performed experiments for both adiabatic and diabatic flow patterns, bubble growth and flow pattern transitions in microchannels under a wide range of test fluids and parameters. Therefore, effort should be made to develop generalized flow pattern maps for microchannels at a wide range of conditions, channels sizes and shapes and fluids. In the channel sizes with diameters from d 0.01 to 3 mm, both adiabatic and diabatic two phase flow patterns can be quite different as the effect of channel confinement. Many studies have been done for channels with diameter>1 mm. However, smaller diameter<1 mm should be focused in future. Extensive experimental studies are also needed for microchannels with enhanced structures.

Bubble dynamics is the fundamental to understanding the flow pattern evolution and transition mechanisms in diabatic phase change processes in microchannels. The confinement effect on the bubble coalescing has not fully understood. Especially, the bubble dynamics at stable and unstable flow boiling conditions may also significantly affect the flow pattern involution but are seldom considered. Diabatic gas liquid two phase flow patterns, bubble dynamics and flow pattern transitions are quite different from those adiabatic two phase flow and heat transfer. Therefore, systematic theoretical knowledge of bubble dynamics including bubble growth and coalescing in microchannels should be developed. Furthermore, the onset of CHF through its corresponding critical vapor quality is an important flow pattern map transition. such transition and flow map have not yet been well developed. Furthermore, unstable and transient flow patterns and their transitions are intrinsically related to bubble formation, growth and coalescing but the relevant research is much less studied. Liquid film plays a major role in understanding both the bubble and flow pattern evolution in microchannel as bubble may also grow from the liquid film and affect the interface between the bubble and the liquid film but such a topic has been less investigated.

There remain many challenges in fundamental understanding of flow patterns and bubble growth in gas liquid two phase flow in microchannels. Considerable experimental and theoretical research is still needed before reliable design tools become available. For instance, reliable prediction methods for flow boiling and flow condensation heat transfer in microchannels based on flow patterns and heat transfer mechanisms are needed. In particular, the heat transfer mechanisms strongly depend on the flow patterns affected by many factors in microchannels.

Although simplified flow boiling heat transfer correlations can be obtained from the experimental data ignoring the details of the flow patterns in microchannels, advanced knowledge of flow patterns allows more suitable assumptions to be applied for each particular flow pattern, leading to more accurate prediction methods for two phase flow and heat transfer in microchannels. Therefore, methods for predicting the occurrence of the major two-phase flow patterns in microchannel are useful and still needed. Current methods for predicting the flow patterns in microchannels are far from perfect. The difficulty and challenges arise out of the extremely varied morphological configurations, especially for flow boiling involving bubble growth which can be significantly affected by the channel confinement while the available experimental data show quite different results from one study to another. Therefore, effort should be made to contribute to both experimental and theoretical studies of two phase flow patterns, bubble dynamics and flow pattern transitions in the future. Furthermore, systematic experimental studies of unstable and transient two phase flow and flow patterns phenomena in microchannels should be conducted to provide accurate flow pattern data in order to further develop comprehensive and advanced knowledge, theory and models.

Declaration of Competing Interest

The authors declare that they have no known competing financial interests or personal relationships that could have appeared to influence the work reported in this paper.

Data availability

No data was used for the research described in the article.

References

[1] L. Cheng, G. Ribatski, J.R. Thome, Gas-liquid two-phase flow patterns and flow pattern maps: fundamentals and applications, ASME Appl. Mech. Rev. 61 (2008), 050802.

[2] L. Cheng, Microscale Flow Patterns and Bubble Growth in Microchannels, in *Microchannel Phase Change Heat Transfer*, Editor: Sujoy Kumar Saha, Elsevier Publisher, pp. 91-140. 2016.

[3] T.G. Karayiannis, M.M. Mahmoud, Flow boiling in microchannels: Fundamentals and applications, Appl. Therm. Eng. 15 (2017) 1372–1397.

[4] S. Szczukiewicz, N. Borhani, J.R. Thome, Two-phase flow operational maps for multi-microchannel evaporators, Int. J. Heat Fluid Flow 42 (2013) 176–189.

[5] L. Cheng, G. Xia, Fundamental issues, mechanisms and models of flow boiling heat transfer in microscale channels, Int. J. Heat Mass Transfer 108 (Part A) (2017) 97–127.

[6] S.G. Kandlikar, Fundamental issues related to flow boiling in minichannels and microchannels, Exp. Therm. Fluid Sci. 26 (2002) 389–407.

[7] L. Cheng, Flow Boiling Heat Transfer with Models in Microchannels, in *Microchannel Phase Change Heat Transfer*, Editor: Sujoy Kumar Saha, Elsevier Publisher, pp.141-191, 2016.

[8] J.R. Thome, A. Cioncolini, Flow Boiling in Microchannels, Adv. Heat Transfer 49 (2017) 157–224.

[9] L. Cheng, G. Xia, J.R. Thome, Flow boiling heat transfer and two phase flow phenomena of CO_2 in macro- and micro-channel evaporators: Fundamentals, applications and engineering design, Appl. Therm. Eng. 195 (2021), 170770.

[10] S. Szczukiewicz, M. Magnini, J.R. Thome, Proposed models, ongoing experiments, and latest numerical simulations of microchannel two-phase flow boiling, Int. J. Multiphase Flow 59 (2014) 84–101.

[11] L. Cheng, G. Xia, High heat flux cooling technologies using microchannel evaporators: fundamentals and challenges, Heat Transfer Eng (2023) in press.

[12] C.B. Tibirica, G. Ribatski, Flow boiling in micro-scale channels e Synthesized literature review, Int. J. Refrig. 36 (2) (2013) 301–324.

[13] G. Ribatski, A critical overview on the recent literature concerning flow boiling and two-phase flows inside micro-scale channels, Exp. Heat Transfer 26 (2–3) (2013) 198–246.

[14] L. Cheng, J.R. Thome, Cooling of microprocessors using flow boiling of CO_2 in a micro-evaporator: preliminary analysis and performance comparison, Appl. Therm. Eng. 29 (2009) 2426–2432.

[15] A. Etminan, Y.S. Muzychka, K. Pope, Liquid film thickness of two-phase slug flows in capillary microchannels: A review paper, Can. J. Chem. Eng. 100 (2022) 325–348.

[16] Y. Wang, Z. Wang, An overview of liquid-vapor phase change, flow and heat transfer in mini- and micro-channels, Int. J. Therm. Sci. 86 (2014) 227–245.

[17] J.R. Thome, L. Cheng, G. Ribatski, L.F. Vales, Flow boiling of ammonia and hydrocarbons: A state-of-the-art review, Int. J. Refrig. 31 (4) (2008) 603–620.

[18] L. Cheng, G. Xia, Study of the effect of the reduced pressure on a mechanistic heat transfer model for flow boiling of CO_2 in macroscale and microscale tubes, Heat Transfer Eng (2023) in press.

[19] L. Cheng, G. Xia, Flow boiling heat transfer and two-phase flow of carbon dioxide: Fundamentals, mechanistic models and applications. Proc. the 4th World Congr. Momentum, Heat Mass Transfer (MHMT'19) Rome, Italy – April 10–12, 2019.

[20] L. Cheng, T. Chen, Comparison of six typical correlations for upward flow boiling heat transfer with kerosene in a vertical smooth tube, Heat Transfer Eng. 21 (5) (2000) 27–34.

[21] V. Kumar, K.D.P. Vikash, Nigam, Multiphase fluid flow and heat transfer characteristics in microchannels, Chem. Eng. Sci. 169 (2017) 34–66.

[22] C. Baldassari, M. Marengo, Flow boiling in microchannels and microgravity, Prog. Energy Combust. Sci. 39 (1) (2013) 1–36.

[23] J.R. Thome, G. Ribatski, State-of-the-art of two-phase flow and flow boiling heat transfer and pressure drop of CO_2 in macro- and micro-channels, Int. J. Refrig. 28 (8) (2005) 1149–1168.

[24] L. Cheng, G. Xia, Q. Li, CO_2 evaporation process modelling: Fundamentals and engineering applications, Heat Transfer Eng. 43 (8–10) (2022) 1–28.

[25] L. Cheng, G. Xia, Q. Li, J.R. Thome, Fundamental issues, technology development, and challenges of boiling heat transfer, critical heat flux, and two-phase flow phenomena with nanofluids, Heat Transfer Eng. 40 (16) (2019) 1301–1336.

[26] S. Zu, X. Liao, Z. Huang, D. Li, Q. Jian, Visualization study on boiling heat transfer of ultra-thin flat heat pipe with single layer wire mesh wick, Int. J. Heat Mass Transfer 173 (2021), 121239.

[27] L. Cheng, Evaluation of correlations for supercritical CO_2 cooling convective heat transfer and pressure drop in macro- and micro-scale tubes, Int. J. Microscale Nanoscale Therm. Fluid Transp. Phenom. 5 (2) (2014) 113–126.

[28] J.R. Thome, The new frontier in heat transfer: microscale and nanoscale technologies, Heat Transfer Eng. 27 (9) (2006) 1–3.

[29] L. Cheng, Microscale and nanoscale thermal and fluid transport phenomena: Rapidly developing research fields, Int. J. Microscale Nanoscale Thermal Fluid Transport Phenomena 1 (2010) 3–6.

[30] L. Cheng, Z. Guo, G. Xia, A review on research and technology development of green hydrogen energy systems with thermal management and heat recovery, Heat Transfer Eng. (2023) accepted.

[31] J. Wang, Theory and practice of flow field designs for fuel cell scaling-up: A critical review, Appl. Energy 157 (2015) 640–663.

[32] S.G. Kandlikar, A roadmap for implementing minichannels in refrigeration and air-conditioning systems - current status and future directions, Heat Transfer Eng. 28 (12) (2007) 973–985.

[33] L. Cheng, D. Mewes, Review of two-phase flow and flow boiling of mixtures in small and mini channels, Int. J. Multiphase Flow 32 (2006) 183–207.

[34] J.R. Thome, State-of-the art overview of boiling and two-phase flows in microschannels, Heat Transfer Eng. 27 (9) (2006) 4–19.

[35] L. Cheng, G. Ribatski, J.R. Thome, Analysis of supercritical CO_2 cooling in macro- and micro-channels, Int. J. Refrig. 31 (8) (2008) 1301–1316.

[36] L. Cheng, E.P. Bandarra Filho, J.R. Thome, Nanofluid two-phase flow and thermal physics: a new research frontier of nanotechnology and its challenges, J. Nanosci. Nanotech. 8 (7) (2008) 3315–3332.

[37] L. Cheng, Fundamental issues of critical heat flux phenomena during flow boiling in microscale-channels and nucleate pool boiling in confined spaces, Heat Transfer Eng. 34 (13) (2013) 1011–1043.

[38] G. Ribatski, L. Wojtan, J.R. Thome, An analysis of experimental data and prediction methods for two-phase frictional pressure drop and flow boiling heat transfer in micro-scale channels, Exp. Therm. Fluid Sci. 31 (2006) 1–19.

[39] S.-M. Kim, I. Mudawar, Review of databases and predictive methods for heat transfer in condensing and boiling mini/micro-channel flows, Int. J. Heat and Mass Transfer 77 (2014) 627–652.

[40] L. Cheng, D. Mewes, A. Luke, Boiling phenomena with surfactants and polymeric additives: a state-of-the-art review, Int. J. Heat Mass Transfer 50 (2007) 2744–2771.

[41] L. Cheng, Critical heat flux in microscale channels and confined spaces: A review on experimental studies and prediction methods, Russian J. General Chemistry 82 (12) (2012) 2116–2131.

[42] T.A. Shedd, Next generation spray cooling: High heat flux management in compact spaces, Heat Transfer Eng. 28 (2) (2007, 2007,) 87–92.

[43] B. Agostini, M. Fabbri, J.E. Park, L. Wojtan, J.R. Thome, B. Michel, State of the art of high heat flux cooling technologies, Heat Transfer Eng. 28 (2007) 258–281.

[44] R.R. Schmidt, B.D. Notohardjono, High-End Server Low-Temperature Cooling, IBM J. Res. & Dev. 46 (6) (2002) 739–751.

[45] E. Costa-Patry, J. Olivierb, J.R. Thome, Heat transfer characteristics in a copper micro-evaporator and flow pattern-based prediction method for flow boiling in microchannels, Front. Heat and Mass Transfer (FHMT) 3 (2012), 013002.

[46] F. Yang, X. Dai, Y. Peles, P. Cheng, J. Khan, C. Li, Flow boiling phenomena in a single annular flow regime in microchannels (I): Characterization of flow boiling heat transfer, Int. J. Heat Mass Transfer 68 (2014) 703–715.

[47] S.-M. Kim, I. Mudawar, Universal approach to predicting saturated flow boiling heat transfer in mini/micro-channels – Part I. Dryout incipience quality, Int. J. Heat Mass Transfer 64 (2013) 1226–1238.

[48] S.-M. Kim, I. Mudawar, Universal approach to predicting saturated flow boiling heat transfer in mini/micro-channels – Part II. Two-phase heat transfer coefficient, Int. J. Heat Mass Transfer 64 (2013) 1239–1256.

[49] L. Cheng, L. Chai, Z. Guo, Thermal energy, process, and transport intensification-a brief review of literature in 2021 and prospects, Heat Transfer Res. 53 (18) (2022) 1–25.

[50] Z. Guo, L. Cheng, H. Cao, H. Zhang, X. Huang, et al., Heat transfer enhancement—A brief review of literature in 2020 and prospects, Heat Transfer Res. 52 (10) (2021) 65–92.

[51] Z. Guo, Heat transfer enhancement – a brief review of 2018 literature, J. Enhanced Heat Transfer 26 (5) (2019) 429–449.

[52] M.R. Özdemir, M.M. Mahmoud, T.G. Karayiannis, Flow Boiling of water in a rectangular metallic microchannel, Heat Transfer Eng. 42 (6) (2019) 492–516.

[53] G. Hedau, P. Dey, R. Raj, S.K. Saha, Combined effect of inlet restrictor and nanostructure on two-phase flow performance of parallel microchannel heat sinks, Int. J. Therm. Sci. 153 (2020), 106339.

[54] R. Diaz, Z. Guo, Enhanced conduction and pool boiling heat transfer on single-layer graphene-coated substrates, J. Enhanced Heat Transfer 26 (2) (2019) 127–143.

[55] S.K. Nayak, P.C. Mishra, Enhanced heat transfer from hot surface by nanofluid based ultrafast cooling: an experimental investigation, J. Enhanced Heat Transfer 26 (4) (2019) 415–428.

[56] H. Kubo, H. Takamatsu, H. Honda, Effects of size and number density of micro-reentrant cavities on boiling heat transfer from a silicon chip immersed in degassed and gas-dissolved FC-72, J. Enhanced Heat Transfer 6 (2–4) (1999) 151–160.

[57] H. Honda, H. Takamatsu, J.J. Wei, Enhanced boiling heat transfer from silicon chips with micro-pin fins immersed in FC-72, J. Enhanced Heat Transfer 10 (2) (2003) 211–224.

[58] U. Sajjad, A. Kumar, Chi-Chuan Wang, Nucleate pool boiling of sintered coated porous surfaces with dielectric liquid, HFE-7200, J. Enhanced Heat Transfer 27 (8) (2020) 767–784.

[59] V.V. Nirgude, S.K. Sahu, Nucleate boiling heat transfer performance of laser textured copper surfaces, J. Enhanced Heat Transfer 26 (6) (2019) 597–618.

[60] M. Piasecka, K. Strąk, Influence of the surface enhancement on the flow boiling heat transfer in a minichannel, Heat Transfer Eng. 40 (13–14) (2019) 1162–1175, https://doi.org/10.1080/01457632.2018.1457264.
[61] L. Cheng, T. Chen, Study of flow boiling heat transfer in a tube with axial microgrooves, Exp. Heat Transfer 14 (1) (2001) 59–73.
[62] D. Deng, L. Zeng, W. Sun, A review on flow boiling enhancement and fabrication of enhanced microchannels of microchannel heat sinks, Int. J. Heat Mass Transfer 175 (2021), 121332.
[63] Y. Li, G. Xia, Y. Jia, Y. Cheng, J. Wang, Experimental Investigation of flow boiling performance in microchannels with and without triangular cavities – A comparative study, Int. J. Heat Mass Transfer 108 (Part B) (2017) 1511–1526.
[64] Y.F. Li, G.D. Xia, D.D. Ma, J.L. Yang, W. Li, Experimental investigation of flow boiling characteristics in microchannel with triangular cavities and rectangular fins, Int. J. Heat Mass Transfer 148 (2020), 119036.
[65] J. Xu, X. Yu, W. Jin, Porous-wall microchannels generate high frequency "eye-blinking" interface oscillation, yielding ultra-stable wall temperatures, Int J Heat Mass Transfer 101 (2016) 341–353.
[66] Y.T. Jia, G.D. Xia, L.X. Zong, D.D. Ma, Y.X. Tang, A comparative study of experimental flow boiling heat transfer and pressure drop characteristics in porous-wall microchannel heat sink, Int J Heat Mass Transfer. 127 (Part A) (2019) 818–833.
[67] G. Xia, Y. Cheng, L. Cheng, Y. Li, Heat transfer characteristics and flow visualization during flow boiling of acetone in semi-open multi-microchannels, Heat Transfer Eng. 40 (16) (2019) 1349–1362.
[68] L.X. Zong, G.D. Xia, Y.T. Jia, L. Liu, D.D. Ma, et al., Flow boiling instability characteristics in microchannels with porous-wall, Int. J. Heat Mass Transfer 146 (2020), 118863.
[69] X. Cheng, H. Wu, Enhanced flow boiling performance in high-aspect-ratio groove-wall microchannels, Int. J. Heat Mass Transfer 164 (2021), 120468.
[70] C. Ren, W. Li, J. Ma, G. Huang, C. Li, Flow boiling in microchannels enhanced by parallel microgrooves fabricated on the bottom surfaces, Int. J. Heat Mass Transfer 166 (2021), 120756.
[71] Q. Zhao, J. Qiu, J. Zhou, M. Lu, Q. Li, et al., Visualization study of flow boiling characteristics in open microchannels with different wettability, Int. J. Heat Mass Transfer 180 (2021), 121808.
[72] W. Li, J. Ma, T. Alam, F. Yang, J. Khan, Flow boiling of HFE-7100 in silicon microchannels integrated with multiple micro-nozzles and reentry micro-cavities, Int. J. Heat Mass Transfer 123 (2018) (2018) 354–366.
[73] W. Li, C. Li, Z. Wang, Y. Chen, Enhanced flow boiling in microchannels integrated with supercapillary pinfin fences, Int. J. Heat Mass Transfer 183 (2022), 122185.
[74] D. Deng, L. Chen, W. Wan, T. Fu, X. Huang, Flow boiling performance in pin fin-interconnected reentrant microchannels heat sink in different operational conditions, Appl. Therm. Eng. 150 (2019) 1260–1272.
[75] D. Deng, Y. Xie, Q. Huang, Y. Tang, L. Huang, et al., Flow boiling performance of Ω-shaped reentrant copper microchannels with different channel sizes, Exp. Therm. Fluid Sci. 69 (2015) 8–18.
[76] S. Lee, V.S. Devahdhanush, I. Mudawar, Investigation of subcooled and saturated boiling heat transfer mechanisms, instabilities, and transient flow regime maps for large length-to-diameter ratio micro-channel heat sinks, Int. J. Heat Mass Transfer 123 (2018) 172–191.
[77] L.E. O'Neill, I. Mudawar, Review of two-phase flow instabilities in macro- and micro-channel systems, Int. J. Heat Mass Transfer 157 (2020), 119738.
[78] Y.K. Prajapati, M. Pathak, M.K. Khan, Bubble dynamics and flow boiling characteristics in three different microchannel configurations, Int. J. Therm. Sci. 112 (2017) 371–382.
[79] Y.K. Prajapati, P. Bhandari, Flow boiling instabilities in microchannels and their promising solutions – A review, Exp. Therm. Fluid Sci. 88 (2017) 576–593.
[80] J. Lee, S.J. Darges, I. Mudawar, Experimental investigation and analysis of parametric trends of instability in two-phase micro-channel heat sinks, Int. J. Heat Mass Transfer 170 (2021), 120980.
[81] H. Huang, J.R. Thome, Local measurements and a new flow pattern based model for subcooled and saturated flow boiling heat transfer in multi-microchannel evaporators, Int. J. Heat Mass Transfer 103 (2016) 701–714.
[82] H. Huang, L. Pan, R. Yan, Flow characteristics and instability analysis of pressure drop in parallel multiple microchannels, Appl. Therm. Eng. 142 (2018) 184–193.
[83] E.M. Fayyadh, M.M. Mahmoud, K. Sefiane, T.G. Karayiannis, Flow boiling heat transfer of R134a in multi microchannels, Int. J. Heat Mass Transfer 110 (2017) 422–436.
[84] Y. Lv, G. Xia, L. Cheng, D. Ma, Experimental investigation into unstable two phase flow phenomena during flow boiling in multi-microchannels, Int. J. Therm. Sci. 166 (2021), 106985.
[85] G. Xia, Y. Lv, L. Cheng, D. Ma, Y. Jia, Experimental study and dynamic simulation of the continuous two phase instable boiling in multiple parallel microchannels, Int. J. Heat Mass Transfer 138 (2019) 961–984.
[86] Y. Lv, G. Xia, L. Cheng, D. Ma, Experimental study on the pressure drop oscillation characteristics of the flow boiling instability with FC-72 in parallel rectangle microchannels, Int. Comm. Heat Mass Transfer 108 (2019), 104289.
[87] Z. Guo, A review on heat transfer enhancement with nanofluids, J. Enhanced Heat Transfer 27 (1) (2020) 1–70.
[88] L. Cheng, L. Liu, Boiling and two phase flow phenomena of refrigerant-based nanofluids: fundamentals, applications and challenges, Int. J. Refrig. 36 (2) (2013) 421–446.
[89] G. Xia, M. Du, L. Cheng, W. Wang, Experimental study on the nucleate boiling heat transfer characteristics of a water-based multi-walled carbon nanotubes nanofluid in a confined space, Int. J. Heat Mass Transfer (113) (2017) 59–69.
[90] R.K., Shah, Classification of Heat Exchangers. In: Heat Exchangers: Thermal Hydraulic Fundamentals and Design (Eidted by Kakac S., Bergles A.E., Mayinger F.), Hemisphere Publishing Corp., Washington DC, 1986, pp 9-46.
[91] S.S. Mehendale, A.M. Jacobi, R.K. Shah, Fluid flow and heat transfer at micro- and meso-scales with application to heat exchanger design, Applied Mech. Revs. 53 (2000) 175–193.
[92] K.A. Triplett, S.M. Ghiaasiaan, S.I. Abdel-Khalik, D.L. Sadowski, Gas-liquid two-phase flow in microchannels. Part I: Two-phase flow patterns, Int. J. Multiphase Flow 25 (1999) 377–394.
[93] P.A. Kew, K. Cornwell, Correlations for the prediction of boiling heat transfer in small-diameter channels, Appl. Thermal Eng. 17 (1997) 705–715.
[94] J. Li, B. Wang, Size effect on two-phase flow regime for condensation in micro/mini tubes, Heat Transfer – Asian Research 32 (2003) 65–71.
[95] N. Brauner, D. Moalem-Maron, Identification of the range of small diameter conduits regarding two-phase flow pattern transitions, Int. Comm. Heat Mass Transfer 19 (1992) 29–39.
[96] T. Harirchian, S.V. Garimella, A comprehensive flow regime map for microchannel flow boiling with quantitative transition criteria, Int. J. Heat Mass Transfer 53 (2010) 2694–2702.
[97] C.L. Ong, J.R. Thome, Macro-to-microchannel transition in two-phase flow: Part 1 – Two-phase flow patterns and film thickness measurements, Exp. Therm. Fluid Sci. 35 (2011) 37–47.
[98] L. Cheng, G. Ribatski, L. Wojtan, J.R. Thome, New flow boiling heat transfer model and flow pattern map for carbon dioxide evaporating inside horizontal tubes, Int. J. Heat Mass Transfer 49 (2006) 4082–4094.
[99] L. Cheng, G. Ribatski, J. Quibén Moreno, J.R. Thome, New prediction methods for CO_2 evaporation inside tubes: Part I – A two-phase flow pattern map and a flow pattern based phenomenological model for two-phase flow frictional pressure drops, Int. J. Heat Mass Transfer 51 (2008) 111–124.
[100] L. Cheng, G. Ribatski, J.R. Thome, New prediction methods for CO_2 evaporation inside tubes: Part II – An updated general flow boiling heat transfer model based on flow patterns, Int. J. Heat Mass Transfer 51 (2008) 125–135.
[101] G.R. Tibirica, Flow boiling heat transfer of R134a and R245fa in a 2.3 mm tube, Int. J. Heat Mass Transfer 53 (2010) 2459–2468.
[102] L. Cheng, L. Liu, Analysis and evaluation of gas-liquid two-phase frictional pressure drop prediction methods for microscale channels, Int. J. Microscale Nanoscale Thermal Fluid Transport Phenomena 2 (2011) 259–280.
[103] L. Cheng, H. Zou, Evaluation of flow boiling heat transfer correlations with experimental data of R134a, R22, R410A and R245fa in microscale channels, Int. J. Microscale Nanoscale Thermal Fluid Transport Phenomena 1 (2010) 363–380.
[104] L. Wojtan, T. Ursenbacher, J.R. Thome, Investigation of flow boiling in horizontal tubes: Part I – A new diabatic two-phase flow pattern map, Int. J. Heat Mass Transfer 48 (2005) 2955–2969.
[105] L. Wojtan, T. Ursenbacher, J.R. Thome, Investigation of flow boiling in horizontal tubes: Part II – development of a new heat transfer model for stratified-wavy, dryout and mist flow regimes, Int. J. Heat Mass Transfer 48 (2005) 2970–2985.
[106] J. Moreno Quibén, L. Cheng, R.J. da Silva Lima, J.R. Thome, Flow boiling in horizontal flattened tubes: part I – two-phase frictional pressure drop results and model, Int. J. Heat Mass Transfer 52 (2009) 3634–3644.
[107] J. Moreno Quibén, L. Cheng, R.J. da Silva Lima, J.R. Thome, Flow boiling in horizontal flattened tubes: part II – flow boiling heat transfer results and model, Int. J. Heat Mass Transfer 52 (2009) 3645–3653.
[108] B. Cai, G. Xia, L. Cheng, Z. Wang, Experimental investigation on spatial phase distributions for various flow patterns and frictional pressure drop characteristics of gas liquid two-phase flow in a horizontal helically coiled rectangular tube, Exp. Therm. Fluid Sci. 142 (2023), 110806.
[109] G. Xia, B. Cai, L. Cheng, Z. Wang, Experimental study and modelling of average void fraction of gas-liquid two-phase flow in a helically coiled rectangular channel, Exp. Therm. Fluid Sci. 94 (2018) 9–22.
[110] G. Xia, B. Cai, L. Cheng, Z. Wang, Flow regime visualization and identification of air–water two-phase flow in a horizontal helically coiled rectangular channel, Heat Transfer Eng. 43 (8 – 10) (2022). pp. 720-736.
[111] A. Gunther, K.F. Jensen, Multiphase microfluidics: from flow characteristics to chemical and materials synthesis, Lab Chip 6 (2006) 1487–1503.
[112] D.R. Link, S.L. Anna, D.A. Weitz, H.A. Stone, Geometrically mediated breakup of drops in microfluidic devices, Phys. Rev. Lett. 92 (2004), 054503.
[113] J.J. Heras, A.J. Sederman, L.F. Gladden, Ultrafast velocity imaging of single- and two-phase flows in a ceramic monolith, Magn. Reson. Imaging 23 (2005) 387–389.
[114] S. Waelchli, Two-phase flow characteristics in gas–liquid microreactors, Dissertation, ETH Zurich No. 16116 (2005).
[115] J.H. Kinney, M.C. Nichols, X-ray tomographic microscopy (XTM) using synchrotron radiation, Annu. Rev. Mater. Sci. 22 (1992) 121–152.
[116] M.A. Le Gros, G. McDermott, C.A. Larabell, X-ray tomography of whole cells, Curr. Opin. Struct. Biol. 15 (2005) 593–600.
[117] N. de Mas, A. Gunther, T. Kraus, M.A. Schmidt, K.F. Jensen, Scaled-out multilayer gas–liquid microreactor with integrated velocimetry sensors, Ind. Eng. Chem. Res. 44 (2005) 8997–9013.
[118] T. Kraus, A. Gunther, N. de Mas, M.A. Schmidt, K.F. Jensen, An integrated multiphase flow sensor for microchannels, Exp. Fluids 36 (6) (2004) 819–832.
[119] B.M.A. Wolffenbuttel, T.A. Nijhuis, A. Stankiewicz, J.A. Moulijn, Novel method for non-intrusive measurement of velocity and slug length in two- and three phase slug flow in capillaries, Meas. Sci. Technol. 13 (2002) 1540–1544.
[120] R. Revellin, V. Dupont, T. Ursenbacher, J.R. Thome, I. Zun, Characterization of diabatic two-phase flows in microchannels: flow parameter results for R-134a in a 0.5 mm channel, Int. J. Multiphase Flow 32 (2006) 755–774.

[121] R. Revellin, J.R. Thome, Experimental investigation of R-134a and R-245fa two-phase flow in microchannels for different flow conditions, Int. J. Heat Fluid Flow 28 (1) (2007) 63–71.
[122] D.C. Lowe, K.S. Rezkallah, Flow regime identification in microgravity two-phase flows using void fraction signals, Int. J. Multiphase Flow 25 (1999) 433–457.
[123] I. Hassan, M. Vaillancourt, K. Pehlivan, Two-phase flow regime transitions in microchannels: A comparative experimental study, Microscale Thermophys. Eng. 9 (2) (2005) 165–182.
[124] F. Ronshin, E. Chinnov, Experimental characterization of two-phase flow patterns in a slit microchannel, Exp. Therm. Fluid Sci. 103 (2019) 262–273.
[125] E.A. Chinnov, F.V. Ronshin, O.A. Kabov, Two-phase flow patterns in short horizontal rectangular microchannels, Int. J. Multiphase Flow 80 (2016) 57–68.
[126] V.V. Kuznetsov, A.S. Shamirzaev, I.A. Kozulin, S.P. Kozlov, Correlation of the flow pattern and flow boiling heat transfer in microchannels, Heat Transfer Eng. 34 (2–3) (2013) 235–245.
[127] S. Hardt, B. Schilder, D. Tiemann, G. Kolb, V. Hessel, P. Stephan, Analysis of flow patterns emerging during evaporation in parallel microchannels, Int. J. Heat Mass Transfer 50 (1–2) (2007) 226–239.
[128] M.H. Matin, S. Moghaddam, Mechanism of transition from elongated bubbles to wavy-annular regime in flow boiling through microchannels, Int. J. Heat Mass Transfer 176 (2021), 121464.
[129] S. Lee, I. Mudawar, Investigation of flow boiling in large micro-channel heat exchangers in a refrigeration loop for space applications, Int. J. Heat Mass Transfer. 97 (2016) 110–129.
[130] Y. Lin, Y. Luo, J. Li, W. Li, Heat transfer, pressure drop and flow patterns of flow boiling on heterogeneous wetting surface in a vertical narrow microchannel, Int. J. Heat Mass Transfer 172 (2021), 121158.
[131] G. Xia, Z. Chen, L. Cheng, D. Ma, Y. Zhai, Y. Yang, Micro-PIV visualization of fluid flow and numerical simulation of flow and heat transfer characteristics in micro pin-fin heat sinks with three different structures, Int. J. Therm. Sci. 119 (2017) 9–23.
[132] J.G. Santiago, S.T. Wereley, C.D. Meinhart, D.J. Beebe, R.J. Adrian, A particle image velocimetry system for microfluidics, Exp. Fluids 25 (1998) 316–319.
[133] C.D. Meinhart, S.T. Wereley, J.G. Santiago, PIV measurements of a microchannel flow, Exp. Fluids 27 (1999) 414–419.
[134] K.V. Sharp, R.J. Adrian, Transition from laminar to turbulent flow in liquid filled microtubes, Exp. Fluids 36 (2004) 741–747.
[135] A.V. Kovalev, A.A. Yagodnitsyna, A.V. Bilsky, Flow hydrodynamics of immiscible liquids with low viscosity ratio in a rectangular microchannel with T-junction, Chem. Eng. J. 352 (2018) 120–132.
[136] N. Shao, A. Gavriilidis, P. Angeli, Flow regimes for adiabatic gas–liquid flow in microchannels, Chem. Eng. Sci. 64 (2009) 2749–2761.
[137] A. Kawahara, P.-M.-Y. Chung, M. Kawaji, Investigation of two-phase flow pattern, void fraction and pressure drop in a microchannel, Int. J. Multiphase Flow 28 (9) (2002) 1411–2135.
[138] P.-M.-Y. Chung, M. Kawaji, The effect of channel diameter on adiabatic two-phase flow characteristics in microchannels, Int. J. Multiphase Flow 30 (2004) 735–761.
[139] M. Kawaji, P.-M.-Y. Chung, Adiabatic gas–liquid flow in microchannels, Microscale Thermophys. Eng. 8 (3) (2004) 239–257.
[140] M. Suo, P. Griffith, Two-phase flow in capillary tubes, J. Basic Eng. 86 (1964) 576–582.
[141] Y. Taitel, A.E. Dukler, A model for predicting flow regime transitions in horizontal and near horizontal gas-liquid flow, AIChE J. 22 (1976) 47–55.
[142] T.S. Zhao, Q.C. Bi, Co-current air-water two-phase flow patterns in vertical triangular microchannels, Int. J. Multiphase Flow 27 (2001) 765–782.
[143] J. Pettersen, Flow vaporization of CO_2 in microchannel tubes, Exp. Thermal Fluid Sci. 28 (2004) 111–121.
[144] B. Lowry, M. Kawaji, Adiabatic vertical two-phase flow in narrow flow channels, AIChE Sym. Ser., Heat Transfer- Houston 1988, pp. 133-139.
[145] C.A. Damianides, J.W. Westwater, Two-phase flow patterns in a compact heat exchanger and in small tubes, in: *Proc. 2nd U.K. National Conf. on Heat Transfer*, 2, 1988, pp. 1257-1268.
[146] D. Liu, S. Wang, Flow pattern and pressure drop of upward two-phase flow in vertical capillaries, Ind. Eng. Chem. Res. 47 (2008) 243–255.
[147] A. Sur, D. Liu, Adiabatic air-water two-phase flow in circular microchannels, Int. J. Therm. Sci. 53 (2012) 18–34.
[148] L. Chen, Y.S. Tian, T.G. Karayiannis, The effect of tube diameter on vertical two-phase flow regimes in small tubes, Int. J. Heat Mass Transfer 49 (2006) 4220–4230.
[149] C.Y. Yang, C.C. Shieh, Flow pattern of air-water and two-phase R-134a in small circular tubes, Int. J. Multiphase Flow 27 (2011) 1163–1177.
[150] A. Serizawa, Z. Feng, Z. Kawara, Two-phase flow in microchannels, Exp. Therm. Fluid Sci. 26 (2002) 703–714.
[151] H. Ide, A. Kariyasaki, T. Fukano, Fundamental data on the gas-liquid two-phase flow in microchannels, Int. J. Thermal Sci. 46 (2007) 519–530.
[152] T. Fukano, A. Kariyasaki, Characteristics of gas-liquid two-phase flow in a capillary tube, Nucl. Eng. Design 141 (1993) 59–68.
[153] T. Cubaud, C.-M. Ho, Transport of bubbles in square Microchannels, Phys. Fluids 16 (2004) 4575–4585.
[154] C.W. Choi, D.I. Yu, M.H. Kim, Adiabatic two-phase flow in rectangular microchannels with different aspect ratios: Part I - Flow pattern, pressure drop and void fraction, Int. J. Heat Mass Transfer 54 (1–3) (2011) 616–624.
[155] S. Saisorn, S. Wongwises, Flow pattern, void fraction and pressure drop of two-phase air–water flow in a horizontal circular micro-channel, Exp. Therm. Fluid Sci. 32 (3) (2008) 748–760.
[156] S. Saisorn, S. Wongwises, The effects of channel diameter on flow pattern, void fraction and pressure drop of two-phase air–water flow in circular micro-channels, Exp. Therm. Fluid Sci. 34 (2010) 454–462.
[157] S. Saisorn, S. Wongwises, Adiabatic two-phase gas–liquid flow behaviors during upward flow in a vertical circular micro-channel, Exp. Therm. Fluid Sci. 69 (2015) 158–168.
[158] X. Wang, Y. Yong, P. Fan, G. Yu, C. Yang, Z.-S. Mao, Flow regime transition for cocurrent gas–liquid flow in micro-channels, Chem. Eng. Sci. 69 (2012) 578–586.
[159] Y. Liu, S. Wang, Distribution of gas-liquid two-phase slug flow in parallel micro-channels with different branch spacing, Int. J. Heat Mass Transfer 132 (2019) 606–617.
[160] E.X. Barreto, J.L.G. Oliveira, J.C. Passos, Analysis of air–water flow pattern in parallel microchannels: A visualization study, Exp. Therm. Fluid Sci. 63 (2015) 1–8.
[161] Y. Zhao, G. Chen, C. Ye, Q. Yuan, Gas–liquid two-phase flow in microchannel at elevated pressure, Chem. Eng. Sci. 87 (2013) 122–132.
[162] H.-C. Shin, S.-M. Kim, Experimental investigation of two-phase flow regimes in rectangular micro-channel with two mixer types, Chem. Eng. J. 448 (2022), 137581.
[163] H.-C. Shin, S.-M. Kim, Generalized flow regime map for two-phase mini/micro-channel flows, Int. J. Heat Mass Transfer 196 (2022), 123298.
[164] V. Haverkamp, V. Hessel, H. Lowe, G. Menges, M.J.F. Warnier, E.V. Rebrov, M.H.J.M. de Croon, J.C. Schouten, M.A. Liauw, Hydrodynamics and mixer-induced bubble formation in micro bubble columns with single and multiple-channels, Chem. Eng. Technol. 29 (9) (2006) 1015–1026.
[165] E.A. Chinnov, F.V. Ron'shin, O.A. Kabov, Regimes of two-phase flow in micro- and minichannels (review), Thermophys. Aeromech. 22 (2015) 265–284.
[166] T. Cubaud, U. Ulmanella, C.M. Ho, Two-phase flow in microchannels with surface modifications, Fluid Dyn. Res. 38 (11) (2006) 772–786.
[167] C.Y. Lee, S.Y. Lee, Influence of surface wettability on transition of two-phase flow pattern in round mini-channels, Int. J. Multiphase Flow 34 (2008) 706–711.
[168] A.M. Barajas, R.L. Panton, The effects of contact angle on twophase flow in capillary tubes, Int. J. Multiphase Flow 19 (1993) 337–346.
[169] C. Choi, D.I. Yu, M. Kim, Surface wettability effect on flow pattern and pressure drop in adiabatic two-phase flows in rectangular microchannels with T-junction mixer, Exp. Therm. Fluid Sci. 35 (2011) 1086–1109.
[170] G. Hetsroni, A. Mosyak, Z. Segal, E. Pogrebnyak, Two-phase flow patterns in parallel micro-channels, Int. J. Multiphase Flow 29 (2003) 341–360.
[171] C.B. Tibiriçá, G. Ribatski, Flow patterns and bubble departure fundamental characteristics during flow boiling in microscale channels, Exp. Therm. Fluid Sci. 59 (2014) 152–165.
[172] T. Harirchian, S.V. Garimella, Effects of channel dimension, heat flux, and mass flux on flow boiling regimes in microchannels, Int. J. Multiphase Flow 35 (2009) 349–362.
[173] G. Wang, P. Cheng, A.E. Bergles, Effects of inlet/outlet configurations on flow boiling instability in parallel microchannels, Int. J. Heat and Mass Transfer 51 (2008) 2267–2281.
[174] G.D. Wang, P. Cheng, H.Y. Wu, Unstable and stable flow boiling in parallel microchannels and in a single microchannel, Int. J. Heat Mass Transfer 50 (2007) 4297–4310.
[175] H. Tuo, P. Hrnjak, Visualization and measurement of periodic reverse flow and boiling fluctuations in a microchannel evaporator of an air-conditioning system, Int. J. Heat and Mass Transfer 71 (2014) 639–652.
[176] W.-C. Liu, C.-Y. Yang, Two-phase flow visualization and heat transfer performance of convective boiling in micro heat exchangers, Exp. Therm. Fluid Sci. 57 (2014) 358–364.
[177] R. Revellin, J.R. Thome, A New type of diabatic flow pattern map for boiling heat transfer in microchannels, J. Micromech. & Microeng. 17 (2007) 788–796.
[178] G.P. Celata, M. Cumo, D. Dossevi, R.T.M. Jilisen, S.K. Saha, G. Zummo, Flow pattern analysis of flow boiling inside a 0.48 mm microtube, Int. J. Therm. Sci. 58 (2012) 1–8.
[179] J.W. Coleman, S. Garimella, Characterization of two-phase flow patterns in small diameter round and rectangular tubes, Int. J. Heat Mass Transfer 42 (1999) 2869–2881.
[180] T. Chen, S.V. Garimella, Measurements and high-speed visualizations of flow boiling of a dielectric fluids in a silicon microchannel heat sink, Int. J. Multiphase Flow 32 (2006) 957–971.
[181] W. Owhaib, B. Palm, C. Martin-Callizo, Flow boiling visualization in a vertical Circular minichannel at high vapor quality, Exp. Therm. Fluid Sci. 30 (2006) 755–763.
[182] E. Sobierska, R. Kulenovic, R. Mertz, M. Groll, Experimental results of flow boiling of water in a vertical microchannels, Exp. Therm. Fluid Sci. 31 (2007) 111–119.
[183] T.H. Yen, M. Shoji, F. Takemura, Y. Suzuki, N. Kasage, Visualization of convective boiling heat transfer in single microchannels with different shaped cross-sections, Int. J. Heat Mass Transfer 49 (2006) 3884–3894.
[184] L. Wojtan, R. Revellin, J.R. Thome, Investigation of critical heat flux in single, uniformly heated microchannels, Exp. Thermal Fluid Sci. 30 (2006) 765–774.
[185] C. Keepaiboon, S.i. Wongwises, Two-phase flow patterns and heat transfer characteristics of R134a refrigerant during flow boiling in a single rectangular micro-channel, Exp. Therm. Fluid Sci. 66 (2015) 36–45.
[186] A. Bar-Cohen, E. Rahim, Modeling and prediction of two-phase microgap channel heat transfer characteristics, Heat Transfer Eng. 30 (2009) 601–625.
[187] J.R. Thome, A. Bar-Cohen, R. Revellin, I. Zun, Unified mechanistic multiscale mapping of two-phase flow patterns in microchannels, Exp. Therm. Fluid Sci. 44 (2013) 1–22.

[188] T. Alam, W. Li, W. Chang, F. Yang, J. Khan, C. Li, Favourably regulating two-phase flow regime of flow boiling HFE-7100 in microchannels using silicon nanowires, Sci. Rep. 11 (2021) 11131.
[189] A. Kalani, S.G. Kandlikar, Flow patterns and heat transfer mechanisms during flow boiling over open microchannels in tapered manifold (OMM), Int. J. Heat Mass Transfer 89 (2015) 494–504.
[190] G. Nema, S. Garimella, B.M. Fronk, Flow regime transitions during condensation in microchannels, Int. J. Refrig. 40 (2014) 227–240.
[191] A.H. Al-Zaidi, M.M. Mahmoud, T.G. Karayiannis, Condensation flow patterns and heat transfer in horizontal microchannels, Exp. Therm. Fluid Sci. 90 (2018) 153–173.
[192] Y. Lei, I. Mudawar, Z. Chen, Computational and experimental investigation of condensation flow patterns and heat transfer in parallel rectangular micro-channels, Int. J. Heat Mass Transfer 149 (2020), 119158.
[193] J. Wu, M. Shi, Y. Chen, X. Li, Visualization study of steam condensation in wide rectangular silicon microchannels, Int. J. Therm. Sci. 49 (2010) 922–930.
[194] X. Ma, X. Fan, Z. Lan, T. Hao, Flow patterns and transition characteristics for steam condensation in silicon microchannels, J. Micromech. Microeng. 21 (2011), 075009.
[195] S.-M. Kim, I. Mudawar, Flow condensation in parallel micro-channels - Part 2: Heat transfer results and correlation technique, Int. J. Heat Mass Transfer 55 (2012) 984–994.
[196] S.-M. Kim, J. Kim, I. Mudawar, Flow condensation in parallel micro-channels - Part 1: Experimental results and assessment of pressure drop correlations, Int. J. Heat Mass Transfer 55 (2012) 971–983.
[197] G. El Achkar, M. Miscevic, P. Lavieille, J. Lluc, J. Hugon, Flow patterns and heat transfer in a square cross-section micro condenser working at low mass flux, Appl. Therm. Eng. 59 (2013) 704–716.
[198] R. Jiang, X. Ma, Z. Lan, Y. Bai, T. Bai, Visualization study of condensation of ethanol–water mixtures in trapezoidal microchannels, Int. J. Heat Mass Transfer 90 (2015) 339–349.
[199] J. Kaew-On, N. Naphattharanun, R. Binmud, S. Wongwises, Condensation heat transfer characteristics of R134a flowing inside mini circular and flattened tubes, Int. J. Heat Mass Transfer 102 (2016) 86–97.
[200] D. Jige, S. Kikuchi, H. Eda, N. Inoue, S. Koyama, Two-phase flow characteristics of R32 in horizontal multiport minichannels: Flow visualization and development of flow regime map, Int. J. Refrig. 95 (2018) 156–164.
[201] H. El Mghari, H. Louahlia-Gualous, Experimental and numerical investigations of local condensation heat transfer in a single square microchannel under variable heat flux, Int. Commun. Heat Mass Transfer 71 (2016) 197–207.
[202] J. Wang, J.M. Li, Y. Hwang, Flow pattern transition during condensation of R134a and R1234ze(E) in microchannel arrays, Appl. Therm. Eng. 115 (2017) 244–255.
[203] G.T. Liang, N. Mascarenhas, I. Mudawar, Analytical and experimental determination of slug flow parameters, pressure drop and heat transfer coefficient in micro-channel condensation, Int. J. Heat Mass Transfer 111 (2017) 1218–1233.
[204] Y. Ding, L. Jia, Study on flow condensation characteristics of refrigerant R410a in a single rectangular micro-channel, Int. J. Heat Mass Transfer 114 (2017) 125–134.
[205] J.C. Chen, Correlation for boiling heat transfer to saturated fluids in convective flow, Industrial and Engineering Chemistry – Process Design and Development 5 (3) (1966) 322–329.
[206] K.E. Gungor, R.H.S. Winterton, A general correlation for flow boiling in tubes and annuli, Int. J. Heat Mass Transfer 29 (3) (1986) 351–358.
[207] Z. Liu, R.H.S. Winterton, A general correlation for saturated and subcooled flow boiling in tubes and annuli, based on a nucleate pool boiling equation, Int. J. Heat Mass Transfer 34 (11) (1991) 2759–2766.
[208] S.G. Kandlikar, A general correlation for two-phase flow boiling heat transfer coefficient inside horizontal and vertical tubes, J. Heat Transfer 102 (1990) 219–228.
[209] S.G. Kandlikar, A model for predicting the two-phase flow boiling heat transfer coefficient in augmented tube and compact heat exchanger geometries, J. Heat Transfer 113 (1991) 966–972.
[210] D. Steiner, J. Taborek, Flow boiling heat transfer in vertical tubes correlated by an asymptotic model, Heat Transfer Eng. 13 (2) (1992) 43–69.
[211] N. Kattan, J.R. Thome, D. Favrat, Flow boiling in horizontal tubes: Part-3: Development of a new heat transfer model based on flow patterns, ASME J. Heat Transfer 120 (1998) 156–165.
[212] W. Zhang, T. Hibiki, K. Mishima, Correlation for flow boiling heat transfer in mini-channels, Int. J. Heat Mass Transfer 47 (2004) 5749–5763.
[213] J. Lee, I. Mudawar, Two-phase flow in high-heat-flux micro-channel heat sink for refrigeration cooling applications: Part II-heat transfer characteristics, Int. J. Heat Mass Transfer 48 (2005) 941–955.
[214] S.S. Bertsch, E.A. Groll, S.V. Garimella, A composite heat transfer correlation for saturated flow boiling in small channels, Int. J. Heat Mass Transfer 52 (2009) 2110–2118.
[215] L. Sun, K. Mishima, An evaluation of prediction methods for saturated methods for saturated flow boiling heat transfer, Int. J. Heat Mass Transfer 52 (2009) 5323–5329.
[216] W. Li, Z. Wu, A general correlation for evaporative heat transfer in micro/mini-channels, Int. J. Heat Mass Transfer 53 (2010) 1778–1787.
[217] X. Huo, L. Chen, Y.S. Tian, T.G. Karayiannis, Flow boiling and flow regimes in small diameter tubes, Appl. Therm. Eng. 24 (2004) 1225–1239.
[218] T. Chen, S.V. Garimella, Measurements and high-speed visualization of flow boiling of a dielectric fluid in a silicon microchannel heat sink, International Journal of Multiphase Flow 32 (8) (2006) 957–971.
[219] T. Chen, S.V. Garimella, Flow boiling heat transfer to a dielectric coolant in a microchannel heat sink, IEEE Trans. Compon. Packag. Technol. 30 (1) (2006) 24–31.
[220] A.M. Jacobi, J.R. Thome, Heat transfer model for evaporation of elongated bubble flows in microchannels, J. Heat Transfer 124 (2002) 1131–1136.
[221] J.R. Thome, V. Dupont, A.M. Jacobi, Heat transfer model for evaporation in microchannels. Part I: Presentation of the model, Int. J. Heat Mass Transfer 47 (2004) 3375–3385.
[222] V. Dupont, J.R. Thome, A.M. Jacobi, Heat transfer model for evaporation in microchannels. Part II: Comparison with the database, Int. J. Heat Mass Transfer 47 (2004) 3387–3401.
[223] D. Shiferaw, T.G. Karayiannis, D.B.R. Kenning, Flow boiling in a 1.1 mm tube with R134a: Experimental results and comparison with model, Int. J. Thermal Sci. 48 (2009) 331–341.
[224] L. Consolini, J.R. Thome, A heat transfer model for evaporation of coalescing bubble in micro-channel flow, Int. J. Heat Fluid Flow 31 (2010) 115–125.
[225] L. Cheng, Modelling of heat transfer of upward annular flow in vertical tubes, Chem. Eng. Comm. 194 (2007) 975–993.
[226] W. Qu, I. Mudawar, Flow boiling heat transfer in two-phase micro-channel heat sinks—II. Annular two-phase flow model, Int. J. Heat Mass Transfer 46 (2003) 2773–2784.
[227] S.-M. Kim, I. Mudawar, Theoretical model for local heat transfer coefficient for annular flow boiling in circular mini/micro-channels, Int. J. Heat Mass Transfer 73 (2014) 731–742.
[228] S.M. Magnini, J.R. Thome, Proposed models, ongoing experiments, and latest numerical simulations of microchannel two-phase flow boiling, Int. J. Multiphase Flow 59 (2014) 84–101.
[229] L. Cheng, G. Ribatski and J.R. Thome, On the prediction of flow boiling heat transfer of CO_2, *The 22nd IIR Int. Congr. Refrig.*, Beijing, P.R. China, August 21-26, 2007.
[230] E. Costa-Patry, J.R. Thome, Flow pattern based flow boiling heat transfer model for microchannel, Int. J. Refrigeration 36 (2013) 414–420.
[231] A. Cioncolini, J.R. Thome, Algebraic Turbulence Modeling in Adiabatic and Evaporating Annular Two- Phase Flow, Int. J. Heat Fluid Flow 32 (2011) 805–817.
[232] J.R. Thome, A. Cioncolini, Unified model suite for two phase flow, convective boiling and condensation in macro- and microchannel, Heat Transfer Eng. 37 (2016) 1148–1157.
[233] G. Hetsroni, A. Mosyak, Z. Segal, G. Ziskind, A uniform temperature heat sink for cooling of electric devices, Int. J. Heat mass Transfer 45 (2002) 3275–3286.
[234] G. Hetsroni, A. Mosyak, Z. Segal, Nonuniform temperature distribution in electric device cooled by flow in parallel microchannel, IEEE Trans. Compon. Pack. technol. 24, 17–23 heat sink for cooling of electric devices Int. J. Heat mass Transfer 45 (2002) (2001) 3275–3286.
[235] H.Y. Wu, P. Cheng, Visualization and measurements of periodic boiling in silicon microchannel heat sinks, Int. J. Heat Mass transfer 46 (2003) 2603–2614.
[236] H. Huang, N. Borhani, J.R. Thome, Thermal response of multi-microchannel evaporators during flow boiling of refrigerants under transient heat loads with flow visualization, J. Electronic Packaging 128 (2016).
[237] D. Bestion, The difficult challenge of a two-phase CFD modelling for all flow regimes, Nucl. Eng. Des. 279 (2014) 116–125.
[238] S. Gedupudi, Y.Q. Zu, T.G. Karayiannis, D.B.R. Kenninga, Y.Y. Yan, Confined bubble growth during flow boiling in a mini/micro-channel of rectangular cross-section Part I: Experiments and 1-D modelling, Int. J. Therm. Sci 50 (3) (2011) 250–266.
[239] C. Zhang, L. Chen, F. Qin, L. Liu, W.-T. Ji, W.-Q. Tao, Lattice Boltzmann study of bubble dynamic behaviors and heat transfer performance during flow boiling in a serpentine microchannel, Appl. Therm. Eng. 218 (2023), 119331.
[240] O.A. Odumosu, H. Xu, T. Wang, Z. Che, Growth of elongated vapor bubbles during flow boiling heat transfer in wavy microchannels, Appl. Therm. Eng. 223 (2023), 119987.